Simulator of photoemission angular distribution for experiments (SPADExp)

Hiroaki Tanaka (ISSP / Graduate School of Science, The Univ. of Tokyo)

August 16, 2023

Contents

Chapter 1

Calculation theory

1.1 Hartree-Fock-Slater equation

Plane waves for photoelectron wave functions are modified by atomic potentials. Here, we explain Hartree-Fock-Slater (HFS) equations to obtain self-consistent atomic potentials.

1.1.1 Atomic units

The following arguments use **the atomic unit**, in which the following physical constants are omitted.

- **Electron mass** $m = 9.109 \times 10^{-31}$ kg
- **Bohr radius** $a_0 = 0.5292$ Å
- **Elementary charge** $e = 1.602 \times 10^{-19}$ C
- **Dirac constant** $\hbar = 1.054 \times 10^{-34}$ J · s

Values in the SI unit are from Ref. [1]. Therefore, the units of energy and wavevector become $E_h = 27.2114$ eV and $1/a_0 = 1.890$ Å^{-1}, respectively. Since Ref. [2] uses Ryberg ($E_h/2$) as the unit, coefficients may differ twice.

1.1.2 Exchange-correlation terms in free electron gas

In the HFS equations, the exchange-correlation term is approximated by the local density approximation (LDA). Here we calculate the term in free electron gas with number density n.

In a three-dimensional space with large enough volume V, wavefunctions of free-electron gases $\psi_{\mathbf{k}}(\mathbf{r})$ and eigenenergies $E(\mathbf{k})$ become

$$\psi_{\mathbf{k}}(\mathbf{r}) = \frac{1}{\sqrt{V}} e^{i\mathbf{k}\cdot\mathbf{r}},\ E(\mathbf{k}) = \frac{1}{2}|\mathbf{k}|^2. \tag{1.1}$$

We represent the Fermi wavevector by k_{F}, and using that the number density coefficient in the reciprocal space is $1/(2\pi)^3$, we obtain the following relationship;

$$n = 2 \times \frac{4}{3}\pi k_{\mathrm{F}}^3 \cdot \frac{1}{(2\pi)^3} = \frac{k_{\mathrm{F}}^3}{3\pi^2}. \tag{1.2}$$

We solve the above equation w.r.t. k_{F}, and then get

$$k_{\mathrm{F}} = (3\pi^2 n)^{1/3}. \tag{1.3}$$

We calculate the exchange-correlation term where $|\mathbf{k}| < k_{\mathrm{F}}$ region is occupied by the Hartree-Fock approximation. Here we calculate the term for only one spin direction.

$$E_{\mathrm{xc}} = -\frac{1}{2}\sum_{i,\ j}\int \mathrm{d}^3\mathbf{r}_1\mathrm{d}^3\mathbf{r}_2\ \psi_i^*(\mathbf{r}_1)\psi_j^*(\mathbf{r}_2)\frac{1}{|\mathbf{r}_1-\mathbf{r}_2|}\psi_j(\mathbf{r}_1)\psi_i(\mathbf{r}_2) \tag{1.4}$$

$$= -\frac{1}{2V^2}\sum_{i,\ j}\int \mathrm{d}^3\mathbf{r}_1\mathrm{d}^3\mathbf{r}_2\ \frac{1}{|\mathbf{r}_1-\mathbf{r}_2|}e^{i(\mathbf{k}_j-\mathbf{k}_i)\cdot(\mathbf{r}_1-\mathbf{r}_2)} \tag{1.5}$$

using $\mathbf{r}_3 = \mathbf{r}_1 - \mathbf{r}_2$ as a new integral variable,

$$= -\frac{1}{2V}\sum_{i,\ j}\int \mathrm{d}^3\mathbf{r}_3\ \frac{1}{|\mathbf{r}_3|}e^{i(\mathbf{k}_j-\mathbf{k}_i)\cdot\mathbf{r}_3} \tag{1.6}$$

in the polar coordinate system with principal axis parallel to $\mathbf{k}_j - \mathbf{k}_i$,

$$= -\frac{1}{2V}\sum_{i,\ j}\int_0^\infty r_3^2\mathrm{d}r_3\int_0^\pi \sin\theta\mathrm{d}\theta\int_0^{2\pi}\mathrm{d}\varphi\ \frac{1}{r_3}e^{iKr_3\cos\theta}\quad (K = |\mathbf{k}_j-\mathbf{k}_i|) \tag{1.7}$$

$$= -\sum_{i,\ j}\frac{\pi}{iKV}\int_0^\infty \left(e^{iKr_3} - e^{-iKr_3}\right)\mathrm{d}r_3 \tag{1.8}$$

Adding a convergence factor $e^{-\eta r}$, finally we get

$$= -\sum_{i,\ j} \frac{2\pi}{K^2 V}. \tag{1.9}$$

Next, we calculate the sum w.r.t. $\mathbf{k}_j$ with fixed $\mathbf{k}_i$,

$$E_{\rm xc} = -\frac{2\pi}{V} \sum_i \int_{|\mathbf{k}_j|<k_{\rm F}} \mathrm{d}^3\mathbf{k}_j \ \frac{1}{K^2} \cdot \frac{V}{(2\pi)^3} \tag{1.10}$$

in polar coordinate system with principal axis parallel to $\mathbf{k}_i$,

$$= -\frac{1}{4\pi^2} \sum_i \int_0^{k_{\rm F}} k_j^2 \mathrm{d}k_j \int_0^{\pi} \ \sin\theta \mathrm{d}\theta \int_0^{2\pi} \mathrm{d}\varphi \frac{1}{k_i^2 + k_j^2 - 2k_i k_j \cos\theta} \quad (k_i = |\mathbf{k}_i|,\ k_j = |\mathbf{k}_j|) \tag{1.11}$$

$$= -\frac{1}{2\pi} \sum_i \frac{1}{k_i} \int_0^{k_{\rm F}} \mathrm{d}k_j \ k_j \Big(\log|k_i + k_j| - \log|k_i - k_j| \Big) \tag{1.12}$$

Using

$$\int_0^b x \log|x+a| \mathrm{d}x = \left[\frac{1}{2}x^2 \log|x+a| - \frac{1}{4}x^2 + \frac{a}{2}x - \frac{a^2}{2} \log|x+a| \right]_0^b \tag{1.13}$$

$$= \frac{b^2 - a^2}{2} \log|b+a| - \frac{1}{4}b^2 + \frac{ab}{2} + \frac{a^2}{2} \log|a|, \tag{1.14}$$

we get

$$E_{\rm xc} = -\frac{1}{2\pi} \sum_i \frac{1}{k_i} \left[\frac{k_{\rm F}^2 - k_i^2}{1} (\log|k_{\rm F} + k_i| - \log|k_{\rm F} - k_i|) + k_{\rm F} k_i \right] \tag{1.15}$$

$$= -\frac{k_{\rm F}}{2\pi} \sum_i \left(1 + \frac{k_{\rm F}^2 - k_i^2}{2k_{\rm F} k_i} \log\left| \frac{k_i + k_{\rm F}}{k_i - k_{\rm F}} \right| \right). \tag{1.16}$$

At last we take the summation w.r.t $\mathbf{k}_i$,

$$E_{\rm xc} = -2k_{\rm F} \int_0^{k_{\rm F}} k_i^2 \mathrm{d}k_i \ \left(1 + \frac{k_{\rm F}^2 - k_i^2}{2k_{\rm F} k_i} \log\left| \frac{k_i + k_{\rm F}}{k_i - k_{\rm F}} \right| \right) \cdot \frac{V}{(2\pi)^3} \tag{1.17}$$

$$= -\frac{k_{\rm F}^4 V}{12\pi^3} + \frac{V}{8\pi^3} \int_0^{k_{\rm F}} \mathrm{d}k_i \ k_i (k_i^2 - k_{\rm F}^2)(\log|k_i + k_{\rm F}| - \log|k_i - k_{\rm F}|) \tag{1.18}$$

Using

$$\int_0^b x(x^2 - a^2) \log|x+a| \mathrm{d}x = \left[\left(\frac{1}{4}x^4 - \frac{a^2}{2}x^2 \right) \log|x+a| - \frac{1}{16}x^4 + \frac{a}{12}x^3 + \frac{a^2}{8}x^2 - \frac{a^3}{4}x + \frac{a^4}{4} \log|x+a| \right]_0^b \tag{1.19}$$

$$= \frac{(b^2 - a^2)^2}{4} \log|b+a| + \frac{1}{48}(-3b^4 + 4ab^3 + 6a^2b^2 - 12a^3 b) - \frac{a^4}{4} \log|a|, \tag{1.20}$$

we get

$$E_{\rm xc} = -\frac{k_{\rm F}^4 V}{12\pi^3} - \frac{k_{\rm F}^4 V}{24\pi^3} = -\frac{k_{\rm F}^4 V}{8\pi^3}. \tag{1.21}$$

Electron with the other spin has the same energy, so the exchange-correlation term per one electron becomes

$$e_{\rm xc} = 2E_{\rm xc} \times \frac{1}{nV} = -\frac{3k_{\rm F}}{4\pi}. \tag{1.22}$$

The exchange-correlation potential becomes twice because the energy is half to avoid double counting. Therefore, the exchange-correlation potential in the LDA approximation is

$$V_{\rm xc} = 2e_{\rm xc} = -3 \left(\frac{3n}{8\pi} \right)^{1/3}. \tag{1.23}$$

1.1.3 HFS equation

The HFS equation is obtained by averaging the Hartree-Fock equation along the angle direction. Since the potential becomes spherically isotropic, the wavefunctions can be separated by radial functions and spherical harmonics;

$$\psi(\mathbf{r}) = \frac{P_{nl}(r)}{r} Y_{lm}(\theta,\ \varphi). \tag{1.24}$$

Here, the HFS equation of $P_{nl}(r)$ becomes

$$\left[-\frac{1}{2}\frac{\mathrm{d}^2}{\mathrm{d}r^2} + \frac{l(l+1)}{2r^2} + V(r)\right] P_{nl}(r) = E_{nl} P_{nl}(r). \tag{1.25}$$

The potential $V(r)$ is the sum of nucleus potential, Hartree term, and Fock term;

$$V(r) = -\frac{Z}{r} + \frac{1}{r}\int_0^r \sigma(r')\mathrm{d}r' + \int_r^\infty \frac{\sigma(r')}{r'}\mathrm{d}r' - 3\left(\frac{3\rho(r)}{8\pi}\right)^{1/3} \tag{1.26}$$

$$\sigma(r) = \sum_{nl} w_{nl}(P_{nl}(r))^2 \tag{1.27}$$

$$\rho(r) = \frac{\sigma(r)}{4\pi r^2}, \tag{1.28}$$

where w_{nl} is the occupation number of each orbital, Z is the atomic number. There are given as input parameters. $\sigma(r)$ is the number density integrated along the angle direction, and $\rho(r)$ is the number density per unit volume. When the atomic potential $V(r)$ becomes self-consistent, that potential is the solution.

1.1.4 Thomas-Fermi potential

When we try to obtain self-consistent potential in the HFS equation, the initial potential is given by the Thomas-Fermi potential [22]. We put the atomic nucleus with charge Z at the coordinate origin and consider Z electrons around it. We represent the potential and electron density by $V(r)$ and $\rho(r)$, respectively. Also, we suppose the relationship $\rho(r) = k_\mathrm{F}(r)^3/3\pi^2$, which is similar to electron gases.

The Fermi level, determined by the potential and Fermi wavevector, should be isotropically uniform, so the relationship

$$E_\mathrm{F} = \frac{1}{2}k_\mathrm{F}(r)^2 + V(r) = \text{const.} = 0 \tag{1.29}$$

hold. We represent k_F as a function of $\rho(r)$, and using $V(r) = -\phi(r)$ where $\phi(r)$ is the electric field, then we get

$$E_\mathrm{F} = \frac{1}{2}(3\pi^2\rho(r))^{2/3} - \phi(r). \tag{1.30}$$

Combining it with the Poisson equation of the electric field

$$\Delta\phi(r) = 4\pi\rho(r) \quad (\rho(r) \text{ is the number density of electrons}), \tag{1.31}$$

then we get

$$\frac{1}{r^2}\frac{\mathrm{d}}{\mathrm{d}r}r^2\frac{\mathrm{d}}{\mathrm{d}r}(\phi(r) + E_\mathrm{F}) = \frac{4}{3\pi}(2(\phi(r) + E_\mathrm{F}))^{3/2}. \tag{1.32}$$

We define a function $f(r)$ by

$$f(r) = \frac{r}{Z}(\phi(r) + E_\mathrm{F}). \tag{1.33}$$

In the limit $r \to 0$, $\phi(r) \to Z/r$ should be dominant, so $f(r) \to 1$. On the other hand, in the limit $r \to \infty$ electron density and the potential becomes zero so $f(r) \to 0$. Using $f(r)$, we get

$$\frac{1}{r}\frac{\mathrm{d}^2}{\mathrm{d}r^2}f(r) = \frac{4}{3\pi}r^{-3/2}Z^{1/2}(2f(r))^{3/2} \tag{1.34}$$

$$\iff \frac{\mathrm{d}^2}{\mathrm{d}r^2}f(r) = \frac{2^{7/2}Z^{1/2}}{3\pi}\frac{1}{r^{1/2}}f(r)^{3/2}. \tag{1.35}$$

To obtain simple coefficients by the scaling $r = \mu x$, using $g(x) = f(r) = f(\mu x)$ we get

$$\frac{1}{\mu^2}\frac{\mathrm{d}^2}{\mathrm{d}x^2}g(x) = \frac{2^{7/2}Z^{1/2}}{3\pi}\frac{1}{(\mu x)^{1/2}}g(x)^{3/2} \tag{1.36}$$

$$\frac{\mathrm{d}^2}{\mathrm{d}x^2}g(x) = \frac{2^{7/2}Z^{1/2}}{3\pi}\frac{\mu^{3/2}}{x^{1/2}}g(x)^{3/2} \quad \therefore \mu = \left(\frac{3\pi}{2^{7/2}Z^{1/2}}\right)^{2/3} = \frac{1}{2Z^{1/3}}\left(\frac{3\pi}{4}\right)^{2/3}. \tag{1.37}$$

Using this scaling, the equation to solve becomes

$$\frac{\mathrm{d}^2}{\mathrm{d}x^2}g(x) = \frac{g(x)^{3/2}}{\sqrt{x}}, \tag{1.38}$$

and the Thomas-Fermi potential is obtained by the following equation;

$$V(r) = -\frac{Z}{r}g(r/\mu), \quad V(\mu x) = -\frac{Z}{\mu x}g(x). \tag{1.39}$$

1.2 Calculations of atomic potentials

We explain the process of numerically calculating atomic potentials based on Hartree-Fock-Slater (HFS) equations.

1.2.1 Numerical solutions of differential equations

Reduction to first-order differential equations

The differential equations in the following discussions can be represented in the form of

$$\frac{\mathrm{d}^2}{\mathrm{d}x^2} f(x) = F(f(x),\ x) \tag{1.40}$$

and are solved in the $x \geq 0$ region. Some of them satisfy the relationship $F(f(x),\ x) = -a(x) \cdot f(x)$[1]. Using $f'(x) = \frac{\mathrm{d}}{\mathrm{d}x} f(x)$, we can transform the equations to a first-order differential equation like

$$\frac{\mathrm{d}}{\mathrm{d}x} \begin{pmatrix} f(x) \\ f'(x) \end{pmatrix} = \begin{pmatrix} f'(x) \\ F(f(x),\ x) \end{pmatrix}. \tag{1.41}$$

Euler method

The Euler method calculates the value at x_{i+1} using only the value at x_i. We take a sequence of points x_i $(i = 0,\ 1,\ \cdots)$ in $x \geq 0$ region satisfying $0 = x_0 < x_1 < \cdots < x_i < x_{i+1} < \cdots$; the distances between two adjacent points $x_{i+1} - x_i$ need not to be uniform. Also, we suppose that the initial values $f(0),\ f'(0)$ are given. In this situation, the values at x_{i+1}, $f(x_{i+1})$ and $f'(x_{i+1})$ can be calculated from those at x_i by the following equations;

$$f(x_{i+1}) = f(x_i) + f'(x_i)(x_{i+1} - x_i) \tag{1.42}$$

$$f'(x_i) = f'(x_i) + F(f(x_i), x_i)(x_{i+1} - x_i). \tag{1.43}$$

Although the Euler method is less precise than the following methods because the error is proportional to the step width [4], it is more general because it does not require an equally-separated grid.

4th-order Runge-Kutta method

First, we describe the general form of the 4th-order Runge-Kutta method. We suppose a first-order differential equation of a vertical vector $\mathbf{y}(x)$ like

$$\frac{\mathrm{d}}{\mathrm{d}x} \mathbf{y}(x) = f(\mathbf{y}(x),\ x), \tag{1.44}$$

where $f(\mathbf{y}(x),\ x)$ is a function that returns a vertical vector of the same dimension as $\mathbf{y}(x)$. Using sequence of points x_i equally-separated with the distance h, $\mathbf{y}_{i+1}$ can be calculated by

$$\mathbf{k}_1 = f(\mathbf{y}(x_i),\ x_i) \tag{1.45}$$

$$\mathbf{k}_2 = f(\mathbf{y}(x_i) + h\mathbf{k}_1/2,\ x_i + h/2) \tag{1.46}$$

$$\mathbf{k}_3 = f(\mathbf{y}(x_i) + h\mathbf{k}_2/2,\ x_i + h/2) \tag{1.47}$$

$$\mathbf{k}_4 = f(\mathbf{y}(x_i) + h\mathbf{k}_3,\ x_i + h) \tag{1.48}$$

$$\mathbf{y}_{i+1} = \mathbf{y}_i + h\left[\frac{1}{6}\mathbf{k}_1 + \frac{1}{3}\mathbf{k}_2 + \frac{1}{3}\mathbf{k}_3 + \frac{1}{6}\mathbf{k}_4\right]. \tag{1.49}$$

This method gives the error proportional to the 4th power of the step h [4].

In our situation, the 4th-order Runge-Kutta method becomes

$$k_1 = f'(x_i) \qquad k'_1 = F(f(x_i),\ x_i) \tag{1.50}$$

$$k_2 = f'(x_i) + hk'_1/2 \qquad k'_2 = F(f(x_i) + hk_1/2,\ x_i + h/2) \tag{1.51}$$

$$k_3 = f'(x_i) + hk'_2/2 \qquad k'_3 = F(f(x_i) + hk_2/2,\ x_i + h/2) \tag{1.52}$$

$$k_4 = f'(x_i) + hk'_3 \qquad k'_4 = F(f(x_i) + hk_3,\ x_i + h) \tag{1.53}$$

$$f(x_{i+1}) = f(x_i) + h\left[\frac{1}{6}k_1 + \frac{1}{3}k_2 + \frac{1}{3}k_3 + \frac{1}{6}k_4\right] \quad f'(x_{i+1}) = f'(x_i) + h\left[\frac{1}{6}k'_1 + \frac{1}{3}k'_2 + \frac{1}{3}k'_3 + \frac{1}{6}k'_4\right]. \tag{1.54}$$

[1] The minus sign is to match the Numerow method.

Numerov method

The Numerov method can be used if the differential equation satisfies $F(f(x),\ x) = -a(x) \cdot f(x)$. We do not use a simultaneous differential equation form like above, but we calculate the value by the following equation;

$$f(x_{i+1}) = \frac{2(1 - 5h^2 a(x_i)/12)f(x_i) - (1 + h^2 a(x_{i-1})/12)f(x_{i-1})}{1 + h^2 a(x_{i+1})/12}, \tag{1.55}$$

where h is the distance between two adjacent points and must be constant.

The above equation is derived as follows[4]. First, using Störmer's formula

$$f(x_{i+1}) - 2f(x_i) + f(x_{i-1}) = \frac{h^2}{12}\Big(F(f(x_{i+1}),\ x_{i+1}) + 10F(f(x_i),\ x_i) + F(f(x_{i-1}),\ x_{i-1})\Big) + O(h^6), \tag{1.56}$$

$F(f(x),\ x)$ terms in the RHS are replaced by $-a(x) \cdot f(x)$. Then gathering $f(x_{i+1})$ in the RHS, we get eq. (1.55).

Sequence of points in actual calculations

In our program, a sequence of points is separated by some blocks, and in each block, points are equally separated. Table 1.1 describes the default sequence.

Table 1.1: Default sequence of points. FP and LP represent the first point and last point.

FP index	LP index	Distance	Number of distances	FP position	LP position
0	40	0.0025	40	0	0.1
40	80	0.005	40	0.1	0.3
80	120	0.01	40	0.3	0.7
120	160	0.02	40	0.7	1.5
160	200	0.04	40	1.5	3.1
200	240	0.08	40	3.1	6.3
240	280	0.16	40	6.3	12.7
280	320	0.32	40	12.7	25.5
320	360	0.64	40	25.5	51.1
360	400	1.28	40	51.1	102.3
400	440	2.56	40	102.3	204.7

1.2.2 Calculations of the Thomas-Fermi potential

The differential equation for the Thomas-Fermi potential is

$$\frac{\mathrm{d}}{\mathrm{d}x^2} g(x) = F(g(x),\ x) = \frac{g(x)^{3/2}}{\sqrt{x}}. \tag{1.57}$$

Since the Numerov method is not applicable to the equation, we solve it by the Euler method or 4th-order Runge-Kutta method. We note that only the Euler method is applicable when we consider points belonging to different blocks because the distance is not uniform.

The boundary condition derives the initial value $g(0) = 1$, but $g'(0)$ can not be determined. Therefore, we need to find appropriate $g'(0)$ satisfying the other boundary condition $g(x) \to 0$ $(x \to \infty)$. In addition, if $g(x_i)$ becomes negative, we can not calculate $g(x_{i+1})$ and further because we cannot perform the three-halves power calculation.

In our actual calculations, we use the bisection method to find $g'(0)$ which gives $g(x_N)$ smaller than the threshold. Here we represent the value $g(x_N)$ calculated with the initial value $g'(0) = g'$ by $g(x_N;\ g')$; if $g(x_i) < 0$ occurs during calculations, we suppose $g(x_N;\ g') = g(x_i)$. The following is the detailed procedure of calculations.

1. Find g'_0 and g'_1, which satisfy $g(x_N;\ g'_0) < 0 < g(x_N;\ g'_1)$.
2. Take $g'_2 = (g'_0 + g'_1)/2$ and calculate $g(x_N;\ g'_2)$.

3. If $g(x_N;\ g_2') < 0$, replace g_0' by g_2'. If $g(x_N;\ g_2') > 0$ and larger than the threshold, replace g_1' by g_2'. If $g(x_N;\ g_2') > 0$ and smaller than the threshold, current $g(x_i)$ is the solution.

4. Unless $g(x_N;\ g_2') > 0$ and smaller than the threshold, go back to 2. and continue calculations.

Figure 1.1 represents $g(x)$ obtained by our numerical calculations, which is approximately equal to the previous research [3].

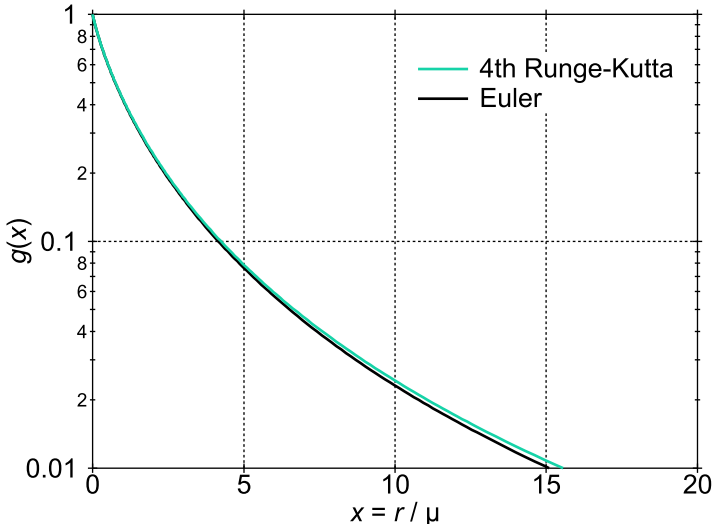

Figure 1.1: Thomas-Fermi potential function $g(x)$。

1.2.3 Schrödiger equation in an isotropic potential

Calculation procedure

The potential in the HFS equation $V(r)$ is isotropic, so we need to solve the Schrödinger equation of the radial part;

$$\left[-\frac{1}{2}\frac{\mathrm{d}^2}{\mathrm{d}r^2} + \frac{l(l+1)}{2r^2} + V(r)\right] P_{nl}(r) = E_{nl} P_{nl}(r). \tag{1.58}$$

Using the Thomas-Fermi scaling $r = \mu x$ and the substitution $P_{nl}(r) = p_{nl}(x),\ V(r) = v(x)$, we get

$$\frac{\mathrm{d}^2}{\mathrm{d}x^2} p_{nl}(x) = \left[\frac{l(l+1)}{x^2} + 2\mu^2(v(x) - E_{nl})\right] p_{nl}(x). \tag{1.59}$$

Since the potential values at points x_i, $v(x_i)$, are given, we can use the Euler method or the Numerov method. We cannot use the 4th-order Runge-Kutta method because it uses the value at $x_i + h/2$. We find the solution with $n - l - 1$ nodes and eigenvalue E_{nl}. Bound solutions, which are regular at the origin, should satisfy $p_{nl}(0) = 0$ and $p_{nl}(x) \to 0$ $(x \to \infty)$. The following condition is approximated to $p_{nl}(x_N) = 0$, where x_N is the last point of calculations.

We can use a similar procedure to that of the Thomas-Fermi potential to obtain $p_{nl}(x_i)$ with initial conditions at the origin $p_{nl}(0) = 0$; for $p_{nl}'(0)$ we can set an arbitrary value. However, this procedure gives large numerical error in large x region, so it is difficult to obtain E_{nl} satisfying $p_{nl}(x_N) = 0$ by the bisection method. Therefore, we use the following procedure to calculate $p_{nl}(x_i)$ with given E_{nl}.

1. The function in the RHS of eq. (1.59), $l(l+1)/x^2 + 2\mu^2(v(x) - E_{nl})$, becomes $-E_{nl} > 0$ in the limit $x \to \infty$. Therefore, if E_{nl} is an appropriate eigenvalue, $p_{nl}(x)$ increases/decreases monotonically and does not have a node in $x > x_0$ region, where x_0 is the last border across which the function changes sign (from negative to positive).

2. We set the calculation region to $0 \le x < x_0 \times$ const. An appropriate const. is around 8, and if the last point is smaller than $x_0 \times$ const., the former is the calculation border.

3. We solve the differential equation from $x = 0$ to outward in $0 \leq x \leq x_0$ region and obtain$p_{nl}^{\rm out}(x_i)$. On the other hand, in $x_0 \leq x$ region, the equation is solved from the border to inward and we obtain $p_{nl}^{\rm in}(x_i)$. In both calculations, the initial values of the differential are given arbitrarily.

4. We count the nodes only in the $0 \leq x \leq x_0$ region.

5. Since eq. (1.59) is a linear differential equation, a solution multiplied by a constant is also a solution. We can scale $p_{nl}^{\rm out}(x_i)$ and $p_{nl}^{\rm in}(x_i)$ so that they are continuous at $x = x_0$. If the differentials are also continuous, the solution is appropriate. We can use the logarithmic derivative $\frac{1}{p_{nl}(x)}\frac{\mathrm{d}}{\mathrm{d}x}p_{nl}(x) = \frac{\mathrm{d}}{\mathrm{d}x}\log\big(p_{nl}(x)\big)$ to judge the continuity of the differential.

6. If the logarithmic derivatives do not coincide, We can estimate the error ΔE by the method in the following subsubsection.

First, we perform 1.-4. to obtain the largest E_{nl} with $n - l - 1$ nodes[2]. After this estimation, we perform 1.-6. to change the estimated value of the eigenenergy. We continue this process until $|\Delta E|$ is smaller than the threshold, and then we obtain the eigenvalue E_{nl}, and the wavefunction is obtained by normalizing $p_{nl}(x_i)$.

Estimation of the eigenenergy error from logarithmic derivatives

Modifying eq. (1.59), we use the following differential equation

$$\frac{\mathrm{d}^2}{\mathrm{d}x^2}p(x) + (V(x) - \varepsilon)p(x) = 0 \tag{1.60}$$

and boundary conditions $p(0) = 0,\ p(x) \to 0\ (x \to \infty)$, where $p(x)$ is the solution and ε is the eigenenergy. Using a solution $q(x) = p(x) + \Delta p(x)$ and eigenenergy $\varepsilon + \Delta\varepsilon$, which satisfies the boundary conditions but is not continuous or differentiable at $x = x_0$, we estimate the eigenenergy error $\Delta\varepsilon$.

Since $q(x)$ and $\varepsilon + \Delta\varepsilon$ satisfy eq. (1.60) at any point other than $x = x_0$, inserting them and taking the first order of the error, we obtain

$$\frac{\mathrm{d}^2}{\mathrm{d}x^2}\Delta p(x) + (V(x) - \varepsilon)\Delta p(x) - \Delta\varepsilon \cdot p(x) = 0. \tag{1.61}$$

Multiplying $p(x)$ and performing integration, we get

$$\int_0^{x_0}\Big[p(x)\frac{\mathrm{d}^2}{\mathrm{d}x^2}\Delta p(x) + (V(x) - \varepsilon)p(x)\Delta p(x) - \Delta\varepsilon \cdot p(x)^2\Big]\mathrm{d}x = 0 \tag{1.62}$$

$$\iff \int_0^{x_0}\Big[p(x)\frac{\mathrm{d}^2}{\mathrm{d}x^2}\Delta p(x) - \Delta p(x)\frac{\mathrm{d}^2}{\mathrm{d}x^2}p(x)\Big]\mathrm{d}x = \Delta\varepsilon\int_0^{x_0} p(x)^2\mathrm{d}x \quad (\because \text{Using eq. (1.60) to } (V(x) - \varepsilon)p(x)) \tag{1.63}$$

$$\iff \left[p(x)\frac{\mathrm{d}}{\mathrm{d}x}\Delta p(x) - \Delta p(x)\frac{\mathrm{d}}{\mathrm{d}x}p(x)\right]_0^{x_0} = \Delta\varepsilon\int_0^{x_0} p(x)^2\mathrm{d}x \tag{1.64}$$

$$\iff \left[p(x)^2\Delta\left(\frac{1}{p(x)}\frac{\mathrm{d}}{\mathrm{d}x}p(x)\right)\right]_0^{x_0} = \Delta\varepsilon\int_0^{x_0} p(x)^2\mathrm{d}x \tag{1.65}$$

$$\iff p(x_0)^2\Delta\left(\frac{1}{p(x_0)}\frac{\mathrm{d}}{\mathrm{d}x}p(x_0)\right) = \Delta\varepsilon\int_0^{x_0} p(x)^2\mathrm{d}x \quad (\because p(0) = 0). \tag{1.66}$$

We can obtain a similar result by changing the integration region to $[x_0,\ \infty]$. Modifying these results by using $q(x)$, we get

$$p(x_0)^2\left[\frac{1}{q(x_0 - 0)}\frac{\mathrm{d}}{\mathrm{d}x}q(x_0 - 0) - \frac{1}{p(x_0)}\frac{\mathrm{d}}{\mathrm{d}x}p(x_0)\right] = \Delta\varepsilon\int_0^{x_0} p(x)^2\mathrm{d}x \tag{1.67}$$

$$-p(x_0)^2\left[\frac{1}{q(x_0 + 0)}\frac{\mathrm{d}}{\mathrm{d}x}q(x_0 + 0) - \frac{1}{p(x_0)}\frac{\mathrm{d}}{\mathrm{d}x}p(x_0)\right] = \Delta\varepsilon\int_{x_0}^{\infty} p(x)^2\mathrm{d}x. \tag{1.68}$$

[2]If the energy increases slightly from E_{nl}, where E_{nl} is a solution satisfying the boundary and node-number conditions, the node increases by 1.

We replace $p(x)$ by $q(x)$ because we cannot obtain $p(x)$, and modifying the equations to remove the second term in the LHS, we get

$$\Delta\varepsilon = \frac{\dfrac{1}{q(x_0-0)}\dfrac{\mathrm{d}}{\mathrm{d}x}q(x_0-0) - \dfrac{1}{q(x_0+0)}\dfrac{\mathrm{d}}{\mathrm{d}x}q(x_0+0)}{\dfrac{1}{q(x_0-0)^2}\displaystyle\int_0^{x_0} q(x)^2\mathrm{d}x + \dfrac{1}{q(x_0+0)^2}\int_{x_0}^{\infty} q(x)^2\mathrm{d}x}. \tag{1.69}$$

As you can see from the equation, we can use $p_{nl}^{\mathrm{out}}(x_i)$ and $p_{nl}^{\mathrm{in}}(x_i)$ without the scaling to the error estimation.

Calculation examples using the Thomas-Fermi potential

Figure 1.2 shows the Z dependence of eigenenergies of the Schrödinger equation with the Thomas-Fermi potential. This result coincides well with the previous research [3].

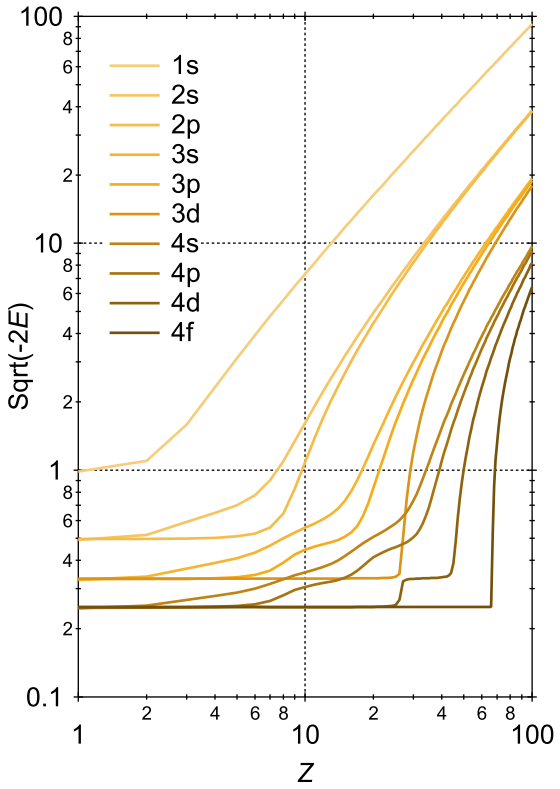

Figure 1.2: Eigenenergies in the Thomas-Fermi potential. Since the previous research [3] uses the Rydberg unit system, the vertical axis is $\sqrt{-2E}$, not $\sqrt{-E}$.

1.2.4 Calculations of self-consistent atomic potentials

Modification of the potential

As discussed above, the potential $V(r)$ in the HFS equation is given by

$$V(r) = -\frac{Z}{r} + \frac{1}{r}\int_0^r \sigma(r')\mathrm{d}r' + \int_r^{\infty}\frac{\sigma(r')}{r'}\mathrm{d}r' - 3\left(\frac{3\rho(r)}{8\pi}\right)^{1/3} \tag{1.70}$$

$$\sigma(r) = \sum_{nl} w_{nl}(P_{nl}(r))^2 \tag{1.71}$$

$$\rho(r) = \frac{\sigma(r)}{4\pi r^2}. \tag{1.72}$$

In our actual calculations, we use the scaling $r = \mu x$, so the equations become

$$V(x_i) = -\frac{Z}{\mu x_i} + \frac{1}{x_i}\sum_{j=0}^{i-1}\sigma(x_j)(x_{j+1} - x_j) + \sum_{j=i}^{N-1}\frac{\sigma(x_j)}{x_j}(x_{j+1} - x_j) - 3\left(\frac{3\rho(x_i)}{8\pi}\right)^{1/3} \tag{1.73}$$

$$\sigma(x_i) = \sum_{nl} w_{nl}(P_{nl}(x_i))^2 \tag{1.74}$$

$$\rho(x_i) = \frac{\sigma(x_i)}{4\pi(\mu x_i)^2}. \tag{1.75}$$

Furthermore, the potential should satisfy $V(x_i) \sim -1/\mu x_i$ in $x \to \infty$ limit, so we add the following modification:

$$V_{\text{modified}}(x_i) = \begin{cases} V(x_i) & V(x_i) < -\dfrac{1}{\mu x_i} \\ -\dfrac{1}{\mu x_i} & V(x_i) > -\dfrac{1}{\mu x_i} \end{cases}. \tag{1.76}$$

The radial Schrödinger equation (1.59) with the modified potential $V_{\text{modified}}(x_i)$ is solved.

SCF convergence

the j-th calculation is performed using the j-th input potential $V^{(j)}(x_i),\ V^{(j)}_{\text{modified}}(x_i)$. After that, the potential for the $j+1$-th calculation is obtained by the simple mixing method. We represent the potential obtained by the j-th calculation by $V(x_i),\ V_{\text{modified}}(x_i)$, and then the $j+1$-th input is

$$V^{(j+1)}(x_i) = (1-A)V(x_i) + A\cdot V^{(j)}(x_i),\ \ V^{(j+1)}_{\text{modified}}(x_i) = (1-A)V_{\text{modified}}(x_i) + A\cdot V^{(j)}_{\text{modified}}(x_i) \tag{1.77}$$

. The mixing ratio A is between 0 and 1, and $A = 0.5$ gave the appropriate convergence.

The convergence is checked by the following parameters $\alpha,\ \beta$.

$$\alpha_j = \max_i \left|\frac{V^{(j)}(x_i) - V^{(j+1)}(x_i)}{V^{(j)}(x_i)}\right| \tag{1.78}$$

$$\beta_j = \max_i \left|\mu x_i V^{(j)}(x_i) - \mu x_i V^{(j+1)}(x_i)\right| \tag{1.79}$$

We finish the calculations when both values are below the thresholds.

Calculation example

In case of the carbon atom, $Z = 6$ and the occupancy is $w_{10} = 2,\ w_{20} = 2,\ w_{21} = 2$. Figure 1.3 shows the calculation result in good coincidence with the previous research [2].

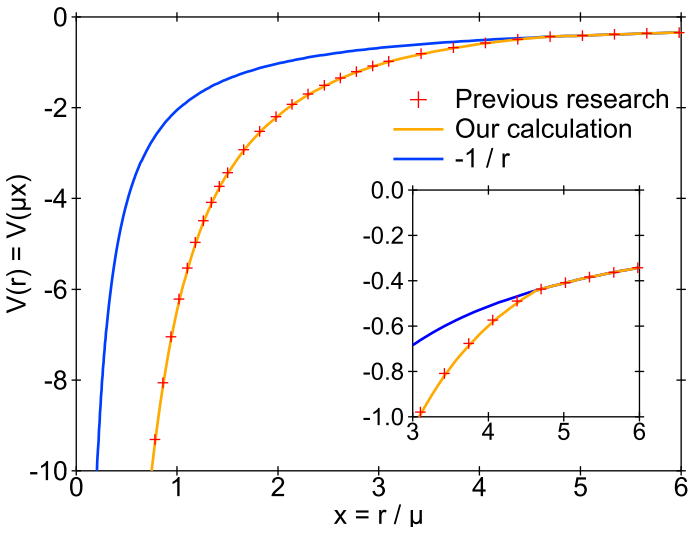

Figure 1.3: Self-consistent atomic potential of a carbon atom. The inset shows the border where the modification $V(x) = -1/\mu x$ starts.

1.3 Special functions for radial wave functions

We discuss the properties of special functions necessary for wave functions in a spherically isotropic potential $V(r)$.

1.3.1 Gamma functions

Definition

The gamma function is the natural extension of the factorial $n!$ defined by

$$\Gamma(x) = \int_0^\infty e^{-t} t^{x-1} \mathrm{d}t. \tag{1.80}$$

Properties

When $x = 1$, we get

$$\Gamma(1) = \int_0^\infty e^{-t} \mathrm{d}t = 1. \tag{1.81}$$

Partial integration gives

$$\Gamma(x) = \int_0^\infty e^{-t} t^{x-1} \mathrm{d}t \tag{1.82}$$

$$= \left[-e^{-t} t^{x-1}\right]_0^\infty + (x-1) \int_0^\infty e^{-t} t^{x-2} \mathrm{d}t = (x-1)\Gamma(x-1). \tag{1.83}$$

From Eqs. (1.81) and (1.83), we get

$$\Gamma(n) = (n-1)(n-2) \cdot 1 \cdot \Gamma(1) = (n-1)! \tag{1.84}$$

where n is a positive integer.

Next, we consider the case where x is a half-integer. Since

$$\Gamma(1/2) = \int_0^\infty e^{-t} t^{-1/2} \mathrm{d}t \tag{1.85}$$

$$= 2 \int_0^\infty e^{-u^2} \mathrm{d}u \ (t = u^2,\ \mathrm{d}t = 2u\mathrm{d}u) \tag{1.86}$$

$$= \sqrt{\pi}, \tag{1.87}$$

we get

$$\Gamma(n + 1/2) = (n - 1/2)(n - 3/2) \cdot 1/2 \cdot \Gamma(1/2) \tag{1.88}$$

$$= \frac{(2n-1)!}{(n-1)! \cdot 2^{n-1}} \sqrt{\pi} \tag{1.89}$$

$$= \frac{(2n-1)!}{(n-1)! \cdot 2^{2n-1}} \sqrt{\pi} \ \ (n \geq 1). \tag{1.90}$$

Multiplying the denominator and numerator by $2n$, we get

$$\Gamma(n + 1/2) = \frac{(2n)!}{n! \cdot 2^{2n}} \sqrt{\pi}, \tag{1.91}$$

which can be applicable for the $n = 0$ case.

Since Eq. (1.80) does not diverge unless x is zero or a negative integer, we can extend the gamma function to the complex space. For an arbitrary complex number z, the following relation holds;

$$\Gamma(z^*) = \int_0^\infty e^{-t} t^{z^*-1} \mathrm{d}t = \left[\int_0^\infty e^{-t} t^{z-1} \mathrm{d}t\right]^* = \Gamma(z)^*. \tag{1.92}$$

1.3.2 Bessel functions, spherical Bessel functions

The solutions of the Schrödinger equation with $V(r) = 0$ can be represented by a spherical Bessel function. Further transformation gives the relation between spherical Bessel functions and Bessel functions.

Transformation of a spherical Bessel function to a Bessel function

The Schrödinger equation with $V(r) = 0$ can be transformed to the spherical Bessel equation by the relation $x = kr$. The spherical Bessel equation is

$$\left[x^2\frac{\mathrm{d}^2}{\mathrm{d}x} + 2x\frac{\mathrm{d}}{\mathrm{d}x} + (x^2 - l(l+1))\right] j_l(x) = 0. \tag{1.93}$$

Then we consider transforming the spherical Bessel equation to the following Bessel equation.

$$\left[x^2\frac{\mathrm{d}^2}{\mathrm{d}x} + x\frac{\mathrm{d}}{\mathrm{d}x} + (x^2 - \nu^2)\right] J_\nu(x) = 0. \tag{1.94}$$

From the relation $j_l(x) = x^{-1/2}f(x)$, we get

$$\frac{\mathrm{d}}{\mathrm{d}x}j_l(x) = x^{-1/2}\frac{\mathrm{d}f(x)}{\mathrm{d}x} - \frac{1}{2}x^{-3/2}f(x) \tag{1.95}$$

$$\frac{\mathrm{d}^2}{\mathrm{d}x^2}j_l(x) = x^{-1/2}\frac{\mathrm{d}^2f(x)}{\mathrm{d}x} - x^{-3/2}\frac{\mathrm{d}f(x)}{\mathrm{d}x} + \frac{3}{4}x^{-5/2}f(x). \tag{1.96}$$

Substituting the above equations, we get

$$\left[x^2\frac{\mathrm{d}^2}{\mathrm{d}x^2} + x\frac{\mathrm{d}}{\mathrm{d}x} + (x^2 - (l+1/2)^2)\right] f(x) = 0. \tag{1.97}$$

The result gives the relation between a spherical Bessel function $j_l(x)$ and a Bessel function $J_\nu(x)$;

$$j_l(x) = \sqrt{\frac{\pi}{2x}}J_{l+1/2}(x). \tag{1.98}$$

The coefficient $\sqrt{\pi/2}$ is multiplied for later convenience.

Series expansion of a Bessel function

We obtain a Bessel function $J_\nu(x)$ by series expansion. Hereafter, some arguments are based on the assumption that ν is a half-integer $l + 1/2$.

First, the Bessel function is expanded like

$$J_\nu(x) = \sum_{j=0}^{\infty} a_j x^{c+j},\ a_0 \neq 0. \tag{1.99}$$

Derivatives of the above equation are

$$\frac{\mathrm{d}}{\mathrm{d}x}J_\nu(x) = \sum_{j=0}^{\infty} a_j(c+j)x^{c+j-1} \tag{1.100}$$

$$\frac{\mathrm{d}^2}{\mathrm{d}x^2}J_\nu(x) = \sum_{j=0}^{\infty} a_j(c+j)(c+j-1)x^{c+j-2}. \tag{1.101}$$

Substituting them, we get

$$\sum_{j=0}^{\infty} a_j\left[((c+j)^2 - \nu^2)x^{c+j} + x^{c+j+2}\right] = 0. \tag{1.102}$$

Looking at only the x^{c+j} terms, we get

$$j = 0,\ 1:\ a_j((c+j)^2 - \nu^2) = 0 \tag{1.103}$$

$$j \geq 2:\ a_j((c+j)^2 - \nu^2) + a_{j-2} = 0 \Longleftrightarrow a_j = \frac{-1}{(c+j)^2 - \nu^2} a_{j-2}\ (\text{when } (c+j)^2 - \nu^2 \neq 0). \tag{1.104}$$

From the condition $a_0 \neq 0$, $c = \pm\nu$ is derived.

Next, we consider the equation for the $j = 1$ case. The term in the parentheses becomes $(c+j)^2 - \nu^2 = \pm 2\nu + 1$, so $a_1 = 0$ is necessary for cases other than $\nu = \pm 1/2$. Therefore, all terms with odd j vanish from Eq. (1.104). The following argument proves that the assumption $a_1 = 0$ does not lose generality even in the $\nu = \pm 1/2$ case. When $\nu = 1/2$, the solution with $c = -\nu = -1/2$ can have nonzero a_1 while $c = \nu = 1/2$ cannot. Here we introduce $X(x, y) = -1/(x^2 - y^2)$, corresponding $x = c + j,\ y = \nu$. Then the solutions are

$$c = \nu = 1/2:\ J_\nu(x) = a_0 x^{1/2} + X(5/2, 1/2) a_0 x^{5/2} + X(9/2, 1/2) X(5/2, 1/2) a_0 x^{9/2} + \cdots \tag{1.105}$$

$$\begin{aligned} c = -\nu = -1/2:\ J_\nu(x) &= a_0 x^{-1/2} + X(3/2, 1/2) a_0 x^{3/2} + X(7/2, 1/2) X(3/2, 1/2) a_0 x^{7/2} \cdots \\ &\quad + a_1 x^{1/2} + X(5/2, 1/2) a_1 x^{5/2} + X(9/2, 1/2) X(5/2, 1/2) a_1 x^{9/2} + \cdots . \end{aligned} \tag{1.106}$$

However, the terms with a_1 in Eq. (1.106) is the same as Eq. (1.105) $\times$ (a constant) so they can be removed. Therefore we can assume $a_1 = 0$. The $\nu = -1/2$ case is also discussed similarly.

From the arguments, a_j can be nonzero when $j = 2k$ ($k = 0,\ 1,\ \cdots$). Since ν is a half-integer, the demoninator in Eq. (1.104) cannot be nonzero because $j = \mp 2\nu$ is not satisfied[3] Therefore, a_{2k} can be obtained inductively from a_0.

First, when $c = \nu$ we get

$$X(c + j,\ \nu) = -\frac{1}{(\nu + j)^2 - \nu^2} = \frac{-1}{j(2\nu + j)}. \tag{1.107}$$

The recursion equation (1.104) gives

$$a_{2k} = \frac{-1}{4k(\nu + k)} a_{2k-2} \tag{1.108}$$

$$= \frac{-1}{4k(k + j)} \frac{-1}{4(k-1)(\nu + k - 1)} a_{2k-4} \tag{1.109}$$

$$= \cdots = \frac{(-1)^k}{2^{2k} k! \cdot (\nu + k) \cdots (\nu + 1)} a_0. \tag{1.110}$$

Since Eq. (1.83) gives

$$(\nu + k) \cdots (\nu + 1) = \frac{\Gamma(\nu + k + 1)}{\Gamma(\nu + 1)}, \tag{1.111}$$

we get

$$a_{2k} = \frac{(-1)^k \Gamma(\nu + 1)}{2^{2k} k! \cdot \Gamma(\nu + k + 1)} a_0, \tag{1.112}$$

and supposing

$$a_0 = \frac{1}{2^\nu \Gamma(\nu + 1)} \tag{1.113}$$

we finally obtain

$$a_{2k} = \frac{(-1)^k}{2^{2k+\nu} k! \cdot \Gamma(\nu + k + 1)} \tag{1.114}$$

[3] if ν is an integer and $c = -\nu$, Eq. (1.104) with the $j = 2\nu$ case gives $a_{2\nu-2} = 0$. Going back to the recursion equation, we get $a_0,\ \cdots,\ a_{2\nu-2} = 0$. Therefore the first nonzero term is $a_{2\nu}$. In this case, the solution is equivalent to the $c = \nu$ case.

となる。

When $c = -\nu$, we get

$$X(c+j,\ \nu) = \frac{-1}{j(-2\nu+j)} \tag{1.115}$$

$$a_{2k} = \frac{(-1)^k}{2^{2k-\nu}k!\cdot\Gamma(-\nu+k+1)} \quad (a_0 = 1/(2^{-\nu}\Gamma(-\nu+1))). \tag{1.116}$$

In summary, two solutions of the Bessel equation are

$$J_\nu(x) = \left(\frac{x}{2}\right)^\nu \sum_{k=0}^{\infty} \frac{(-1)^k}{k!\cdot\Gamma(\nu+k+1)} \left(\frac{x}{2}\right)^{2k} \tag{1.117}$$

and $J_{-\nu}(x)$.

Neumann functions

When ν is not an integer, $J_\nu(x)$ and $J_{-\nu}(x)$ are linearly independent solutions of the Bessel equation. The Neumann function defined by

$$Y_\nu(x) = \frac{1}{\sin(\nu\pi)}(\cos(\nu\pi)J_\nu(x) - J_{-\nu}(x)) \tag{1.118}$$

is frequently used instead of $J_{-\nu}(x)$. However, when $\nu = l + 1/2$ the difference between $Y_{l+1/2}(x)$ and $J_{-(l+1/2)}(x)$ is only the sign since

$$Y_{l+1/2}(x) = (-1)^{l+1}J_{-(l+1/2)}(x) \tag{1.119}$$

$y_l(x) = \sqrt{\pi/2x}\cdot Y_{l+1/2}(x)$ is called the spherical Neumann function, which diverges at $x = 0$.

Recursion formula of Bessel functions

$J_\nu(x)$ satisfies the following recursion formula;

$$\frac{\mathrm{d}}{\mathrm{d}x}\left(x^{-\nu}J_\nu(x)\right) = -x^{-\nu}J_{\nu+1}(x). \tag{1.120}$$

The series expansion gives the proof as follows;

$$\frac{\mathrm{d}}{\mathrm{d}x}\left(x^{-\nu}J_\nu(x)\right) = \sum_{k=0}^{\infty} \frac{(-1)^k}{k!\cdot\Gamma(\nu+k+1)} \frac{2kx^{2k-1}}{2^{2k+\nu}} \tag{1.121}$$

$$= \sum_{k=1}^{\infty} \frac{(-1)^k}{(k-1)!\cdot\Gamma(\nu+k+1)} \frac{x^{2k-1}}{2^{2k+\nu-1}} \quad (k=0 \text{ term is zero}) \tag{1.122}$$

$$= \sum_{K=0}^{\infty} \frac{-(-1)^K}{K!\cdot\Gamma(\nu+K+2)} \frac{x^{2K+1}}{2^{2K+\nu+1}} \quad (K = k-1) \tag{1.123}$$

$$= -x^{-\nu} \sum_{K=0}^{\infty} \frac{(-1)^K}{K!\cdot\Gamma(\nu+K+2)} \left(\frac{x}{2}\right)^{2K+\nu+1} \tag{1.124}$$

$$= -x^{-\nu}J_{\nu+1}(x). \tag{1.125}$$

The Bessel functions also satisfy the following formula;

$$\frac{\mathrm{d}}{\mathrm{d}x}\left(x^{\nu}J_\nu(x)\right) = x^{\nu}J_{\nu-1}(x). \tag{1.126}$$

The series expansion gives

$$\frac{\mathrm{d}}{\mathrm{d}x}\left(x^{\nu}J_{\nu}(x)\right) = \sum_{k=0}^{\infty}\frac{(-1)^k}{k!\cdot\Gamma(\nu+k+1)}\frac{(2k+2\nu)x^{2k+2\nu-1}}{2^{2k+\nu}} \tag{1.127}$$

$$= \sum_{k=1}^{\infty}\frac{(-1)^k}{(k-1)!\cdot\Gamma(\nu+k)}\frac{x^{2k+2\nu-1}}{2^{2k+\nu-1}} \quad (\because \Gamma(\nu+k+1)=(\nu+k)\Gamma(\nu+k)) \tag{1.128}$$

$$= x^{\nu}\sum_{k=0}^{\infty}\frac{(-1)^k}{k!\cdot\Gamma(\nu+k)}\left(\frac{x}{2}\right)^{2k+\nu-1} \tag{1.129}$$

$$= x^{\nu}J_{\nu-1}(x). \tag{1.130}$$

Spherical Bessel functions and spherical Neumann functions

The recursion formula above and the Bessel function with $\nu = 1/2$,

$$J_{1/2}(x) = \sqrt{\frac{x}{2}}\sum_{k=0}^{\infty}\frac{(-1)^k}{k!\cdot\Gamma(k+1+1/2)}\left(\frac{x}{2}\right)^{2k} \tag{1.131}$$

$$= \sqrt{\frac{x}{2}}\sum_{k=0}^{\infty}\frac{(-1)^k(k+1)!\cdot 2^{2k+2}}{k!\cdot(2k+2)!\cdot\sqrt{\pi}}\left(\frac{x}{2}\right)^{2k} \quad (\because (1.91)) \tag{1.132}$$

$$= \sqrt{\frac{2}{\pi x}}\sum_{k=0}^{\infty}\frac{(-1)^k}{(2k+1)!}x^{2k+1} = \sqrt{\frac{2}{\pi x}}\sin x, \tag{1.133}$$

the Bessel function when ν is a positive half-integer becomes

$$J_{l+1/2}(x) = -x^{l-1/2}\frac{\mathrm{d}}{\mathrm{d}x}\left(x^{-(l-1/2)}J_{l-1/2}(x)\right) \tag{1.134}$$

$$= -x^{l-1/2}\frac{\mathrm{d}}{\mathrm{d}x}\left(-\frac{1}{x}\frac{\mathrm{d}}{\mathrm{d}x}\left(x^{-(l-3/2)}J_{l-3/2}(x)\right)\right) \tag{1.135}$$

$$= (-1)^l x^{l+1/2}\left(\frac{1}{x}\frac{\mathrm{d}}{\mathrm{d}x}\right)^l x^{-1/2}J_{1/2}(x) \tag{1.136}$$

$$= \sqrt{\frac{2}{\pi}}(-1)^l x^{l+1/2}\left(\frac{1}{x}\frac{\mathrm{d}}{\mathrm{d}x}\right)^l\frac{\sin x}{x}. \tag{1.137}$$

The spherical Bessel function is represented by

$$j_l(x) = (-1)^l x^l\left(\frac{1}{x}\frac{\mathrm{d}}{\mathrm{d}x}\right)^l\frac{\sin x}{x}. \tag{1.138}$$

The following are spherical Bessel functions from $l = 0$ to $l = 4$.

$$j_0(x) = \frac{\sin x}{x} \tag{1.139}$$

$$j_1(x) = \frac{\sin x - x\cos x}{x^2} \tag{1.140}$$

$$j_2(x) = \frac{(3-x^2)\sin x - 3x\cos x}{x^3} \tag{1.141}$$

$$j_3(x) = \frac{(15-6x^2)\sin x + (x^3-15x)\cos x}{x^4} \tag{1.142}$$

$$j_4(x) = \frac{(x^4-45x^2+105)\sin x + (10x^3-105x)\cos x}{x^5} \tag{1.143}$$

The Bessel function with $\nu = -1/2$ is

$$J_{-1/2}(x) = \sqrt{\frac{2}{x}} \sum_{k=0}^{\infty} \frac{(-1)^k}{k! \cdot \Gamma(k+1/2)} \left(\frac{x}{2}\right)^{2k} \tag{1.144}$$

$$= \sqrt{\frac{2}{x}} \sum_{k=0}^{\infty} \frac{(-1)^k k! \cdot 2^{2k}}{k! \cdot (2k)! \cdot \sqrt{\pi}} \left(\frac{x}{2}\right)^{2k} \quad (\because (1.91)) \tag{1.145}$$

$$= \sqrt{\frac{2}{\pi x}} \sum_{k=0}^{\infty} \frac{(-1)^k}{(2k)!} x^{2k} = \sqrt{\frac{2}{\pi x}} \cos x. \tag{1.146}$$

Therefore, the Bessel function when ν is a negative half-integer is

$$J_{-l-1/2}(x) = x^{l-1/2} \frac{\mathrm{d}}{\mathrm{d}x} \left(x^{-l+1/2)} J_{-l+1/2}(x)\right) \tag{1.147}$$

$$= x^{l-1/2} \frac{\mathrm{d}}{\mathrm{d}x} \left(\frac{1}{x} \frac{\mathrm{d}}{\mathrm{d}x} \left(x^{-l+3/2)} J_{-l+3/2}(x)\right)\right) \tag{1.148}$$

$$= x^{l+1/2} \left(\frac{1}{x} \frac{\mathrm{d}}{\mathrm{d}x}\right)^l x^{-1/2} J_{-1/2}(x) \tag{1.149}$$

$$= \sqrt{\frac{2}{\pi}} x^{l+1/2} \left(\frac{1}{x} \frac{\mathrm{d}}{\mathrm{d}x}\right)^l \frac{\cos x}{x}. \tag{1.150}$$

The spherical Neumann function is

$$y_l(x) = (-1)^{l+1} x^l \left(\frac{1}{x} \frac{\mathrm{d}}{\mathrm{d}x}\right)^l \frac{\cos x}{x}. \tag{1.151}$$

Asymptotic forms

The asymptotic form with $x \to 0$ is dominated by the lowest power of x in the series expansion. Therefore, we get

$$J_\nu(x) \sim \left(\frac{x}{2}\right)^\nu \frac{1}{\Gamma(\nu+1)} \tag{1.152}$$

and

$$j_l(x) \sim \sqrt{\frac{\pi}{2x}} \left(\frac{x}{2}\right)^{l+1/2} \frac{1}{\Gamma(l+1+1/2)} \tag{1.153}$$

$$= \sqrt{\frac{\pi}{2x}} \left(\frac{x}{2}\right)^{l+1/2} \frac{(l+1)! \cdot 2^{2l+2}}{(2l+2)! \cdot \sqrt{\pi}} \quad (\because (1.91)) \tag{1.154}$$

$$= \frac{2^l l!}{(2l+1)!} x^l. \tag{1.155}$$

The asymptotic form with $x \to \infty$ is dominated by the term obtained by the differentiations of the trigonometric function. Therefore, the form of the spherical Bessel function is

$$j_l(x) \sim (-1)^l \frac{1}{x} \frac{\mathrm{d}^l}{\mathrm{d}x^l} \sin x \tag{1.156}$$

$$= \frac{1}{x} \frac{(-1)^l}{2i} \left(i^l \mathrm{cis}(x) - (-i)^l \mathrm{cis}(-x)\right) \tag{1.157}$$

$$= \frac{1}{x} \frac{\mathrm{cis}(x - l\pi/2) - \mathrm{cis}(-(x - l\pi/2))}{2i} \tag{1.158}$$

$$= \frac{\sin(x - l\pi/2)}{x} \tag{1.159}$$

and that of the spherical Neumann function is

$$y_l(x) \sim (-1)^{l+1}\frac{1}{x}\frac{\mathrm{d}^l}{\mathrm{d}x^l}\cos x \tag{1.160}$$
$$= \frac{1}{x}\frac{(-1)^{l+1}}{2}\Big(i^l\mathrm{cis}(x) + (-i)^l\mathrm{cis}(-x)\Big) \tag{1.161}$$
$$= \frac{-1}{x}\frac{\mathrm{cis}(x - l\pi/2) + \mathrm{cis}(-(x - l\pi/2))}{2} \tag{1.162}$$
$$= -\frac{\cos(x - l\pi/2)}{x}, \tag{1.163}$$

where $\mathrm{cis}(x) = e^{ix} = \cos x + i\sin x$.

1.3.3 Coulomb wave functions

A Coulomb function is a solution of the Schrödinger equation with the Coulomb potential $V(r) = -1/r$.

Transformation to a confluent hypergeometric function

Substituting $E = k^2/2$ and $r = x/k$ in the radial Schrödinger equation with the Coulomb potential, we get

$$\left[\frac{\mathrm{d}^2}{\mathrm{d}x^2} + 1 + \frac{2}{kx} - \frac{l(l+1)}{x^2}\right] f(x) = 0. \tag{1.164}$$

First, the equation is transformed into the Whittaker equation

$$\left[\frac{\mathrm{d}^2}{\mathrm{d}z^2} - \frac{1}{4} + \frac{\kappa}{z} + \frac{1/4 - \mu^2}{z^2}\right] g(z) = 0. \tag{1.165}$$

Using the relation $x = z/2i$, we get

$$(1.164) \iff \left[-4\frac{\mathrm{d}^2}{\mathrm{d}z^2} + 1 + \frac{4i}{kz} + \frac{4l(l+1)}{z^2}\right] f(z/2i) = 0 \tag{1.166}$$
$$\iff \left[\frac{\mathrm{d}^2}{\mathrm{d}z^2} - \frac{1}{4} - \frac{i}{kz} + \frac{1/4 - (l+1/2)^2}{z^2}\right] f(z/2i) = 0. \tag{1.167}$$

Therefore we get the following relation;

$$g(z) = f(x) = f(z/2i),\ \kappa = -\frac{i}{k},\ \mu = l + \frac{1}{2}. \tag{1.168}$$

Next, the Whittaker equation is transformed to the confluent hypergeometric equation

$$\left[z\frac{\mathrm{d}^2}{\mathrm{d}z^2} + (b - z)\frac{\mathrm{d}}{\mathrm{d}z} - a\right] h(z) = 0. \tag{1.169}$$

Assuming the relation $g(z) = e^{-z/2}z^{\mu+1/2}h(z)$, the derivatives of it are

$$\frac{\mathrm{d}}{\mathrm{d}z}g(z) = -\frac{1}{2}e^{-z/2}z^{\mu+1/2}h(z) + (\mu + 1/2)e^{-z/2}z^{\mu-1/2}h(z) + e^{-z/2}z^{\mu+1/2}\frac{\mathrm{d}h(z)}{\mathrm{d}z} \tag{1.170}$$
$$\frac{\mathrm{d}^2}{\mathrm{d}z^2}g(z) = \frac{1}{4}e^{-z/2}z^{\mu+1/2}h(z) + (\mu^2 - 1/4)e^{-z/2}z^{\mu-3/2}h(z) + e^{-z/2}z^{\mu+1/2}\frac{\mathrm{d}^2h(z)}{\mathrm{d}z^2}$$
$$+2\left[-\frac{\mu + 1/2}{2}e^{-z/2}z^{\mu-1/2}h(z) - \frac{1}{2}e^{-z/2}z^{\mu+1/2}\frac{\mathrm{d}h(z)}{\mathrm{d}z} + (\mu + 1/2)e^{-z/2}z^{\mu-1/2}\frac{\mathrm{d}h(z)}{\mathrm{d}z}\right]. \tag{1.171}$$

Therefore, we get

$$(1.165) \iff \left[\frac{\mathrm{d}^2}{\mathrm{d}z^2} + \left(-1 + \frac{2\mu+1}{z}\right)\frac{\mathrm{d}}{\mathrm{d}z} + \frac{\kappa - (\mu + 1/2)}{z}\right] h(z) = 0 \tag{1.172}$$
$$\iff \left[z\frac{\mathrm{d}^2}{\mathrm{d}z^2} + (2\mu + 1 - z)\frac{\mathrm{d}}{\mathrm{d}z} - (\mu - \kappa + 1/2)\right] h(z) = 0. \tag{1.173}$$

The relation between the Whittaker equation and the confluent hypergeometric equation becomes

$$b = 2\mu + 1 = 2(l+1),\ a = \mu - \kappa + \frac{1}{2} = l + 1 + \frac{i}{k}. \tag{1.174}$$

Regular and irregular solutions of the confluent hypergeometric function are represented by $M(a,\ b,\ z)$ and $U(a,\ b,\ z)$, respectively. $M(a,\ b,\ z)$ is

$$M(a,\ b,\ z) = \sum_{s=0}^{\infty} \frac{(a)_s}{(b)_s s!} z^s, \tag{1.175}$$

where $(a)_s$ is the Pochhammer symbol defined by

$$(a)_s = a(a+1)\cdots(a+s-1),\ (a)_0 = 1. \tag{1.176}$$

$U(a,\ b,\ z)$ has different representations depending on a and b. In this case, $U(a,\ b,\ z)$ is

$$\begin{aligned} U(a,\ n+1,\ z) = {} & \frac{(-1)^{n+1}}{n!\Gamma(a-n)} \sum_{k=0}^{\infty} \frac{(a)_k}{(n+1)_k k!} z^k (\log z + \psi(a+k) - \psi(1+k) - \psi(n+k+1)) \\ & + \frac{1}{\Gamma(a)} \sum_{k=1}^{n} \frac{(k-1)!(1-a+k)_{n-k}}{(n-k)!} z^{-k},\ n = 0,\ 1,\ \cdots, a \neq 0,\ -1,\ \cdots \end{aligned} \tag{1.177}$$

$$\psi(x) = \frac{1}{\Gamma(x)} \frac{\mathrm{d}\Gamma(x)}{\mathrm{d}x}. \tag{1.178}$$

$\psi(x)$ is called the digamma function.

Normalization based on the asymptotic forms

The asymptotic forms of $M(a,\ b,\ z)$ and $U(a,\ b,\ z)$ with $z \to \infty$ are

$$\begin{aligned} M(a,\ b,\ z) \sim {} & \frac{\Gamma(b)}{\Gamma(a)} e^z z^{a-b} \sum_{s=0}^{\infty} \frac{(1-a)_s (b-a)_s}{s!} z^{-s} \\ & + \frac{\Gamma(b)}{\Gamma(b-a)} e^{i\pi a} z^{-a} \sum_{s=0}^{\infty} \frac{(a)_s (a-b+1)_s}{s!} (-z)^{-s},\ -\frac{\pi}{2} + \delta \leq \arg z \leq \frac{3\pi}{2} - \delta \end{aligned} \tag{1.179}$$

$$U(a,\ b,\ z) \sim z^{-a} \sum_{s=0}^{\infty} \frac{(a)_s (a-b+1)_s}{s!} (-z)^{-s},\ |\arg z| \leq \frac{3\pi}{2} - \delta. \tag{1.180}$$

Since $z = 2ix$ and $x \geq 0$, the argument of z becomes $\frac{\pi}{2}$

We extract the highest power of x in the asymptotic forms. For $M(a,\ b,\ z)$, the highest power from the first term is z^{a-b}, that from the second term is z^{-a}, and

$$z^{a-b} = (2ix)^{-(l+1)+i/k} \tag{1.181}$$

$$= (2x)^{-(l+1)+i/k} \times \exp\left(\frac{\pi i}{2} \cdot (-(l+1) + i/k)\right) \tag{1.182}$$

$$= (2x)^{-(l+1)} e^{-\pi/2k} \mathrm{cis}\left[\frac{\log(2x)}{k} - \frac{\pi(l+1)}{2}\right] \tag{1.183}$$

$$z^{-a} = (2ix)^{-(l+1)-i/k} \tag{1.184}$$

$$= (2x)^{-(l+1)-i/k} \times \exp\left(\frac{\pi i}{2} \cdot (-(l+1) - i/k)\right) \tag{1.185}$$

$$= (2x)^{-(l+1)} e^{\pi/2k} \mathrm{cis}\left[-\frac{\log(2x)}{k} - \frac{\pi(l+1)}{2}\right]. \tag{1.186}$$

Since these are in the same order, both of them are taken into account, and by multiplying the conversion coefficient $e^{-z/2}z^{\mu+1/2}$, we get

$$e^{-ix}(2ix)^{l+1}\left[\frac{\Gamma(2(l+1))}{\Gamma(l+1+i/k)}e^{2ix}(2x)^{-(l+1)}e^{-\pi/2k}\mathrm{cis}\left(\frac{\log(2x)}{k}-\frac{\pi(l+1)}{2}\right)\right.$$
$$\left.+\frac{\Gamma(2(l+1))}{\Gamma(l+1-i/k)}e^{i\pi(l+1+i/k)}(2x)^{-(l+1)}e^{\pi/2k}\mathrm{cis}\left(-\frac{\log(2x)}{k}-\frac{\pi(l+1)}{2}\right)\right] \tag{1.187}$$
$$= i^{l+1}(2l+1)!e^{-\pi/2k}\left[\frac{e^{ix}}{\Gamma(l+1+i/k)}\mathrm{cis}\left(\frac{\log(2x)}{k}-\frac{\pi(l+1)}{2}\right)\right.$$
$$\left.+\frac{e^{-ix}}{\Gamma(l+1-i/k)}\mathrm{cis}\left(-\frac{\log(2x)}{k}+\frac{\pi(l+1)}{2}\right)\right] \tag{1.188}$$
$$= \frac{(-i)i^{l+1}(2l+1)!e^{-\pi/2k}}{|\Gamma(l+1+i/k)|}\left[\mathrm{cis}\left(x+\frac{\log(2x)}{k}-\frac{l\pi}{2}+\arg\,\Gamma(l+1-i/k)\right)-\text{c.c.}\right] \tag{1.189}$$
$$= \frac{2\cdot i^{l+1}(2l+1)!e^{-\pi/2k}}{|\Gamma(l+1+i/k)|}\sin\left(x+\frac{\log(2x)}{k}-\frac{l\pi}{2}+\arg\,\Gamma(l+1-i/k)\right). \tag{1.190}$$

Eq. (1.92) is used during the transformation and c.c. represents the complex conjugate of the first term. $f(x)$ is normalized as follows

$$f_1(x) = \frac{|\Gamma(l+1+i/k)|\cdot e^{\pi/2k}}{2k\cdot(2l+1)!}e^{-ix}(2x)^{l+1}M(l+1+i/k,\ 2l+2,\ 2ix) \tag{1.191}$$
$$f_1(kr) \to \frac{1}{k}\sin\left(kr+\frac{\log(2kr)}{k}-\frac{l\pi}{2}+\arg\,\Gamma(l+1-i/k)\right), \tag{1.192}$$

so that the asymptotic form of $f(kr)/r$ becomes similar to that of the spherical Bessel function $j_l(kr)\to \sin(kr-l\pi/2)/kr$.

For $U(a,\ b,\ z)$, the asymptotic form of the highest power is z^{-a} so

$$e^{-ix}(2ix)^{l+1}(2ix)^{-(l+1)-i/k} = e^{\pi/2k}\mathrm{cis}(-x-\log(2x)/k) \tag{1.193}$$

is the asymptotic form of the Coulomb wave function. A linear combination of it and $f(x)$ gives the solution with the following asymptotic form

$$f_2(kr) \to \frac{1}{k}\cos\left(kr+\frac{\log(2kr)}{k}-\frac{l\pi}{2}+\arg\,\Gamma(l+1-i/k)\right). \tag{1.194}$$

At last, we discuss the behavior of $f_1(x)$ around $x\to 0$. Since $M(a,\ b,\ z)\to 1$, we get

$$f_1(x) \to \frac{|\Gamma(l+1+i/k)|\cdot e^{\pi/2k}}{2k\cdot(2l+1)!}(2x)^{l+1}. \tag{1.195}$$

Therefore, we need to set the sign of $f_1(x)$ so that the first derivative is positive.

Real function

We prove that

$$f_0(x) = e^{-ix}(2x)^{l+1}M(l+1+i/k,\ 2l+2,\ 2ix), \tag{1.196}$$

obtained by removing real coefficients in $f_1(x)$, is a real function

From Eq. (1.175), we get

$$M(a,\ b,\ z)^* = M(a^*,\ b^*,\ z^*). \tag{1.197}$$

Also, using the relation derived from the confluent hypergeometric equation

$$M(a,\ b,\ z) = e^z M(b-a,\ b,\ -x), \tag{1.198}$$

We get

$$f_0^*(x) = e^{ix}(2x)^{l+1}M(l+1-i/k,\ 2l+2,\ -2ix) \tag{1.199}$$
$$= e^{ix}(2x)^{l+1}e^{-2ix}M(l+1+i/k,\ 2l+2,\ 2ix) \tag{1.200}$$
$$= e^{-ix}(2x)^{l+1}M(l+1+i/k,\ 2l+2,\ 2ix) = f_0(x). \tag{1.201}$$

Therefore $f_0(x)$ is a real function.

1.3.4 Spherical harmonics

A spherical harmonic is an eigenstate of the angular momentum operator.

Conversion of the polar coordinate system and cartesian coordinate system

The position vector $\mathbf{r}$ is represented by polar and cartesian coordinates like

$$\mathbf{r} = \begin{pmatrix} x \\ y \\ z \end{pmatrix} = \begin{pmatrix} r\sin\theta\cos\varphi \\ r\sin\theta\sin\varphi \\ r\cos\theta \end{pmatrix}. \tag{1.202}$$

The partial derivative of a function with respect to the distance r gives

$$f(r+\Delta r,\ \theta,\ \varphi) - f(r,\ \theta,\ \varphi) = \Delta r \frac{\partial}{\partial r} f(\mathbf{r}). \tag{1.203}$$

When we represent the relation using the cartesian coordinates, we get

$$f(r+\Delta r,\ \theta,\ \varphi) - f(r,\ \theta,\ \varphi) = f(x+\Delta r\sin\theta\cos\varphi,\ y+\Delta r\sin\theta\sin\varphi,\ z+\Delta r\cos\theta) - f(x,\ y,\ z) \tag{1.204}$$

$$= \Delta r\left[\sin\theta\cos\varphi\frac{\partial}{\partial x} + \sin\theta\sin\varphi\frac{\partial}{\partial y} + \cos\theta\frac{\partial}{\partial z}\right] f(\mathbf{r}). \tag{1.205}$$

Comparing them, we get

$$\frac{\partial}{\partial r} = \sin\theta\cos\varphi\frac{\partial}{\partial x} + \sin\theta\sin\varphi\frac{\partial}{\partial y} + \cos\theta\frac{\partial}{\partial z}. \tag{1.206}$$

Similar arguments give

$$\frac{\partial}{\partial\theta} = r\cos\theta\cos\varphi\frac{\partial}{\partial x} + r\cos\theta\sin\varphi\frac{\partial}{\partial y} - r\sin\theta\frac{\partial}{\partial z} \tag{1.207}$$

$$\frac{\partial}{\partial\varphi} = -r\sin\theta\sin\varphi\frac{\partial}{\partial x} + r\sin\theta\cos\varphi\frac{\partial}{\partial y}, \tag{1.208}$$

and the inverse transformations are

$$\frac{\partial}{\partial x} = \sin\theta\cos\varphi\frac{\partial}{\partial r} + \frac{\cos\theta\cos\varphi}{r}\frac{\partial}{\partial\theta} - \frac{\sin\varphi}{r\sin\theta}\frac{\partial}{\partial\varphi} \tag{1.209}$$

$$\frac{\partial}{\partial y} = \sin\theta\sin\varphi\frac{\partial}{\partial r} + \frac{\cos\theta\sin\varphi}{r}\frac{\partial}{\partial\theta} + \frac{\cos\varphi}{r\sin\theta}\frac{\partial}{\partial\varphi} \tag{1.210}$$

$$\frac{\partial}{\partial z} = \cos\theta\frac{\partial}{\partial r} - \frac{\sin\theta}{r}\frac{\partial}{\partial\theta}. \tag{1.211}$$

Using these relations, the following relations can be proved;

$$\Delta = \frac{1}{r^2}\frac{\partial}{\partial r}r^2\frac{\partial}{\partial r} - \frac{\mathbf{L}^2}{r^2},\ \mathbf{L} = \mathbf{r}\times\mathbf{p} = -i\mathbf{r}\times\nabla \tag{1.212}$$

$$L_z = -i\left(x\frac{\partial}{\partial y} - y\frac{\partial}{\partial x}\right) = -i\frac{\partial}{\partial\varphi} \tag{1.213}$$

$$L_\pm = L_x \pm iL_y = e^{\pm i\varphi}\left(\pm\frac{\partial}{\partial\theta} + i\frac{\cos\theta}{\sin\theta}\frac{\partial}{\partial\varphi}\right). \tag{1.214}$$

Derivation of spherical harmonics

We obtain the eigenstate of $\mathbf{L}^2$ and L_z satisfying

$$\mathbf{L}^2 Y_{lm}(\theta,\ \varphi) = l(l+1)Y_{lm}(\theta,\ \varphi) \tag{1.215}$$

$$L_z Y_{lm}(\theta,\ \varphi) = mY_{lm}(\theta,\ \varphi). \tag{1.216}$$

First, from Eqs. (1.213) and (1.216) the spherical harmonic can be decomposed like

$$Y_{lm}(\theta,\ \varphi) = \Theta(\theta)\Phi(\varphi) \tag{1.217}$$

$$L_z\Phi(\varphi) = -i\frac{\partial}{\partial\varphi}\Phi(\varphi) = m\Phi(\varphi). \tag{1.218}$$

The normalization is defined so that the integrals with respect to θ and φ become 1;

$$\int_0^\pi \sin\theta \mathrm{d}\theta \int_0^{2\pi} \mathrm{d}\varphi |Y_{lm}(\theta,\ \varphi)|^2 = \int_0^\pi |\Theta(\theta)|^2 \sin\theta \mathrm{d}\theta \int_0^{2\pi} |\Phi(\varphi)|^2 \mathrm{d}\varphi = 1 \times 1. \tag{1.219}$$

The differential equation with respect to φ can be easily solved; the solution is

$$\Phi_m(\varphi) = \frac{1}{\sqrt{2\pi}} e^{im\varphi}. \tag{1.220}$$

The coefficient $1/\sqrt{2\pi}$ is for the normalization.

Next we obtain $\Theta(\theta)$. From the properties of the ladder operator $L_\pm$, when $m = l$ we get

$$L_+\Big(\Theta_{ll}(\theta)\Phi_l(\varphi)\Big) = 0 \tag{1.221}$$

$$\iff \left[\frac{\partial}{\partial\theta} - l\frac{\cos\theta}{\sin\theta}\right]\Theta_{ll}(\theta) = 0. \tag{1.222}$$

The solution to the above equation is

$$\Theta_{ll}(\theta) = (-1)^l \sqrt{\frac{(2l+1)!}{2}} \frac{1}{2^l l!} \sin^l\theta. \tag{1.223}$$

The normalization of the solution is determined from

$$I_l = \frac{2l}{2l+1}\frac{2l-2}{2l-1}\cdots\frac{2}{3}I_0 = \frac{2\cdot(2^l l!)^2}{(2l+1)!}, \tag{1.224}$$

which is obtained from

$$I_l = \int_0^\pi \sin^{2l+1}\theta \mathrm{d}\theta = 2l\int_0^\pi (1-\sin^2\theta)\sin^{2l-1}\mathrm{d}\theta = 2l(I_{l-1} - I_l) \tag{1.225}$$

$$\therefore I_l = \frac{2l}{2l+1} I_{l-1} \tag{1.226}$$

and $I_0 = 2$. The coefficient $(-1)^l$ is multiplied for later convenience.

Since we get $\Theta_{ll}(\theta)$, we can calculate Θ_{lm} from the properties of the latter operator

$$L_- Y_{lm}(\theta,\ \varphi) = \sqrt{(l+m)(l-m+1)}\, Y_{lm-1}(\theta,\ \varphi). \tag{1.227}$$

Since

$$L_-\Theta_{lm}(\theta)\Phi_m(\varphi) = \left(-\frac{\partial}{\partial\theta} - m\frac{\cos\theta}{\sin\theta}\right)\Theta_{lm}(\theta)\Phi_{m-1}(\varphi) \tag{1.228}$$

holds, we get

$$\Theta_{lm-1}(\theta) = -\frac{1}{\sqrt{(l+m)(l-m+1)}}\left(\frac{\mathrm{d}}{\mathrm{d}\theta} + m\frac{\cos\theta}{\sin\theta}\right)\Theta_{lm}(\theta). \tag{1.229}$$

Here we introduce the conversion $x = \cos\theta$. Since $\mathrm{d}x = -\sin\theta\mathrm{d}\theta$,

$$\sin^{1-m}\theta\frac{\mathrm{d}}{\mathrm{d}x}\Big[\sin^m\theta\cdot f(\theta)\Big] = \sin\theta\frac{\mathrm{d}}{\mathrm{d}x}f(\theta) - m\cos\theta\frac{\mathrm{d}\theta}{\mathrm{d}x}f(\theta) = -\left(\frac{\mathrm{d}}{\mathrm{d}\theta} + m\frac{\cos\theta}{\sin\theta}\right)f(\theta) \tag{1.230}$$

holds. Substituting it, we get

$$\Theta_{lm-1}(\theta) = \frac{\sin^{1-m}\theta}{\sqrt{(l+m)(l-m+1)}}\frac{\mathrm{d}}{\mathrm{d}x}\Big[\sin^m\theta\cdot\Theta_{lm}(\theta)\Big]. \tag{1.231}$$

Using it repeatedly, finally, we get

$$\Theta_{lm}(\theta) = \sqrt{\frac{(l+m)!}{(2l)!(l-m)!}} \frac{1}{\sin^m \theta} \left(\frac{\mathrm{d}}{\mathrm{d}x}\right)^{l-m} \sin^l \theta \cdot \Theta_{ll}(\theta) \tag{1.232}$$

$$= (-1)^l \sqrt{\frac{2l+1}{2} \frac{(l+m)!}{(l-m)!}} \frac{1}{2^l l!} \frac{1}{\sin^m \theta} \left(\frac{\mathrm{d}}{\mathrm{d}x}\right)^{l-m} \sin^{2l} \theta. \tag{1.233}$$

Similar argument gives

$$\Theta_{lm+1}(\theta) = -\frac{\sin^{1+m} \theta}{\sqrt{(l-m)(l+m+1)}} \frac{\mathrm{d}}{\mathrm{d}x} \Big[\sin^{-m} \theta \cdot \Theta_{lm}(\theta)\Big]. \tag{1.234}$$

Especially when $m = 0$, the spherical harmonic becomes

$$\Theta_{l0}(\theta) = (-1)^l \sqrt{\frac{2l+1}{2}} \frac{1}{2^l l!} \left(\frac{\mathrm{d}}{\mathrm{d}x}\right)^l \sin^{2l} \theta = \sqrt{\frac{2l+1}{2}} P_l(\cos\theta), \tag{1.235}$$

where

$$P_l(x) = \frac{1}{2^l l!} \left(\frac{\mathrm{d}}{\mathrm{d}x}\right)^l (x^2-1)^l \tag{1.236}$$

is the Legendre polynomial derived by the Rodrigues formula. Here we obtain Θ_{lm} from Θ_{l0}; the result is

$$\Theta_{lm}(\theta) = (-1)^m \sqrt{\frac{2l+1}{2} \frac{(l-m)!}{(l+m)!}} \sin^m \theta \left(\frac{\mathrm{d}}{\mathrm{d}x}\right)^m P_l(x) \tag{1.237}$$

$$\Theta_{l-m}(\theta) = \sqrt{\frac{2l+1}{2} \frac{(l-m)!}{(l+m)!}} \sin^m \theta \left(\frac{\mathrm{d}}{\mathrm{d}x}\right)^m P_l(x) = (-1)^m \Theta_{lm}(\theta), \tag{1.238}$$

where m is limited so that $m \geq 0$.

Explicit formulae

First, the Legendre polynomials are

$$P_0(x) = 1 \tag{1.239}$$

$$P_1(x) = x \tag{1.240}$$

$$P_2(x) = \frac{3}{2}x^2 - \frac{1}{2} \tag{1.241}$$

$$P_3(x) = \frac{5}{2}x^3 - \frac{3}{2}x \tag{1.242}$$

$$P_4(x) = \frac{35}{8}x^4 - \frac{15}{4}x^2 + \frac{3}{8}. \tag{1.243}$$

Applying the ladder operators on $\Theta_{ll}(\theta)$, we can obtain the explicit formulae of $\Theta_{lm}(\theta)$. In the following $\Theta_{l-m}(\theta)$ are omitted because the relation $(-1)^m \Theta_{lm}(\theta)$gives $\Theta_{l-m}(\theta)$.

$$\Theta_{00}(\theta) = \frac{1}{\sqrt{2}} \tag{1.244}$$

$$\Theta_{11}(\theta) = -\frac{\sqrt{3}}{2} \sin\theta \tag{1.245}$$

$$\Theta_{10}(\theta) = \sqrt{\frac{3}{2}} \cos\theta \tag{1.246}$$

$$\Theta_{22}(\theta) = \frac{\sqrt{15}}{4}\sin^2\theta \tag{1.247}$$
$$\Theta_{21}(\theta) = -\frac{\sqrt{15}}{2}\sin\theta\cos\theta \tag{1.248}$$
$$\Theta_{20}(\theta) = \frac{1}{2}\sqrt{\frac{5}{2}}(3\cos^2\theta - 1) \tag{1.249}$$

$$\Theta_{33}(\theta) = -\frac{\sqrt{70}}{8}\sin^3\theta \tag{1.250}$$
$$\Theta_{32}(\theta) = \frac{\sqrt{105}}{4}\sin^2\theta\cos\theta \tag{1.251}$$
$$\Theta_{31}(\theta) = -\frac{\sqrt{42}}{8}(5\cos^2\theta - 1)\sin\theta \tag{1.252}$$
$$\Theta_{30}(\theta) = \frac{1}{2}\sqrt{\frac{7}{2}}(5\cos^2\theta - 3)\cos\theta \tag{1.253}$$

$$\Theta_{44}(\theta) = \frac{3\sqrt{35}}{16}\sin^4\theta \tag{1.254}$$
$$\Theta_{43}(\theta) = -\frac{3\sqrt{70}}{8}\sin^3\theta\cos\theta \tag{1.255}$$
$$\Theta_{42}(\theta) = \frac{3\sqrt{5}}{8}(7\cos^2\theta - 1)\sin^2\theta \tag{1.256}$$
$$\Theta_{41}(\theta) = -\frac{3\sqrt{10}}{8}(7\cos^2\theta - 3)\sin\theta\cos\theta \tag{1.257}$$
$$\Theta_{40}(\theta) = \frac{3\sqrt{2}}{16}(35\cos^4\theta - 30\cos^2\theta + 3) \tag{1.258}$$

1.3.5 Addition theorem of spherical harmonics

We consider two polar coordinates $(\theta,\ \varphi)$ and $(\theta'',\ \varphi'')$ and define ω as the angle between them. We show the following formula:

$$P_l(\cos\omega) = \frac{4\pi}{2l+1}\sum_m Y^*_{lm}(\theta'',\ \varphi'')Y_{lm}(\theta,\ \varphi). \tag{1.259}$$

The proof is based on Ref. [7].

First, we transform (1.235) to get

$$P_l(\cos\omega) = \sqrt{\frac{4\pi}{2l+1}}\Theta_{l0}(\theta')\Phi_0(\varphi') = \sqrt{\frac{4\pi}{2l+1}}Y_{l0}(\theta',\ \varphi'), \tag{1.260}$$

where $(\theta',\ \varphi')$ is the polar coordinate with the $(\theta'',\ \varphi'')$ direction being the pole. Therefore $P_l(\cos\omega)$ is an eigenstate of the angular momentum, so it should be expanded using spherical harmonics with respect to the $(\theta,\ \varphi)$ direction. We represent the expansion coefficient by E_{lm}. Then we get

$$P_l(\cos\omega) = \sum_m E_{lm}Y_{lm}(\theta,\ \varphi). \tag{1.261}$$

The cartesian coordinate with the $(\theta'',\ \varphi'')$ direction being the pole (the z direction) can be constructed, for example, by

$$\mathbf{e}''_x = (\cos\theta''\cos\varphi'',\ \cos\theta''\sin\varphi'', -\sin\theta'') \tag{1.262}$$
$$\mathbf{e}''_y = (-\sin\varphi'',\ \cos\varphi'',\ 0) \tag{1.263}$$
$$\mathbf{e}''_z = (\sin\theta''\cos\varphi'',\ \sin\theta''\sin\varphi'', \cos\theta''). \tag{1.264}$$

The conversion formulae are

$$x = \cos\theta'' \cos\varphi'' x'' - \sin\varphi'' y'' + \sin\theta'' \cos\varphi'' z'' \tag{1.265}$$
$$y = \cos\theta'' \sin\varphi'' x'' + \cos\varphi'' y'' + \sin\theta'' \sin\varphi'' z'' \tag{1.266}$$
$$z = -\sin\theta'' x'' + \cos\theta'' z'' \tag{1.267}$$
$$x'' = \cos\theta'' \cos\varphi'' x + \cos\theta'' \sin\varphi'' y - \sin\theta'' z \tag{1.268}$$
$$y'' = -\sin\varphi'' x + \cos\varphi'' y \tag{1.269}$$
$$z'' = \sin\theta'' \cos\varphi'' x + \sin\theta'' \sin\varphi'' y + \cos\theta'' z. \tag{1.270}$$

Here, we consider applying the angular momentum operator $L_{z''}$ to a function $f(x,\ y,\ z)$. We obtain

$$L_{z''} f(x,\ y\ z) = -i\left(x'' \frac{\partial}{\partial y''} - y'' \frac{\partial}{\partial x''}\right) f(x,\ y,\ z) \tag{1.271}$$
$$= -i \begin{pmatrix} (\cos\theta'' \cos\varphi'' x + \cos\theta'' \sin\varphi'' y - \sin\theta'' z)\left(-\sin\varphi'' \frac{\partial}{\partial x} + \cos\varphi'' \frac{\partial}{\partial z}\right) \\ -(-\sin\varphi'' x + \cos\varphi'' y)\left(\cos\theta'' \cos\varphi'' \frac{\partial}{\partial x} + \cos\theta'' \sin\varphi'' \frac{\partial}{\partial y} - \sin\theta'' \frac{\partial}{\partial z}\right) \end{pmatrix} f(x,\ y,\ z) \tag{1.272}$$
$$= \left[\cos\theta'' L_z + \sin\theta'' \cos\varphi'' L_x + \sin\theta'' \sin\varphi'' L_y\right] f(x,\ y,\ z) \tag{1.273}$$
$$= \left[\cos\theta'' L_z + \frac{1}{2}\sin\theta'' e^{-i\varphi''} L_+ + \frac{1}{2}\sin\theta'' e^{i\varphi''} L_-\right] f(x,\ y,\ z). \tag{1.274}$$

We apply the result to $P_l(\cos\omega) \sim Y_{l0}(\theta',\ \varphi')$, and we extract the Y_{lm} term; we get

$$m\cos\theta'' E_{lm} + \frac{1}{2}\sin\theta'' e^{-i\varphi''}\sqrt{(l-m+1)(l+m)} E_{lm-1} + \frac{1}{2}\sin\theta'' e^{i\varphi''}\sqrt{(l+m+1)(l-m)} E_{lm+1} = 0. \tag{1.275}$$

On the other hand, equation (1.214) can be transformed to

$$e^{-i\varphi} L_+ + e^{i\varphi} L_- + 2\frac{\cos\theta}{\sin\theta} L_z = 0. \tag{1.276}$$

Applying it to $Y_{lm}(\theta'',\ \varphi'')$, then we get

$$m\cos\theta'' Y_{lm}(\theta'',\ \varphi'') + \frac{1}{2}\sin\theta'' e^{-i\varphi''}\sqrt{(l-m)(l+m+1)} Y_{lm+1}(\theta'',\ \varphi'') + \frac{1}{2}\sin\theta'' e^{i\varphi}\sqrt{(l+m)(l-m+1)} Y_{lm-1}(\theta'',\ \varphi'') = 0. \tag{1.277}$$

The above formula corresponds well with the complex conjugate of equation (1.275), so we get the solution $E_{lm} = c \times Y^*_{lm}(\theta'',\ \varphi'')$. c is a constant determined below.

At last, we discuss the $\theta'' = 0$ case. We need to elucidate the condition where $Y_{lm}(0,\ \varphi)$ becomes nonzero. In equation (1.233), the $l - m$ differential operators with respect to $x(= \cos\theta)$ are applied to $\sin^{2l}\theta = (1-x^2)^l$. Therefore at least m $1-x^2$ terms are not differentiated, they becomes $\sin^{2m}\theta$. Even considering the $\sin^m\theta$ term in the denominator, $m = 0$ is necessary to obtain a nonzero value when θ is zero. A similar statement holds for Θ_{l-m} because only the sign can be different from Θ_{lm}. Therefore, $m = 0$ is necessary. In this case, we differentiate $(1-x^2)^l$ l times, we need to differentiate all terms. Otherwise, remaining $1-x^2$ terms becomes zero at $\theta = 0$ $(x = 1)$. Therefore, the nonzero term is

$$\Theta_{l0}(0) = (-1)^l \sqrt{\frac{2l+1}{2}} \frac{1}{2^l l!} \cdot l! \cdot (-2)^l = \sqrt{\frac{2l+1}{2}}. \tag{1.278}$$

Inserting the above equation to equation (1.260), we get

$$\sqrt{\frac{4\pi}{2l+1}} \Theta_{l0}(\theta') \frac{1}{\sqrt{2\pi}} = c\sqrt{\frac{2l+1}{2}} \frac{1}{\sqrt{2\pi}} \cdot \Theta_{l0}(\theta) \frac{1}{\sqrt{2\pi}} \quad \therefore c = \frac{4\pi}{2l+1}. \tag{1.279}$$

1.3.6 Partial wave expansion

The plane wave $e^{i\mathbf{k}\cdot\mathbf{r}}$ can be expanded by spherical Bessel functions and spherical harmonics.

When $\mathbf{k}$ is parallel to the z axis, the partial wave expansion is

$$e^{ikr\cos\theta} = \sum_l i^l(2l+1)j_l(kr)P_l(\cos\theta). \tag{1.280}$$

The proof is as follows.

The plane wave $e^{ikr\cos\theta}$ is a solution of the Schrödinger equation without potential ($E = k^2/2$). On the other hand, $j_l(kr)Y_{lm}(\theta,\ \varphi)$ are also solutions with the same eigenenergy, and they form a complete set. Therefore the plane wave should be represented by a linear combination of them. The φ-independent property shows that we only need to consider the $m = 0$ case, we assume

$$e^{ikr\cos\theta} = \sum_l c_l j_l(kr)P_l(\cos\theta). \tag{1.281}$$

The asymptotic form of the spherical Bessel function with $r \to 0$ is given by Eq. (1.155), which shows that $j_l(kr)$ is the l-th power of r. The l-th power terms in $P_l(x)$ is obtained from Eq. (1.236) like

$$\frac{1}{2^l l!}\left(\frac{\mathrm{d}}{\mathrm{d}x}\right)^l x^{2l} = \frac{(2l)!}{2^l(l!)^2}x^l. \tag{1.282}$$

Comparing the $(kr\cos\theta)^l$ terms of the left hand side and the right hand side, finally, we obtain

$$\frac{1}{l!}(ikr\cos\theta)^l = c_l\frac{2^l l!(kr)^l}{(2l+1)!}\frac{(2l)!\cdot\cos^l\theta}{2^l(l!)^2} = \frac{c_l}{(2l+1)l!}(kr\cos\theta)^l \quad \therefore c_l = i^l(2l+1). \tag{1.283}$$

Next, we consider an arbitrary $\mathbf{k}$. We represent the directions of $\mathbf{r}$ and $\mathbf{k}$ by $(\theta,\ \varphi)$ and $(\theta_k,\ \varphi_k)$, and the angle between $\mathbf{r}$ and $\mathbf{k}$ by ω. Then we get

$$e^{i\mathbf{k}\cdot\mathbf{r}} = e^{ikr\cos\omega} = \sum_l i^l(2l+1)j_l(kr)P_l(\cos\omega). \tag{1.284}$$

Using the addition theorem of spherical harmonics

$$P_l(\cos\omega) = \frac{4\pi}{2l+1}\sum_m Y^*_{lm}(\theta_k,\ \varphi_k)Y_{lm}(\theta,\ \varphi), \tag{1.285}$$

finally, we obtain

$$e^{i\mathbf{k}\cdot\mathbf{r}} = 4\pi\sum_{lm} i^l j_l(kr)Y^*_{lm}(\theta_k,\ \varphi_k)Y_{lm}(\theta,\ \varphi). \tag{1.286}$$

1.4 Unoccupied state calculations in the Kohn-Sham system

.

We calculate the wave functions of unoccupied states in the Kohn-Sham system of OpenMX.

1.4.1 Schrödinger equation

The kinetic energy of a photoelectron $E_{\rm kin} = \frac{1}{2}|\mathbf{k}|^2$ is determined from the binding energy and photon energy; we set the vacuum level to zero. Since the in-plane wavevector $\mathbf{k}_{/\!/}$ is specified, the wave function in the vacuum is

$$\psi_{\rm vac}(\mathbf{r}) = e^{i\mathbf{k}\cdot\mathbf{r}+\theta} \tag{1.287}$$

$$\mathbf{k} = (\mathbf{k}_{/\!/}, k_z) \quad (k_z > 0) \tag{1.288}$$

$$|\mathbf{k}|^2 = |\mathbf{k}_{/\!/}|^2 + k_z^2. \tag{1.289}$$

We note that the degree of freedom in θ remains.

Wave function in a crystal ($0 < z < z_0$) $\psi_{\rm sol}(\mathbf{r})$ is determined to satisfy the following conditions.

- It has the same eigenenergy $E_{\rm kin}$.
- The in-plane wavevector is the same as $\mathbf{k}_{/\!/}$ in the Bloch space. The k_z component is ill-defined in the crystal.
- It is connected to $e^{i\mathbf{k}\cdot\mathbf{r}+\theta}$ in the vacuum.

In the system with collinear spins or neglected spin, the Schrödinger equation for $\psi_{\rm sol}(\mathbf{r})$ is

$$\left[-\frac{1}{2}\Delta + V(\mathbf{r}) + \hat{V}_{\rm nonloc}\right]\psi_{\rm sol}(\mathbf{r}) = E_{\rm kin}\psi_{\rm sol}(\mathbf{r}). \tag{1.290}$$

$V(\mathbf{r})$ is the potential distribution in the real space; we can obtain it as the Gaussian Cube format for both spins. $\hat{V}_{\rm nonloc}$ represents the non-local part of pseudopotential. It is in the separable form

$$\hat{V}_{\rm nonloc} = \sum_{plm} \lambda_{pl}|\beta_{pl}Y_{lm}\rangle\langle Y_{lm}\beta_{pl}|. \tag{1.291}$$

λ_{pl} is a constant and $|\beta_{pl}\rangle$ is a radial part; both are obtained from the pseudopotential file.

1.4.2 Separable non-local pseudopotential

Pseudopotentials in OpenMX include relativistic effects, so they depend on not only the angular momentum $\mathbf{L}$ but also the spin angular momentum $\mathbf{S}$. Indeed, separable non-local pseudopotentials uses the coupled angular momentum $\mathbf{J} = \mathbf{L} + \mathbf{S}$ and its eigenvalue $j = l \pm \frac{1}{2}$. When we use specified multiplicity p and angular momentum l, the separable potential becomes

$$\hat{V}_{{\rm nonloc},pl} = \sum_{j}^{l\pm1/2} \lambda_{pj}|\beta_{pj}\Phi_j\rangle\langle\Phi_j\beta_{pj}|. \tag{1.292}$$

$|\Phi_j\rangle$ is an eigenstate of $\mathbf{J}$ by coupling spherical harmonics $|Y_{lm}\rangle$ and spin wave function $|\sigma\rangle$ The following equations separate them into orbital and spin parts:

$$\hat{V}_{{\rm nonloc},pl} = \hat{V}^{\rm orb}_{{\rm nonloc},pl} + \hat{V}^{\rm spin}_{{\rm nonloc},pl} \tag{1.293}$$

$$\hat{V}^{\rm orb}_{{\rm nonloc},pl} = \lambda_{pl}|\beta_{pl}Y_{lm}\rangle\langle Y_{lm}\beta_{pl}| \tag{1.294}$$

$$\hat{V}^{\rm spin}_{{\rm nonloc},pl} = \lambda^{\rm spin}_{pl}|\beta^{\rm spin}_{pl}Y_{lm}\rangle\mathbf{L}\cdot\mathbf{S}\langle Y_{lm}\beta^{\rm spin}_{pl}| \tag{1.295}$$

$$\lambda_{pl} = \frac{1}{2l+1}\Big[(l+1)\lambda_{p,l+1/2} + l\lambda_{p,l-1/2}\Big] \tag{1.296}$$

$$\beta_{pl}(r) = \frac{1}{2l+1}\Big[(l+1)\beta_{p,l+1/2} + l\beta_{p,l-1/2}\Big] \tag{1.297}$$

$$\lambda^{\rm spin}_{pl} = \frac{2}{2l+1}\Big[\lambda_{p,l+1/2} - \lambda_{p,l-1/2}\Big] \tag{1.298}$$

$$\beta_{pl}(r) = \frac{2}{2l+1}\Big[\beta_{p,l+1/2} - \beta_{p,l-1/2}\Big]. \tag{1.299}$$

These equations can be justified by considering that $\mathbf{L}\cdot\mathbf{S}$ becomes $\frac{l}{2}, -\frac{l+1}{2}$ for the $j = l \pm \frac{1}{2}$ cases. In cases other than non-collinear spin, we discard the $\hat{V}^{\mathrm{spin}}_{\mathrm{nonloc},pl}$ term.

1.4.3 Wave functions in the region without the non-local term

Since the non-local potentials affect within the pseudopotential cutoff, most of the slab is affected by only the local potential $V(\mathbf{r})$. We calculate wave functions in the system with only the local potential and then discuss the effect of the non-local potential.

Fourier expansion

Based on in-plane periodicity, the Fourier expansion can be applied to a wave function;

$$\psi_{\mathrm{sol}}(\mathbf{r}) = \sum_{\mathbf{g}_{/\!/}} \psi_{\mathbf{g}_{/\!/}}(z) e^{\mathrm{i}(\mathbf{k}_{/\!/}+\mathbf{g}_{/\!/})\cdot\mathbf{r}_{/\!/}}. \tag{1.300}$$

$\mathbf{g}_{/\!/}$ represents an in-plane reciprocal vector and $\mathbf{r} = (\mathbf{r}_{/\!/},\ z)$ holds. The boundary conditions at the termination surface $z = z_0$ are

$$\psi_{\mathbf{g}_{/\!/}}(z_0) = 0 \quad (\mathbf{g}_{/\!/} \neq \mathbf{0}) \tag{1.301}$$

$$\left.\frac{\mathrm{d}\psi_{\mathbf{g}_{/\!/}}}{\mathrm{d}z}\right|_{z=z_0} = 0 \quad (\mathbf{g}_{/\!/} \neq \mathbf{0}) \tag{1.302}$$

$$\psi_{\mathbf{0}}(z_0) = e^{\mathrm{i}k_z z_0} \tag{1.303}$$

$$\left.\frac{\mathrm{d}\psi_{\mathbf{0}}}{\mathrm{d}z}\right|_{z=z_0} = \mathrm{i}k_z e^{\mathrm{i}k_z z_0}. \tag{1.304}$$

Inserting it into the Schrödinger equation (1.290) without the non-local term, we get

$$\sum_{\mathbf{g}_{/\!/}} \left[\frac{1}{2}|\mathbf{k}_{/\!/}+\mathbf{g}_{/\!/}|^2 \psi_{\mathbf{g}_{/\!/}}(z) e^{\mathrm{i}(\mathbf{k}_{/\!/}+\mathbf{g}_{/\!/})\cdot\mathbf{r}_{/\!/}} - \frac{1}{2}\frac{\mathrm{d}^2\psi_{\mathbf{g}_{/\!/}}(z)}{\mathrm{d}z^2} e^{\mathrm{i}(\mathbf{k}_{/\!/}+\mathbf{g}_{/\!/})\cdot\mathbf{r}_{/\!/}} + (V(\mathbf{r}) - E_{\mathrm{kin}})\psi_{\mathbf{g}_{/\!/}}(z) e^{\mathrm{i}(\mathbf{k}_{/\!/}+\mathbf{g}_{/\!/})\cdot\mathbf{r}_{/\!/}} \right] = 0. \tag{1.305}$$

Dividing it by $e^{\mathrm{i}\mathbf{k}\cdot\mathbf{r}_{/\!/}}$, then we get

$$\sum_{\mathbf{g}_{/\!/}} \left[-\frac{1}{2}\frac{\mathrm{d}^2\psi_{\mathbf{g}_{/\!/}}(z)}{\mathrm{d}z^2} e^{\mathrm{i}\mathbf{g}_{/\!/}\cdot\mathbf{r}_{/\!/}} + \left(\frac{1}{2}|\mathbf{k}_{/\!/}+\mathbf{g}_{/\!/}|^2 + V(\mathbf{r}) - E_{\mathrm{kin}} \right) \psi_{\mathbf{g}_{/\!/}}(z) e^{\mathrm{i}\mathbf{g}_{/\!/}\cdot\mathbf{r}_{/\!/}} \right] = 0. \tag{1.306}$$

Furthermore, since the local potential $V(\mathbf{r})$ has in-plane periodicity, it can be Fourier-expanded like

$$V(\mathbf{r}) = \sum_{\mathbf{g}} V_{\mathbf{g}_{/\!/}}(z) e^{\mathrm{i}\mathbf{g}_{/\!/}\cdot\mathbf{r}_{/\!/}} \tag{1.307}$$

$$V_{\mathbf{g}_{/\!/}}(z) = \frac{1}{S}\int V(\mathbf{r}) e^{-\mathrm{i}\mathbf{g}_{/\!/}\cdot\mathbf{r}_{/\!/}} \mathrm{d}^2\mathbf{r}_{/\!/}. \tag{1.308}$$

S represents the area of the in-plane unit cell. Inserting the result and extracting the $e^{\mathrm{i}\mathbf{g}_{/\!/}\cdot\mathbf{r}_{/\!/}}$ term, finally we get

$$-\frac{1}{2}\frac{\mathrm{d}^2\psi_{\mathbf{g}_{/\!/}}(z)}{\mathrm{d}z^2} + \left[\frac{1}{2}|\mathbf{k}_{/\!/}+\mathbf{g}_{/\!/}|^2 - E_{\mathrm{kin}} \right] \psi_{\mathbf{g}_{/\!/}}(z) + \sum_{\mathbf{g}'_{/\!/}} V_{\mathbf{g}'_{/\!/}}(z)\psi_{\mathbf{g}_{/\!/}-\mathbf{g}'_{/\!/}}(z) = 0. \tag{1.309}$$

We arrange the equation for the Numerov method; it is transformed to

$$\frac{\mathrm{d}^2\Psi_{/\!/}(z)}{\mathrm{d}z^2} = -\Big[(2E_{\mathrm{kin}} - |\mathbf{k}_{/\!/}+\mathbf{g}_{/\!/}|^2) I - 2V_{\mathbf{g}_{/\!/1}\mathbf{g}_{/\!/2}}(z) \Big] \Psi_{/\!/}(z). \tag{1.310}$$

$\Psi_{/\!/}(z) = (\psi_{\mathbf{g}_{/\!/}}(z))$ is a vertical vector, I is the identity matrix, $V_{\mathbf{g}_{/\!/1}\mathbf{g}_{/\!/2}}(z)$is a matrix including $V_{\mathbf{g}_{/\!/1}-\mathbf{g}_{/\!/2}}(z)$.

When we solve the differential equation by the Numerov method, we need to limit $\mathbf{g}_{/\!/}$ to satisfy $|\mathbf{k}_{/\!/}+\mathbf{g}_{/\!/}|^2/2 < E_{\mathrm{kin}}$. Otherwise, the solution becomes unstable because the solutions at $\mathbf{g}_{/\!/}$ not satisfying the above condition are exponential functions, not waves.

Solution using bulk wave functions

First, since the potential in the slab other than the topmost layer is sufficiently periodic along the z direction, we calculate unoccupied states in the three-dimensionally periodic bulk. We Fourier-expand the potential and wave functions along the z, and we get

$$V(\mathbf{r}) = \sum_{\mathbf{g}} V_{\mathbf{g}} e^{\mathrm{i}\mathbf{g}\cdot\mathbf{r}} \tag{1.311}$$

$$\psi^{\mathrm{bulk}}(\mathbf{r}) = \sum_{\mathbf{g}} \psi_{\mathbf{g}} e^{\mathrm{i}(\mathbf{k}+\mathbf{g})\cdot\mathbf{r}}, \quad \mathbf{k} = (\mathbf{k}_{/\!/},\ k_z - \mathrm{i}\kappa_z), \quad \mathbf{g} = (\mathbf{g}_{/\!/},\ g_z). \tag{1.312}$$

The z component of the Bloch wave vector $k_z - \mathrm{i}\kappa_z$ is determined so that the eigenvalue becomes E_{kin} Inserting them into the Schrödinger equation and then we get

$$|\mathbf{k}+\mathbf{g}|^2\psi_{\mathbf{g}} + 2\sum_{\mathbf{g}'} V_{\mathbf{g}'}\psi_{\mathbf{g}-\mathbf{g}'} = 2E_{\mathrm{kin}}\psi_{\mathbf{g}} \quad (|\mathbf{v}|^2 = v_x^2 + v_y^2 + v_z^2). \tag{1.313}$$

Therefore, the Hamiltonian matrix $H_{\mathbf{g}_1\mathbf{g}_2}$ is

$$H_{\mathbf{g}_1\mathbf{g}_2} = \mathrm{diag}(|\mathbf{k}+\mathbf{g}|^2) + 2V_{\mathbf{g}_1-\mathbf{g}_2}. \tag{1.314}$$

We note that $H_{\mathbf{g}_1\mathbf{g}_2}$ is not Hermite and eigenvalues are not always real because of the complex component $-\mathrm{i}\kappa_z$.

After we get eigenstates of the bulk, we put them on the slab. The linear combination coefficients a_m are determined later. We represent the upper edge of the bulk region by $z = z_{\mathrm{b}}$ and then the bulk wave function becomes

$$\psi_{\mathrm{in}}(\mathbf{r}) = \sum_m a_m \psi_m^{\mathrm{bulk}}(\mathbf{r} - z_{\mathrm{b}}) \tag{1.315}$$

$$= \sum_{m\mathbf{g}} a_m \psi_{m\mathbf{g}} e^{\mathrm{i}(\mathbf{k}_m+\mathbf{g})\cdot(\mathbf{r}-z_{\mathrm{b}})} \tag{1.316}$$

$$= \sum_{\mathbf{g}_{/\!/}} \left[\sum_{g_z m} a_m \psi_{m\mathbf{g}} e^{\mathrm{i}(k_{mz}+g_z)\cdot(z-z_{\mathrm{b}})} e^{\kappa_{mz}(z-z_{\mathrm{b}})} \right] e^{\mathrm{i}(\mathbf{k}_{/\!/}+\mathbf{g}_{/\!/})\cdot\mathbf{r}_{/\!/}}. \tag{1.317}$$

Comparing the equations in the above section, we transform it into

$$\psi_{\mathbf{g}_{/\!/}}(z) = \sum_{g_z m} a_m \psi_{mg} e^{\mathrm{i}(k_{mz}+g_z)\cdot(z-z_{\mathrm{b}})} e^{\kappa_{mz}(z-z_{\mathrm{b}})} \tag{1.318}$$

$$\Psi_{/\!/}(z) = B_m(z) \times \mathbf{a}. \tag{1.319}$$

$\Psi(z) = (\psi_{g_{/\!/}}(z)\}$ and $\mathbf{a} = (a_m)$ are $\#\mathbf{g}_{/\!/}$-dimensional and $\#m$-dimensional vertical vectors and $B_m(z)$ is a $\#\mathbf{g}_{/\!/} \times \#m$ matrix.

We take a lattice point z_0 as the furthest point satisfying $z_0 < z_{\mathrm{b}}$. Also, we set $z = z_1$ as the edge of the slab. The second derivative of the vertical vector $\Psi = (\psi_{\mathbf{g}_{/\!/}}(z_0 + hi)\}$ is

$$\frac{\mathrm{d}^2\Psi}{\mathrm{d}z} = \begin{pmatrix} & A_{\mathbf{g}_{/\!/1}\mathbf{g}_{/\!/2}} & \end{pmatrix} \begin{pmatrix} \Psi \end{pmatrix} + \begin{pmatrix} \psi_{\mathbf{g}_{/\!/}}(z_0 - h)/h^2 \\ 0 \\ \delta_{\mathbf{g}_{/\!/}\mathbf{0}} e^{\mathrm{i}k_z(z_1+h)}/h^2 \end{pmatrix} \tag{1.320}$$

$$A_{\mathbf{g}_{/\!/1}\mathbf{g}_{/\!/2}} = \frac{\delta_{\mathbf{g}_{/\!/1}\mathbf{g}_{/\!/2}}}{h^2} \begin{pmatrix} -2 & 1 & & & & \\ 1 & -2 & 1 & & & \\ & 1 & \ddots & \ddots & & \\ & & \ddots & 1 & -2 & 1 \\ & & & & 1 & -2 \end{pmatrix}. \tag{1.321}$$

Therefore, the differential equation becomes

$$\begin{pmatrix} & A_{\mathbf{g}_{/\!/1}\mathbf{g}_{/\!/2}} + M_{\mathbf{g}_{/\!/1}\mathbf{g}_{/\!/2}} & \end{pmatrix} \begin{pmatrix} \Psi \end{pmatrix} = \begin{pmatrix} -\psi_{\mathbf{g}_{/\!/}}(z_0 - h)/h^2 \\ 0 \\ -\delta_{\mathbf{g}_{/\!/}\mathbf{0}} e^{\mathrm{i}k_z(z_1+h)}/h^2 \end{pmatrix} \tag{1.322}$$

$$M_{\mathbf{g}_{/\!/1}\mathbf{g}_{/\!/2}} = \delta_{\mathbf{g}_{/\!/1}\mathbf{g}_{/\!/2}}(2E_{\mathrm{kin}} - |\mathbf{k}_{/\!/} + \mathbf{g}_{/\!/1}|^2)I - 2V_{\mathbf{g}_{/\!/1}\mathbf{g}_{/\!/2}}(z_0 + hi). \tag{1.323}$$

We represent the inverse matrix of $A_{\mathbf{g}_{/\!/1}\mathbf{g}_{/\!/2}} + M_{\mathbf{g}_{/\!/1}+\mathbf{g}_{/\!/2}}$ by H^{-1} and divide it into upper edge, lower edge, and center;

$$H^{-1} = \left(\begin{array}{c|c|c} H^{-1}_{\mathbf{g}_{/\!/1}\mathbf{g}_{/\!/2}\mathrm{LL}} & H^{-1}_{\mathbf{g}_{/\!/1}\mathbf{g}_{/\!/2}\mathrm{LC}} & H^{-1}_{\mathbf{g}_{/\!/1}\mathbf{g}_{/\!/2}\mathrm{LR}} \\ \hline H^{-1}_{\mathbf{g}_{/\!/1}\mathbf{g}_{/\!/2}\mathrm{CL}} & H^{-1}_{\mathbf{g}_{/\!/1}\mathbf{g}_{/\!/2}\mathrm{CC}} & H^{-1}_{\mathbf{g}_{/\!/1}\mathbf{g}_{/\!/2}\mathrm{CR}} \\ \hline H^{-1}_{\mathbf{g}_{/\!/1}\mathbf{g}_{/\!/2}\mathrm{RL}} & H^{-1}_{\mathbf{g}_{/\!/1}\mathbf{g}_{/\!/2}\mathrm{RC}} & H^{-1}_{\mathbf{g}_{/\!/1}\mathbf{g}_{/\!/2}\mathrm{RR}} \end{array}\right). \tag{1.324}$$

Since we only need the corner values, we do not obtain the inverse matrix. Instead, we solve simultaneous equations which give the corner values. The solving procedure gives the LU decomposition, we use it in the last process calculating Ψ. We can get the vertical vectors including $\psi_{\mathbf{g}_{/\!/}}(z_0)$ and $\psi_{\mathbf{g}_{/\!/}}(z_1)$ by the following equations;

$$\Big(\psi_{\mathbf{g}_{/\!/}}(z_0)\Big) = \Big(H^{-1}_{\mathbf{g}_{/\!/1}\mathbf{g}_{/\!/2}\mathrm{LL}}\Big)\Big(-g_{\mathbf{g}_{/\!/}}(z_0-h)/h^2\Big) + \Big(H^{-1}_{\mathbf{g}_{/\!/1}\mathbf{g}_{/\!/2}\mathrm{LR}}\Big)\Big(-\delta_{\mathbf{g}_{/\!/}\mathbf{0}}e^{\mathrm{i}k_z(z_1+h)}/h^2\Big) \tag{1.325}$$

$$\Big(g_{\mathbf{g}_{/\!/}}(z_1)\Big) = \Big(H^{-1}_{\mathbf{g}_{/\!/1}\mathbf{g}_{/\!/2}\mathrm{RL}}\Big)\Big(-\psi_{\mathbf{g}_{/\!/}}(z_0-h)/h^2\Big) + \Big(H^{-1}_{\mathbf{g}_{/\!/1}\mathbf{g}_{/\!/2}\mathrm{RR}}\Big)\Big(-\delta_{\mathbf{g}_{/\!/}\mathbf{0}}e^{\mathrm{i}k_z(z_1+h)}/h^2\Big). \tag{1.326}$$

They need to be equal to $\Big(B(z_0)\times\mathbf{a}\Big)$ and $\Big(\delta_{\mathbf{g}_{/\!/}\mathbf{0}}e^{\mathrm{i}k_z z_1}\Big)$ respectively. Therefore we need to solve

$$\Big[h^2B(z_0) + H^{-1}_{\mathrm{LL}}B(z_0-h)\Big]\mathbf{a} = -H^{-1}_{\mathrm{LR}}\Big(\delta_{\mathbf{g}_{/\!/}\mathbf{0}}e^{\mathrm{i}k_z(z_1+h)}\Big) \tag{1.327}$$

$$\Big[H^{-1}_{\mathrm{RL}}B(z_0-h)\Big]\mathbf{a} = -H^{-1}_{\mathrm{RR}}\Big(\delta_{\mathbf{g}_{/\!/}\mathbf{0}}e^{\mathrm{i}k_z(z_1+h)}\Big) - h^2\Big(\delta_{\mathbf{g}_{/\!/}\mathbf{0}}e^{\mathrm{i}k_z z_1}\Big). \tag{1.328}$$

However, the dimension of $\mathbf{a}$ is $\#n$ and is smaller than the dimension of the equations $2\#\mathbf{g}_{/\!/}$, we obtain the least norm solution. From the obtained $\mathbf{a}$ vector, we calculate $\psi_{\mathbf{g}_{/\!/}}(z_0-h) = B(z_0-h)\times\mathbf{a}$, and solve simultaneous equations to obtain Ψ.

Searching for bulk eigenstates

We discuss the distribution of the wavevector z component (k_z, κ_z) with the eigenenergy E_{kin}. First, when $\kappa_z = 0$ holds, all eigenvalues are real because $H_{\mathbf{g}_1\mathbf{g}_2}$ is Hermite. We can define continuous band dispersion, so we search for a band and a k_z value crossing E_{kin} and then define the precise position by the bisection method or the linear interpolation.

When $\kappa_z = 0$ does not hold, not all eigenvalues are real because the Hamiltonian matrix is not Hermite. Therefore we can not define the band index, so we can not apply the same strategy as we do for the real axis. Eigenvalues can be real when $k_z = 0$ holds, on the imaginary axis. In case of free electrons or constant potential, eigenstates are represented by single $\mathbf{g}$ being one and the other being zero, and eigenvalues are $|\mathbf{k}+\mathbf{g}|^2/2 = (|\mathbf{k}_{/\!/}+\mathbf{g}_{/\!/}|^2 + (g_z + k_z - \mathrm{i}\kappa_z)^2)/2$. They become real when $\kappa_z = 0$ (real axis) and $k_z = 0$ (imaginary axis). The latter needs another condition $g_z = 0$, and the eigenvalues become $(|\mathbf{k}_{/\!/}+\mathbf{g}_{/\!/}|^2 - \kappa_z^2)/2$. Therefore, the hole band dispersions appear on the imaginary axis. Next, we perturbatively change the potential to the realistic one. Then the change of eigenvalues is real, so the z component with the eigenvalue E_{kin} moves along the imaginary axis. Another case is when E_{kin} appears between the energy gap of nearly-free electron dispersion. The model Hamiltonian around the energy gap is

$$H(k) = \begin{pmatrix} ak & t \\ t & -ak \end{pmatrix}. \tag{1.329}$$

The eigenvalue equation is

$$E^2 = (ak)^2 + t^2, \tag{1.330}$$

so the eigenvalue becomes real when k is on the real axis or on the imaginary axis. The band dispersions along the real axis have an energy gap $2t$ and two bands connecting them appear on the imaginary axis. Such gapped dispersions appear frequently on the $k_z = 0$ and $k_z = \pm\pi/c$ axes and sometimes on arbitrary k_z. The former is investigated by calculating band dispersion with real eigenvalues for the $k_z = 0$ and $k_z = \pi/c$ axes and the latter is by searching around the energy gap minimum. In more detail, we discretize the complex plane $(k_z,\ \kappa_z)$ and calculate the determinant of $H_{\mathbf{g}_1\mathbf{g}_2} - E_{\mathrm{kin}}$ for the corners of a discretized cell. If the traces of determinants encloses zero, there is a wavevector with zero determinant, in other words, with $H_{\mathbf{g}_1\mathbf{g}_2}$ having eigenvalue E_{kin}. We apply the bisection method for cells and finish the search when the cell becomes small enough.

Solution by simultaneous equations

The Numerov method is unstable when $|\mathbf{k}_{/\!/}+\mathbf{g}_{/\!/}|^2/2 > E_{\rm kin}$ holds. To avoid it, we can solve the equation for whole elements of $\psi_{/\!/}(z)$. In this strategy, the boundary conditions at the lower edge are variables, and we tune them to satisfy the connection condition at the upper edge.

We represent the step along the z by h and the number of elements by N; $z_1 = (N-1)h$ holds. g represents the number of $\mathbf{g}_{/\!/}$'s. The vertical vector Ψ includes Ng elements;

$$\Psi_{\mathbf{g}_{/\!/}i} = \psi_{\mathbf{g}_{/\!/}}(hi). \tag{1.331}$$

The second derivative for Ψ becomes

$$\frac{\mathrm{d}^2\Psi(z)}{\mathrm{d}z} = \begin{pmatrix} & A_{\mathbf{g}_{/\!/1}\mathbf{g}_{/\!/2}} & \end{pmatrix} \begin{pmatrix} \\ \Psi \\ \\ \end{pmatrix} + \begin{pmatrix} \psi_{\mathbf{g}_{/\!/}}(-h)/h^2 \\ 0 \\ \delta_{\mathbf{g}_{/\!/}\mathbf{0}} e^{\mathrm{i}k_z(z_0+h)}/h^2 \end{pmatrix} \tag{1.332}$$

$$A_{\mathbf{g}_{/\!/1}\mathbf{g}_{/\!/2}} = \frac{\delta_{\mathbf{g}_{/\!/1}\mathbf{g}_{/\!/2}}}{h^2} \begin{pmatrix} -2 & 1 & & & & \\ 1 & -2 & 1 & & & \\ & 1 & \ddots & \ddots & & \\ & & \ddots & 1 & -2 & 1 \\ & & & & 1 & -2 \end{pmatrix}. \tag{1.333}$$

Therefore, the differential equation can be rearranged to

$$\begin{pmatrix} & A_{\mathbf{g}_{/\!/1}\mathbf{g}_{/\!/2}} + M_{\mathbf{g}_{/\!/1}\mathbf{g}_{/\!/2}} & \end{pmatrix} \begin{pmatrix} \\ \Psi_{\mathbf{g}_{/\!/}} \\ \\ \end{pmatrix} = \begin{pmatrix} -\psi_{\mathbf{g}_{/\!/}}(-h)/h^2 \\ 0 \\ -\delta_{\mathbf{g}_{/\!/}\mathbf{0}} e^{\mathrm{i}k_z(z_0+h)}/h^2 \end{pmatrix} \tag{1.334}$$

$$M_{\mathbf{g}_{/\!/1}\mathbf{g}_{/\!/2}} = \delta_{\mathbf{g}_{/\!/1}\mathbf{g}_{/\!/2}}(2E_{\rm kin} - |\mathbf{k}+\mathbf{g}_{/\!/}|^2)I - 2V_{\mathbf{g}_{/\!/1}\mathbf{g}_{/\!/2}}(hi). \tag{1.335}$$

The right hand side represents boundary condition at the upper edge $z = z_1 + h$ and the lower edge $z = -h$.

We represent the inverse matrix of $A_{\mathbf{g}_{/\!/1}\mathbf{g}_{/\!/2}} + M_{\mathbf{g}_{/\!/1}\mathbf{g}_{/\!/2}}$ by H^{-1} and divide it into upper edge, lower edge, and center;

$$H^{-1} = \left(\begin{array}{c|c|c} H^{-1}_{\mathbf{g}_{/\!/1}\mathbf{g}_{/\!/2}\mathrm{LL}} & H^{-1}_{\mathbf{g}_{/\!/1}\mathbf{g}_{/\!/2}\mathrm{LC}} & H^{-1}_{\mathbf{g}_{/\!/1}\mathbf{g}_{/\!/2}\mathrm{LR}} \\ \hline H^{-1}_{\mathbf{g}_{/\!/1}\mathbf{g}_{/\!/2}\mathrm{CL}} & H^{-1}_{\mathbf{g}_{/\!/1}\mathbf{g}_{/\!/2}\mathrm{CC}} & H^{-1}_{\mathbf{g}_{/\!/1}\mathbf{g}_{/\!/2}\mathrm{CR}} \\ \hline H^{-1}_{\mathbf{g}_{/\!/1}\mathbf{g}_{/\!/2}\mathrm{RL}} & H^{-1}_{\mathbf{g}_{/\!/1}\mathbf{g}_{/\!/2}\mathrm{RC}} & H^{-1}_{\mathbf{g}_{/\!/1}\mathbf{g}_{/\!/2}\mathrm{RR}} \end{array}\right). \tag{1.336}$$

We solve simultaneous equations which give $H^{-1}_{\mathbf{g}_{/\!/1}\mathbf{g}_{/\!/2}\mathrm{RL}} \succeq H^{-1}_{\mathbf{g}_{/\!/1}\mathbf{g}_{/\!/2}\mathrm{RR}}$. The solving process gives the LU decomposition; we use it at the last procedure obtaining $\psi_{\mathbf{g}_{/\!/}}$. The vertical vector containing $\psi_{\mathbf{g}_{/\!/}}(z_0)$ can be calculated from

$$\left(\psi_{\mathbf{g}_{/\!/}}(z_0)\right) = \left(H^{-1}_{\mathbf{g}_{/\!/1}\mathbf{g}_{/\!/2}\mathrm{RL}}\right)\left(-\psi_{\mathbf{g}_{/\!/}}(-h)/h^2\right) + \left(H^{-1}_{\mathbf{g}_{/\!/1}\mathbf{g}_{/\!/2}\mathrm{RR}}\right)\left(-\delta_{\mathbf{g}_{/\!/}\mathbf{0}} e^{\mathrm{i}k_z(z_0+h)}/h^2\right). \tag{1.337}$$

Since it need to be equal to $\left(\delta_{\mathbf{g}_{/\!/}\mathbf{0}} e^{\mathrm{i}k_z z_0}\right)$, the equation is

$$\left(H^{-1}_{\mathbf{g}_{/\!/1}\mathbf{g}_{/\!/2}\mathrm{RL}}\right)\left(\psi_{\mathbf{g}_{/\!/}}(-h)\right) = \left(H^{-1}_{\mathbf{g}_{/\!/1}\mathbf{g}_{/\!/2}\mathrm{RR}}\right)\left(-\delta_{\mathbf{g}_{/\!/}\mathbf{0}} e^{\mathrm{i}k_z(z_0+h)}\right) + \left(-\delta_{\mathbf{g}_{/\!/}\mathbf{0}} e^{\mathrm{i}k_z z_0} h^2\right). \tag{1.338}$$

We set $\psi_{\mathbf{g}_{/\!/}}(-h) = 0$ if $\mathbf{g}_{/\!/}$ satisfies $|\mathbf{k}_{/\!/}+\mathbf{g}_{/\!/}|^2/2 > E_{\rm kin}$ because wave function components can not exist in vacuum. Since the dimension of the simultaneous equations is larger than the number of variables, we obtain the least norm solution. From the obtained $\left(\psi_{\mathbf{g}_{/\!/}}(-h)\right)$, we calculate the solution $\psi_{\mathbf{g}_{/\!/}}$.

1.4.4 Wave function in the region with the non-local terms

Lebedev integral

Since the non-local terms affect near the nuclei, the potential is supposed to be isotropic. Therefore we sometimes need to calculate the spherical integral

$$I = \int_0^{\pi} \sin\theta \mathrm{d}\theta \int_0^{2\pi} \mathrm{d}\varphi \; f(\theta,\varphi). \tag{1.339}$$

It can be calculated precisely by the Lebedev integral

$$I = 4\pi \sum_{i}^{N} w_i f(\mathbf{r}_i). \tag{1.340}$$

The number of sampling points N is associated with the precision. The weight coefficients are calculated up to $N = 5810$ [25]。

Schrödinger equation

We can suppose that the local potential is isotropic. In this case, the Schrödinger equation is also isotropic, so the solutions can be represented by spherical harmonics;

$$\psi_{\mathrm{sol}}(\mathbf{r}) = \sum_{lm} \frac{P_{lm}(r)}{r} Y_{lm}(\theta, \varphi). \tag{1.341}$$

The radial Schrödinger equation becomes

$$\left[-\frac{1}{2}\frac{\mathrm{d}^2}{\mathrm{d}r^2} + \frac{l(l+1)}{2r^2} + V(r) + \sum_{p} \lambda_{pl} |\beta_{pl}\rangle\langle\beta_{pl}| \right] P_{lm}(r) = E_{\mathrm{kin}} P_{lm}(r). \tag{1.342}$$

$V(r)$ represents the averaged local potential. The boundary condition is $P_{lm}(0) = 0$ and the connection at the cutoff position $r = r_c$.[4] The latter is determined by integrating $\psi_{\mathrm{sol}}(\mathbf{r})$ and spherical harmonics at $r = r_c$;

$$P_{lm}(r_c) = r_c \int_0^{\pi} \sin\theta \mathrm{d}\theta \int_0^{2\pi} \mathrm{d}\varphi \; Y^*_{lm}(\theta, \varphi) \psi_{\mathrm{sol}}(r_c, \theta, \varphi). \tag{1.343}$$

Since the differential equation is linear and homogeneous, we can suppose $P_{lm}(r_c) = \text{const.}$ when we obtain the solution $P_l(r)$.[5] After that, we multiply something to satisfy the boundary condition. We calculate wave function up to $l = 4$ because ground states include at most $l = 3$.

We derive the formula to calculate $P^{\mathrm{loc}}_{lm}(r_c)$;

$$P^{\mathrm{loc}}_{lm}(r_c) = r_c \int_0^{\pi} \sin\theta \mathrm{d}\theta \int_0^{2\pi} \mathrm{d}\varphi \; Y^*_{lm}(\theta, \varphi) \psi_{\mathrm{sol}}(\mathbf{r}). \tag{1.344}$$

We note that the polar coordinate center is $\boldsymbol{\tau}_i$. Inserting the Fourier-expanded form of $\psi_{\mathrm{sol}}(\mathbf{r})$, we get

$$P^{\mathrm{loc}}_{lm}(r_c) = r_c \int_0^{\pi} \sin\theta \mathrm{d}\theta \int_0^{2\pi} \mathrm{d}\varphi Y^*_{lm}(\theta, \varphi) \sum_{\mathbf{G}} f_{\mathbf{G}}(z) e^{\mathrm{i}(\mathbf{k}+\mathbf{G})\cdot(\mathbf{r}_{//}+\boldsymbol{\tau}_i)}. \tag{1.345}$$

After applying the partial wave expansion

$$e^{\mathrm{i}(\mathbf{k}+\mathbf{G})\mathbf{r}} = 4\pi \sum_{l'm'} \mathrm{i}^{l'} j_{l'}(kr) Y^*_{l'm'}((\hat{\mathbf{k}+\mathbf{G}})) Y_{l'm'}(\theta, \varphi), \quad k = |\mathbf{k}+\mathbf{G}|, \tag{1.346}$$

only the $m = m'$ terms remain. Therefore, we get

$$P^{\mathrm{loc}}_{lm}(r_c) = 4\pi r_c \sum_{\mathbf{G}l'} e^{\mathrm{i}(\mathbf{k}+\mathbf{G})\boldsymbol{\tau}_i} \mathrm{i}^{l'} j_{l'}(kr_c) Y^*_{l'm}((\hat{\mathbf{k}+\mathbf{G}})) \int_0^{\pi} \sin\theta f_{\mathbf{G}}(\tau_z + r_c\cos\theta) \Theta_{l'm}(\theta) \Theta_{lm}(\theta) \mathrm{d}\theta. \tag{1.347}$$

To judge the reproducibility of wave function $\psi_{\mathrm{sol}}(r_c, \theta, \varphi)$ by $P^{\mathrm{loc}}_{lm}(r_c)$'s up to $l = 4$, we can use the norm ratio N.

$$N = N_1/N_2 \tag{1.348}$$

$$N_1 = \int_0^{\pi} \sin\theta \mathrm{d}\theta \int_0^{2\pi} \mathrm{d}\varphi \sum_{l'm'} Y^*_{l'm'}(\theta, \varphi) \frac{P^{*\mathrm{loc}}_{l'm'}(r_c)}{r_c} \cdot \sum_{lm} Y_{lm}(\theta, \varphi) \frac{P^{\mathrm{loc}}_{lm}(r_c)}{r_c} \tag{1.349}$$

$$N_2 = \int_0^{\pi} \sin\theta \mathrm{d}\theta \int_0^{2\pi} \mathrm{d}\varphi \sum_{\mathbf{G}'} f^*_{\mathbf{G}'}(z) e^{-\mathrm{i}(\mathbf{k}+\mathbf{G}')\cdot(\mathbf{r}_{//}+\boldsymbol{\tau}_i)} \cdot \sum_{\mathbf{G}} f_{\mathbf{G}}(z) e^{\mathrm{i}(\mathbf{k}+\mathbf{G})\cdot(\mathbf{r}_{//}+\boldsymbol{\tau}_i)} \tag{1.350}$$

[4]The cutoff position can depend on p. We use the longest cutoff position

[5]We omit the suffix m because this boundary condition is independent of m.

For N_1, the orthogonality of spherical harmonics extinguishes terms other than the $l' = l,\ m' = m$ terms, then we get

$$N_1 = \sum_{lm} \frac{|P_{lm}^{\mathrm{loc}}(r_c)|^2}{r_c^2}. \tag{1.351}$$

N_2 can be rearranged by the partial wave expansion;

$$\begin{aligned} N_2 = \sum_{\mathbf{G}\mathbf{G}'ll'm} & 16\pi^2 \mathrm{i}^{l-l'} j_{l'}(k'r) j_l(kr) Y_{l'm}((\mathbf{k} + \hat{\mathbf{G}'})) Y_{lm}^*((\mathbf{k} + \hat{\mathbf{G}})) e^{\mathrm{i}(\mathbf{G}-\mathbf{G}')\boldsymbol{\tau}_i} \\ & \int_0^\pi \sin\theta f_{\mathbf{G}'}^*(\tau_z + r\cos\theta) f_{\mathbf{G}}(\tau_z + r\cos\theta) \Theta_{l'm}(\theta) \Theta_{lm}(\theta) \mathrm{d}\theta \end{aligned} \tag{1.352}$$

$$k' = |\mathbf{k} + \mathbf{G}'|,\ k = |\mathbf{k} + \mathbf{G}|. \tag{1.353}$$

Solution by simultaneous equations

First, we need to transform the Schrödinger equation to adjust the logarithmic lattice $r = e^x$, used in the potential term. Derivatives of $f(r) = f(e^x)$ with respect to x are

$$\frac{\mathrm{d}}{\mathrm{d}x} f(e^x) = \left.\frac{\mathrm{d}}{\mathrm{d}r} f(r)\right|_{r=e^x} \cdot e^x \tag{1.354}$$

$$\frac{\mathrm{d}^2}{\mathrm{d}x^2} f(e^x) = \left.\frac{\mathrm{d}^2}{\mathrm{d}r^2} f(r)\right|_{r=e^x} \cdot e^{2x} + \left.\frac{\mathrm{d}}{\mathrm{d}r} f(r)\right|_{r=e^x} \cdot e^x. \tag{1.355}$$

From these equations, we get

$$\left.\frac{\mathrm{d}^2}{\mathrm{d}r^2} f(r)\right|_{r=e^x} = \frac{1}{r^2}\left[\frac{\mathrm{d}^2}{\mathrm{d}x^2} f(e^x) - \frac{\mathrm{d}}{\mathrm{d}x} f(e^x)\right]. \tag{1.356}$$

Inserting the result into equation (1.342), we get

$$\left[\frac{\mathrm{d}^2}{\mathrm{d}x^2} - \frac{\mathrm{d}}{\mathrm{d}x} - \Big(l(l+1) + 2r^2(V(r) - E_{\mathrm{kin}})\Big) - 2r^2 \sum_p \lambda_{pl} |\beta_{pl}\rangle\langle\beta_{pl}|\right] P_l(r) = 0. \tag{1.357}$$

While the $l(l+1)/r^2$ term in equation (1.342) is unstable near $r = 0$, we could successfully remove it. We note that the equation is independent of the wavevector $\mathbf{k}$; it only depends on the kinetic energy E_{kin}. Also, we note that the projector operator $|\beta_{pl}\rangle$ does not include the r^2 term, which is necessary for the polar axis integration. Since $P_l(r) = rR_l(r)$ includes a r term, we need to multiply r to $|\beta_{pl}\rangle$ before the integration.

The differential equation can be solved as simultaneous equations. The wave function is transformed to the vertical vector $\Psi_i = P_l(r_i)$ $(i = 0,\ \cdots,\ N-1)$, satisfying the boundary condition $P_l(0) = 0$. We can suppose $P_l(r_N) = 1$ due to the linearity and homogeneity of the equation. We can construct the

simultaneous equation matrix from the following relations;

$$\frac{\mathrm{d}^2}{\mathrm{d}x^2}P_l(r) = \frac{1}{\Delta x^2}\begin{pmatrix} -2 & 1 & & & & & \\ 1 & -2 & 1 & & & & \\ & & \ddots & & & & \\ & & & 1 & -2 & 1 \\ & & & & 1 & -2 \end{pmatrix}\begin{pmatrix} P_l(r_0) \\ P_l(r_1) \\ \vdots \\ P_{lm}(r_{N-2}) \\ P_{lm}(r_{N-1}) \end{pmatrix} + \begin{pmatrix} 0 \\ 0 \\ \vdots \\ 0 \\ 1/\Delta x^2 \end{pmatrix} \tag{1.358}$$

$$\frac{\mathrm{d}}{\mathrm{d}x}P_{lm}(r) = \frac{1}{2\Delta x}\begin{pmatrix} 0 & 1 & & & & & \\ -1 & 0 & 1 & & & & \\ & & \ddots & & & & \\ & & & -1 & 0 & 1 \\ & & & & -1 & 0 \end{pmatrix}\begin{pmatrix} P_l(r_0) \\ P_l(r_1) \\ \vdots \\ P_l(r_{N-2}) \\ P_l(r_{N-1}) \end{pmatrix} + \begin{pmatrix} 0 \\ 0 \\ \vdots \\ 0 \\ 1/\Delta x \end{pmatrix} \tag{1.359}$$

$$\Big(l(l+1) + 2r^2(V(r) - E_{\mathrm{kin}})\Big)P_l(r) = \mathrm{diag}\Big(l(l+1) + 2r_i^2(V(r_i) - E_{\mathrm{kin}})\Big)\begin{pmatrix} P_l(r_0) \\ P_l(r_1) \\ \vdots \\ P_l(r_{N-2}) \\ P_l(r_{N-1}) \end{pmatrix} \tag{1.360}$$

$$2r^2\sum_p \lambda_{pl}|\beta_{pl}\rangle\langle\beta_{pl}|P_l(r) = \sum_p \begin{pmatrix} 2r_0^2\lambda_{pl}\beta_{pl,0} \\ \vdots \\ 2r_{N-1}^2\lambda_{pl}\beta_{pl,N-1} \end{pmatrix}\begin{pmatrix} \beta_{pl,0}\Delta r_0 \dots \beta_{pl,N-1}\Delta r_{N-1} \end{pmatrix}\begin{pmatrix} P_l(r_0) \\ P_l(r_1) \\ \vdots \\ P_l(r_{N-2}) \\ P_l(r_{N-1}) \end{pmatrix} \tag{1.361}$$

$$\Delta x = x_i - x_{i-1} = \log r_i - \log r_{i-1} \tag{1.362}$$

$$\Delta r_i = r_i - r_{i-1} \quad (r_{-1} = 0). \tag{1.363}$$

1.5 Photoemission angular distribution calculations

We explain the method to calculate the matrix element of the photoemission based on the one-electron approximation and dipole approximation.

1.5.1 Overview

In the photoemission process, the perturbation Hamiltonian due to the light irradiation $\delta H(t)$ is

$$\delta H(t) = \frac{1}{2}(\hat{\mathbf{p}} \cdot \mathbf{A}(t) + \mathbf{A}(t) \cdot \hat{\mathbf{p}}) \tag{1.364}$$

$$= \frac{A_0}{2}(\hat{\mathbf{p}} \cdot \mathbf{e}e^{\mathrm{i}\mathbf{k}^{\mathrm{L}}\cdot\mathbf{r}} + \mathbf{e}e^{\mathrm{i}\mathbf{k}^{\mathrm{L}}\cdot\mathbf{r}} \cdot \hat{\mathbf{p}})e^{-\mathrm{i}\omega t} \tag{1.365}$$

$$= \delta H e^{-\mathrm{i}\omega t}, \tag{1.366}$$

where $\hat{\mathbf{p}}$ is the momentum operator, $\mathbf{A}(t)$ the vector potential of the light, $\mathbf{e}$ a unit vector representing the polarization, $\mathbf{k}^{\mathrm{L}}$ the wavevector of the light, and ω is the angular frequency of the light. We represent the time-independent part of the perturbation by δH as used in Eq. (1.366). According to Fermi's golden rule, the excitation probability by the perturbation is

$$p(|\psi^{\mathrm{I}}\rangle \to |\psi^{\mathrm{F}}\rangle) = 2\pi\delta(E^{\mathrm{F}} - E^{\mathrm{I}} - \omega)\left|\langle\psi^{\mathrm{F}}|\delta H|\psi^{\mathrm{I}}\rangle\right|^2, \tag{1.367}$$

where $|\psi^{\mathrm{I}}\rangle$ and E^{I} are the wave function and the eigenenergy for the initial state, $|\psi^{\mathrm{F}}\rangle$ and E^{F} are those for the final state, and the delta function represents the energy conservation law. Therefore, we need to obtain initial and final states and a perturbation term due to the light electric field to calculate the matrix element in the excitation probability equation.

1.5.2 Initial states

An initial state is a Bloch state with a wavevector $\mathbf{k}$ and a band index μ and is represented by a linear combination of pseudo-atomic orbitals (LCAO) in OpenMX;

$$\psi_\mu^{(\mathbf{k})}(\mathbf{r}) = \frac{1}{\sqrt{N}}\sum_n^N e^{\mathrm{i}\mathbf{R}_n\cdot\mathbf{k}}\sum_{i\alpha\sigma} c_{\mu,i\alpha}^{\sigma(\mathbf{k})}\phi_{i\alpha}(\mathbf{r} - \boldsymbol{\tau}_i - \mathbf{R}_n)|\sigma\rangle. \tag{1.368}$$

In the equation above, $\mathbf{R}_n$ is a lattice vector, i an atom position index, $\alpha = (plm)$ an organized orbital index with the multiplicity index p, angular quantum number l, and magnetic quantum number m, σ ($\uparrow$ or $\downarrow$) a spin index, $\phi(\mathbf{r})$ a pseudo-atomic orbital, and $\boldsymbol{\tau}_i$ an atom position vector. In this paper, the Bloch wavevector $\mathbf{k}$ is in the extended zone scheme. We distinguish an imaginary unit i and an index i by capital and italic letters, respectively. $c_{\mu,i\alpha}^{\sigma(\mathbf{k})}$ is an LCAO coefficient of the wave function and can be directly obtained from OpenMX. See Sec. 2.1 for the details of the pseudo-atomic orbitals.

1.5.3 Final States

A final state, the wavefunction of a photoelectron, is roughly a plane wave, but it should be modified inside a solid crystal.

First, we discuss it based on the three-step model [18]. In the three-step model, the wave function is supposed to have a wavevector $\mathbf{k}$ even in a solid; within this assumption, the eigenenergy and the wave function shape are modified. First, the eigenenergy of the final state with the wavevector $\mathbf{k}$ becomes $\frac{1}{2}|\mathbf{k}|^2 - V_0$, where V_0 is the inner potential of the material. The dispersion of final states should be considered when we determine possible $\mathbf{k}$ values where the photoemission occurs based on the energy conservation law. Second, atomic potentials can change the eigenstate from a simple plane wave to a plane wave plus an ingoing spherical wave [23]. The modification details are discussed after the derivation of the matrix element equation. At last, the wave functions of final states can rapidly decay into the bulk when we consider the surface sensitivity of ARPES measurements [20].

If the three-step model is not adopted, the wave function is determined from the kinetic energy and the Schrödinger equation. In a vacuum, plane waves are eigenstates with eigenenergy $\frac{1}{2}|\mathbf{k}|^2$. The in-plane wavevector can differ only by reciprocal vectors. However, this condition and the energy conservation law can not determine the wavevectors included in the wave function. The amplitude of the photoelectron

wave packet with momentum $\hbar\mathbf{k}$ is associated with the matrix element calculated using the wave function which is a plane wave with the reciprocal vector $\mathbf{k}$ in a vacuum [24]. Therefore, such an eigenstate is adopted in the calculation. The wave function in a solid is determined to connect to the wave function in a vacuum. At last, the decay related to surface sensitivity is applied.

1.5.4 Perturbation term

As discussed, the perturbation term due to the electric field is like Eq. 1.365. Since the initial state is a linear combination of localized PAOs or AOs, we can approximate $e^{\mathrm{i}\mathbf{k}^{\mathrm{L}}\cdot\mathbf{r}}$ by $e^{\mathrm{i}\mathbf{k}^{\mathrm{L}}\cdot(\boldsymbol{\tau}_i+\mathbf{R}_n)}$, where $\boldsymbol{\tau}_i+\mathbf{R}_n$ is the position of the ith atom. This constant is neglected because $\mathbf{k}^{\mathrm{L}}$ is much smaller than $\mathbf{k}$. By this dipole approximation and the relation $\hat{\mathbf{p}}=\frac{\mathrm{d}}{\mathrm{d}t}\hat{\mathbf{r}}$, we get

$$p(|\psi^{\mathrm{I}}\rangle\to|\psi^{\mathrm{F}}\rangle)=2\pi\delta(E^{\mathrm{F}}-E^{\mathrm{I}}-\omega)(A_0\omega)^2\left|\langle\psi^{\mathrm{F}}|\mathbf{r}\cdot\mathbf{e}|\psi^{\mathrm{I}}\rangle\right|^2. \tag{1.369}$$

Whatever the light polarization is, the $\mathbf{r}\cdot\mathbf{e}$ term can be represented by the linear combination of $rY_{1j}(\theta,\ \varphi)$ like $\mathbf{r}\cdot\mathbf{e}=\sum_{j=-1}^{1}e_j rY_{1j}(\theta,\ \varphi)$, where e_j are coefficients depending on the light polarization and direction.

We note that the position operator in the dipole $\mathbf{r}\cdot\mathbf{e}$ represents the position from each atomic origin. Although this modification neglects the $\boldsymbol{\tau}_i\cdot\mathbf{e}$ term, the matrix element becomes independent of the origin selection.

1.5.5 Matrix element calculation (three-step model)

Since initial states are decomposed into atomic orbitals centered at $\boldsymbol{\tau}_i+\mathbf{R}+n$, we calculate the matrix element for each orbital and sum it up. The sum with respect to $\mathbf{R}_n$ gives the momentum conservation law; the matrix element can be nonzero if the initial and final state wavevectors are different only by a reciprocal vector. In the extended zone scheme, we can limit ourselves to the case where both wavevectors are identical.

At this point, we introduce atomic potentials on final states to calculate the matrix element. When we calculate it for an orbital centered at $\boldsymbol{\tau}_i+\mathbf{R}_n$, we set the origin of the polar coordinate system at $\boldsymbol{\tau}_i+\mathbf{R}_n$, for an easier understanding of equations. The wave function of the orbital specified by $\alpha=(plm)$ is

$$\phi^{(\mathbf{k})\mathrm{I}}_{\alpha in}(\mathbf{r})=e^{i\mathbf{k}\cdot\mathbf{R}_n}Y_{lm}(\theta,\ \varphi)\frac{P^{\mathrm{I}}_{ipl}(r)}{r}. \tag{1.370}$$

The plane wave, a final state neglecting the atomic potential, is

$$\psi^{(\mathbf{k})\mathrm{F}}_{in}(\mathbf{r})=4\pi e^{\mathrm{i}\mathbf{k}\cdot(\boldsymbol{\tau}_i+\mathbf{R}_n)}\sum_{l'm'}\mathrm{i}^{l'}Y^*_{l'm'}(\hat{\mathbf{k}})Y_{l'm'}(\theta,\ \varphi)j_{l'}(kr). \tag{1.371}$$

In the equation, the partial wave expansion is applied, $\hat{\mathbf{k}}$ represents the angles θ and φ of the vector $\mathbf{k}$, $j_l(x)$ is the spherical Bessel function, and k is equal to $|\mathbf{k}|$. When the potential $V_{\mathrm{at}}(r)$ is taken into account, the modified final state becomes the sum of the plane wave and an ingoing spherical wave like

$$\psi^{(\mathbf{k})\mathrm{F}}_{in}(\mathbf{r})=4\pi e^{\mathrm{i}\mathbf{k}\cdot(\boldsymbol{\tau}_i+\mathbf{R}_n)}\sum_{l'm'}\mathrm{i}^{l'}e^{-\mathrm{i}\delta_{il'}}Y^*_{l'm'}(\hat{\mathbf{k}})Y_{l'm'}(\theta,\ \varphi)\frac{P^{\mathrm{F}}_{il'}(r)}{r}. \tag{1.372}$$

Derivation of the above form is as follows. We can assume that $V_{\mathrm{at}}(r)$ is very localized around $r=0$ due to the screening effect of valence electrons. Therefore, we define r_0 so that $V_{\mathrm{at}}(r)=0$ if $r>r_0$ and the radial wave function outside of r_0 should have the following asymptotic form;

$$P^{\mathrm{F}}_{il'}(r)\to\frac{1}{k}\sin(kr-l\pi/2+\delta_{il'}). \tag{1.373}$$

The asymptotic form without $\delta_{il'}$ is identical to that of $rj_{l'}(kr)$, the solution without $V_{\mathrm{at}}(r)$. The Schrödinger equation with $V_{\mathrm{at}}(r)$ gives $P^{\mathrm{F}}_{il'}(r)$, and the phase shift $\delta_{il'}$ is determined by the behavior of $P^{\mathrm{F}}_{il'}(r)$ at large r (Eq. 1.373). The $e^{-\mathrm{i}\delta_{il'}}$ term is multiplied to remove outgoing spherical waves.

The integration of the initial state, the final state, and the perturbation term can be separated into the spherical harmonics part and the radial part. The spherical harmonics part is the integration of

$Y^*_{l'm'}Y_{1j}Y_{lm}$, and the integral becomes nonzero when $l' = l \pm 1$ and $m' = m + j$ are satisfied [21].

$$\int Y^*_{l+1,m}Y_{1,0}Y_{lm}\sin\theta \mathrm{d}\theta\mathrm{d}\varphi = \sqrt{\frac{3}{4\pi}}\sqrt{\frac{(l+1)^2-m^2}{(2l+3)(2l+1)}} \tag{1.374}$$

$$\int Y^*_{l-1,m}Y_{1,0}Y_{lm}\sin\theta \mathrm{d}\theta\mathrm{d}\varphi = \sqrt{\frac{3}{4\pi}}\sqrt{\frac{l^2-m^2}{(2l-1)(2l+1)}} \tag{1.375}$$

$$\int Y^*_{l+1,m+1}Y_{1,1}Y_{lm}\sin\theta \mathrm{d}\theta\mathrm{d}\varphi = \sqrt{\frac{3}{4\pi}}\sqrt{\frac{(l+m+2)(l+m+1)}{2(2l+3)(2l+1)}} \tag{1.376}$$

$$\int Y^*_{l-1,m+1}Y_{1,0}Y_{lm}\sin\theta \mathrm{d}\theta\mathrm{d}\varphi = -\sqrt{\frac{3}{4\pi}}\sqrt{\frac{(l-m)(l-m-1)}{2(2l-1)(2l+1)}} \tag{1.377}$$

$$\int Y^*_{l+1,m-1}Y_{1,-1}Y_{lm}\sin\theta \mathrm{d}\theta\mathrm{d}\varphi = \sqrt{\frac{3}{4\pi}}\sqrt{\frac{(l-m+2)(l-m+1)}{2(2l+3)(2l+1)}} \tag{1.378}$$

$$\int Y^*_{l-1,m-1}Y_{1,-1}Y_{lm}\sin\theta \mathrm{d}\theta\mathrm{d}\varphi = -\sqrt{\frac{3}{4\pi}}\sqrt{\frac{(l+m)(l+m-1)}{2(2l-1)(2l+1)}} \tag{1.379}$$

This integral is related to the Gaunt coefficient [6], and we denote it as $g(l',\ m+j;\ l,\ m)$. The radial part is numerically calculated.

Summing up the integral over $\boldsymbol{\tau}_i$, $\mathbf{R}_n$, and α, we finally obtain

$$\langle\psi^{(\mathbf{k})\mathrm{F}}_\sigma|\mathbf{r}\cdot\mathbf{e}|\psi^{(\mathbf{k})\mathrm{I}}_\mu\rangle = 4\pi\sqrt{N}\sum_{i\alpha}\sum_{l'}^{l\pm1}\sum_{j=-1}^{1}(-\mathrm{i})^{l'}Y_{l',m+j}(\hat{\mathbf{k}})e^{\mathrm{i}(\delta_{il'}-\mathbf{k}\cdot\boldsymbol{\tau}_i)}e_j c^{\sigma(\mathbf{k})}_{\mu,i\alpha}g(l',\ m{+}j;\ l,\ m)\int_0^\infty rP^{\mathrm{F}}_{il'}(r)P^{\mathrm{I}}_{ipl}(r)\mathrm{d}r. \tag{1.380}$$

Neglecting the $4\pi\sqrt{N}$ term in the beginning, we use the norm of the matrix element to draw the PAD. Since the final states are spin-degenerated, we can calculate the matrix element for each spin separately.

Since it is difficult to calculate the screened potential in solids, we instead use wave functions of excited states in an atom as discussed in Sec. 1.2. Since the potential becomes $-1/r$ at large r, the asymptotic form is slightly changed to

$$P_{il}(r) \to \frac{1}{k}\sin(kr - l\pi/2 + \log(2kr)/k + \delta_{il}). \tag{1.381}$$

The asymptotic form is similar to that of the Coulomb wave function (see Sec. 1.3.3 for the details).

1.5.6 Matrix element calculation (not three-step model)

The matrix element calculation is performed using the polar coordinate system with each atom position being the center.

Region without the non-local term

Atomic orbital specified by the position $\boldsymbol{\tau}_i + \mathbf{R}_n$ and orbital $\alpha = (plm)$ is

$$\phi^{(\mathbf{k})\mathrm{I}}_{\alpha in} = e^{\mathrm{i}\mathbf{R}_n\cdot\mathbf{k}}Y_{lm}(\theta,\ \varphi)\frac{P^{\mathrm{I}}_{ipl}(r)}{r}. \tag{1.382}$$

The final state wave function in the region without the non-local term ($r > r_c$) is

$$\psi^{(\mathbf{k})\mathrm{F}}_{\mathrm{loc}} = \sum_{\mathbf{g}}\psi_{\mathbf{g}_{/\!/}}(r\cos\theta + \tau_z)e^{\mathrm{i}(\mathbf{k}_{/\!/}+\mathbf{g}_{/\!/})\cdot(\mathbf{r}+\boldsymbol{\tau}_i+\mathbf{R}_n)}, \tag{1.383}$$

where the polar coordinate center is $\boldsymbol{\tau}_i + \mathbf{R}_n$. The sum with respect to n becomes constant because $\mathbf{g}_{/\!/}\cdot\mathbf{R}_n = 2m\pi$ holds. Therefore, the matrix element is

$$\langle\psi^{\mathrm{F}}|\mathbf{r}\cdot\mathbf{e}|\phi^{\mathrm{I}}_{\alpha in}\rangle = \sqrt{N}\sum_{\mathbf{g}_{/\!/}j}e_j e^{-\mathrm{i}(\mathbf{k}_{/\!/}+\mathbf{g}_{/\!/})\boldsymbol{\tau}_i}\int_{r_c}^\infty\mathrm{d}r\int_0^\pi\mathrm{d}\theta\int_0^{2\pi}\mathrm{d}\varphi r^2\sin\theta \\ e^{-\mathrm{i}(\mathbf{k}_{/\!/}+\mathbf{g}_{/\!/})\mathbf{r}_{/\!/}}\psi^*_{\mathbf{g}_{/\!/}}(r\cos\theta+\tau_z)Y_{1j}(\theta,\ \varphi)Y_{lm}(\theta,\ \varphi)P^{\mathrm{I}}_{ipl}(r). \tag{1.384}$$

Using the partial wave expansion for a plane wave $e^{\mathrm{i}(\mathbf{k}_{/\!/}+\mathbf{g}_{/\!/})\mathbf{r}_{/\!/}}$, we get

$$e^{\mathrm{i}(\mathbf{k}_{/\!/}+\mathbf{g}_{/\!/})\mathbf{r}_{/\!/}} = 4\pi \sum_{l'm'} \mathrm{i}^{l'} j_{l'}(kr) Y^*_{l'm'}((\mathbf{k}_{/\!/} \hat{+} \mathbf{g}_{/\!/})) Y_{l'm'}(\theta,\ \varphi), \quad k = |\mathbf{k}_{/\!/} + \mathbf{g}_{/\!/}|. \tag{1.385}$$

Therefore, the integration with respect to φ becomes nonzero when $m' = m + j$ holds. Neglecting the constant term $4\pi\sqrt{N}$, finally we get

$$\begin{aligned}\langle \psi^{\mathrm{F}} | \mathbf{r}\cdot\mathbf{e} | \phi^{\mathrm{I}}_{\alpha i n} \rangle = \sum_{\mathbf{G}jl'} \frac{(-\mathrm{i})^{l'}}{\sqrt{2\pi}} e_j e^{-\mathrm{i}(\mathbf{k}_{/\!/}+\mathbf{g}_{/\!/})\boldsymbol{\tau}_i} Y_{l'm'}((\mathbf{k}_{/\!/} \hat{+} \mathbf{g}_{/\!/})) \\ \int_{r_c}^{\infty} \mathrm{d}r \int_0^{\pi} \mathrm{d}\theta r^2 j_{l'}(kr) P^{\mathrm{I}}_{ipl}(r) \psi^*_{\mathbf{g}_{/\!/}}(r\cos\theta + \tau_z) \Theta_{l'm'}(\theta) \Theta_{1j}(\theta) \Theta_{lm}(\theta) \sin\theta.\end{aligned} \tag{1.386}$$

In this integration, we use the pseudo-atomic orbital because it is identical to the atomic orbital outside of the cutoff.

We define the spherical Bessel function at $r = 0$ by

$$j_l(0) = \delta_{l0}, \tag{1.387}$$

because the partial wave expansion in the $\mathbf{k}_{/\!/} + \mathbf{g}_{/\!/} = \mathbf{0}$ case should be

$$1 = 4\pi j_0(0 \times r) \frac{1}{\sqrt{4\pi}} \frac{1}{\sqrt{4\pi}}, \quad j_0(0) = \lim_{x\to 0} \frac{\sin x}{x} = 1 \tag{1.388}$$

In this case, the values in the $l = m = 0$ case, $Y_{00} = 1/\sqrt{4\pi}$, is used for Y_{lm}. This result mediates the difficulty of determining the polar angles when r is zero.

1.5.7 Region with the non-local terms

The final state wave function in the region with the non-local terms ($r < r_c$) can be represented using the polar coordinate system;

$$\psi^{(\mathbf{k})\mathrm{F}}_{\mathrm{nonloc}} = \sum_{lm} P^{\mathrm{loc}}_{lm}(r_c) Y_{lm}(\theta,\ \varphi) \frac{P^{\mathrm{nonloc}}_l(r)}{r}. \tag{1.389}$$

$P^{\mathrm{nonloc}}_l(r)$ is a radial wave function discussed in Sec. 1.4. We normalize it so that $P^{\mathrm{nonloc}}_l(r_c) = 1$ holds. Since the initial state is

$$\phi^{(\mathbf{k})\mathrm{I}}_{\alpha i n} = Y_{lm}(\theta,\ \varphi) \frac{P^{\mathrm{I}}_{ipl}(r)}{r}, \tag{1.390}$$

the matrix element can be calculated by the following equation

$$\langle \psi^{(\mathbf{k})\mathrm{F}}_{\mathrm{nonloc}} | \mathbf{r}\cdot\mathbf{e} | \phi^{(\mathbf{k})\mathrm{I}}_{\alpha i n} \rangle = \sum_{l'}^{l\pm1} \sum_{j=-1}^{1} P^{\mathrm{loc}*}_{l',m+j}(r_c) e_j g(l', m+j; l, m) \int_0^{r_c} r P^{\mathrm{nonloc}}_l(r) P^{\mathrm{I}}_{ipl}(r) \mathrm{d}r. \tag{1.391}$$

Since the 4π term is omitted in the no non-local area calculation, we need to divide it by 4π.

Chapter 2

Software

2.1 Atomic and pseudo-atomic orbitals in OpenMX and ADPACK

OpenMX[9] is a first-principles calculation software package using localized basis sets, and the pseudopotentials (PPs) for OpenMX are generated by ADPACK[10]. We explain the method to obtain the relationship between atomic orbitals (AOs) in the all-electron (AE) potential and pseudo-atomic orbitals (PAOs) in the PP. See Ref. [11] for properties of PPs.

2.1.1 Modification of ADPACK

ADPACK can perform AE, PP, and PAO calculations depending on the value of `calc.type` (`ALL`, `VPS`, and `PAO` respectively). We modified ADPACK as described in Table 2.1 to calculate AOs and PAOs up to unoccupied states. The modified package is available from this repository.

Table 2.1: Modification of ADPACK.

File name	Line number	Modifications
`adpack.h`	24-25	Constants `ASIZE11`, `ASIZE12` are enlarged.
`adpack.h`	38	`max_N`, the largest principal quantum number in AO calculations, is added.
`adpack.h`	185	The function `All_Electron_NSCF` is added.
`readfile.c`	123	It reads `max_N` from the keyword `max.N`.
`adpack.c`	145-146	It calculates of unoccupied states in AE calculations.
`All_Electron.c`	42-48, 655-659	It exchanges the flag value so that the AE calculations (`Calc_Type=0`) become identical to those for PAO calculations (`Calc_Type=2`).
`All_Electron_NSCF.c`	All	`All_Electron.c` is copied to `All_Electron_NSCF.c`, and then modified to calculate unoccupied AOs using the methods in Sec. 1.2.3.
`Output.c`	743-781	It outputs the AOs in `Output_AllBases` by the same format as the PAOs (ll. 927-944 in `Output_PAOBases2`)
`makefile`	29	`All_Electron_NSCF.o` is added in `OBJS`.

2.1.2 Comparison of orbitals

Here we use `C6.0.pao` as PAOs and `C_CA19.vps` as a PP. While they are used as inputs for OpenMX, parameters in the beginning can be used as the input for ADPACK. We performed AO and PAO calculations based on these input data, although they were slightly modified.

We note that the core potential for a carbon atom includes only the $1s$ orbital. Therefore, p and d orbitals have no change due to the pseudization.

AOs and PAOs (PP input)

We calculated AOs (wave functions in the AE potential) and PAOs (those in the PP) based on the input parameters in the PP file `C_CA19.vps`. Figure 2.1 shows the result for the $2s$ orbital. Since the $1s$ is included in the PP, the $2s$ orbital is the lowest eigenstate with no node.

Optimization of PAOs (PAO input)

Calculated PAOs are for an atom, so they differ slightly in solids or molecules. OpenMX optimizes PAOs by linear combinations to represent bonded states in solids and molecules by fewer bases [12]. The optimization can be checked by comparing PAOs (after the optimization) in the PAO file `C6.0.pao` and those recalculated from input parameters in the file (before the optimization) (Fig. 2.2). The linear combination coefficients are included in PAO files [13], and same values can be calculated by the inner product of the optimized PAOs and recalculated PAOs.

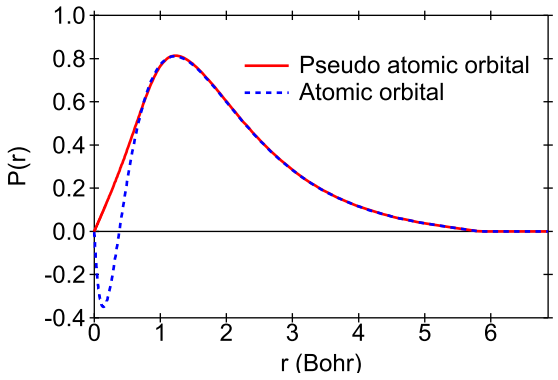

Figure 2.1: 2s AO and PAO for a carbon atom using the PP file as the input.

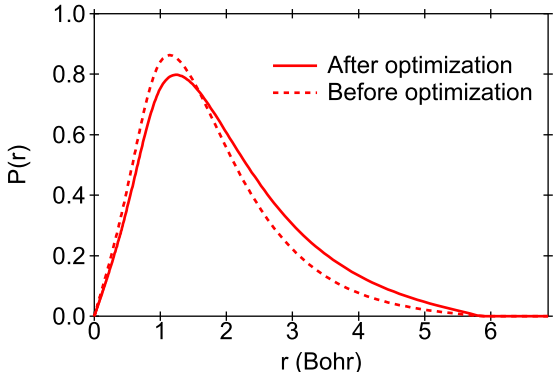

Figure 2.2: 2s PAOs before and after the optimization using the PAO file as the input.

We need to be careful that the atom for PAO calculations may differ from that for PP calculations. In the case of a carbon atom, AE calculations for PAOs use the 1s orbital occupied by 1.5 electrons (not 2.0). Therefore the 2s orbitals are slightly different (Fig. 2.3).

Optimized PAOs, and corresponding AOs

The above arguments show that PAOs used in OpenMX are optimized, and they are represented by linear combinations of original PAOs, eigenstates with the PP. AE calculations during PP calculations give correspondence PAOs (before optimization) and AOs. Therefore, AOs corresponding to optimized PAOs can be obtained by linear combination with the same coefficients as PAOs. Figure 2.4 shows the result for the carbon 2s orbital. The vertical line in the figure shows the cutoff of PP calculations (1.3 Bohr), and we can confirm that the PAO and AO are identical out of the cutoff.

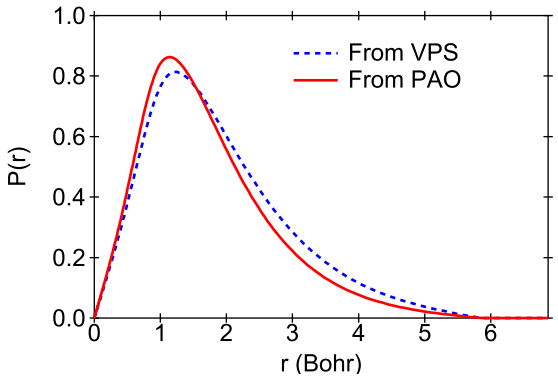

Figure 2.3: 2*s* PAOs using the PP and PAO files as the inputs.

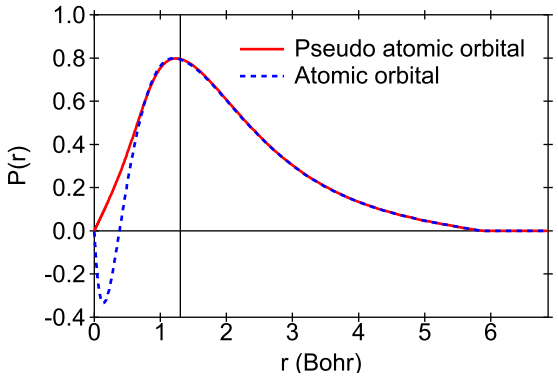

Figure 2.4: Optimized 2*s* PAO for a carbon atom and corresponding AO.

2.2 GUI_tools directory

Tools included in the GUI_tools directory are described. While they are unnecessary for actual photoemission calculations, they are useful for data visualization.

2.2.1 Overview

The following tools use Python 3.7 and libraries listed in Table 2.2.

Table 2.2: Python libraries necessary for the tools. The versions are those for the development environment.

Library	Version
PyQt5	5.15.2
pyqtgraph	0.12.3
h5py	3.2.0
numpy	1.20.1
scipy	1.7.1

Each directory contains the template file Config_example.py. Users need to copy it to Config.py to execute the programs. Since Config.py is out of the Git control, they can modify it by themselves.

2.2.2 OpenMX_viewer

Data blocks beginning by <*keyword* and ending by *keyword*> frequently appear in OpenMX files. The tool can read it and draw a graph.

Figure 2.5 shows a pseudo-atomic orbital in C6.0.pao. In the case of a function of the distance r like pseudo-atomic orbitals, the first column is $x = \log(r)$, the second column is r, and the other columns are values of the function [14].

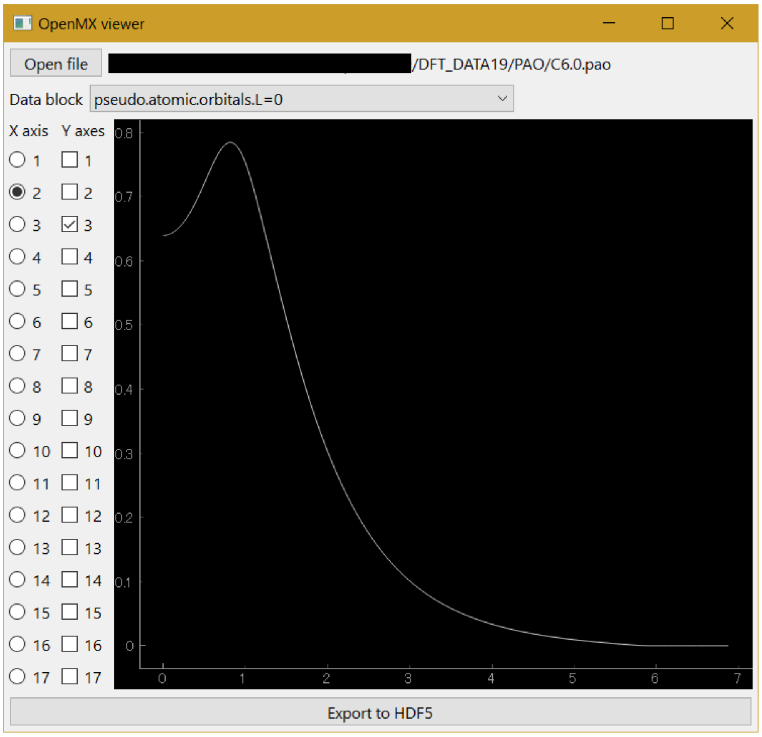

Figure 2.5: Example of OpenMX_viewer.py.

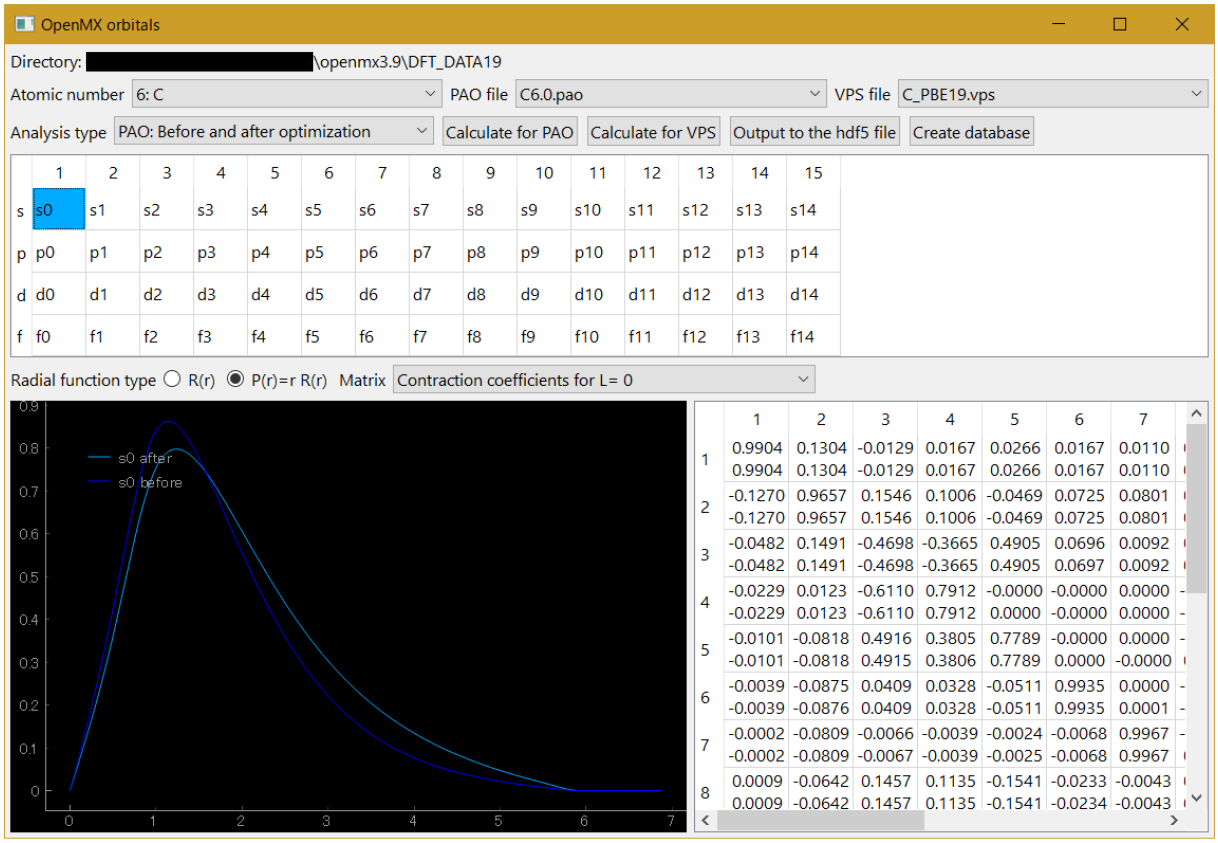

Figure 2.6: Example of `OpenMX_orbitals.py` showing pseudo-atomic orbitals before and after the optimization.

2.2.3 `OpenMX_orbitals`

The tool calculates AOs corresponding to optimized PAOs according to the method in Sec. 2.1. Since pseudopotential and pseudo-atomic orbital files in OpenMX include input parameters for ADPACK, these parameters are used for the following calculations.

1. Pseudo-atomic orbital calculations using the pseudopotential file
2. Atomic orbital calculations using the pseudopotential file
3. Pseudo-atomic orbital (before optimization) calculations using the pseud-atomic potential file

Users need to set `workingDirectory` (the directory containing pseudopotentials and pseudo-atomic orbitals of OpenMX) and `adpack` (the modified ADPACK executable) in `Config.py` before the execution. Since ADPACK needs a C compiler, `OpenMX_orbitals.py` also needs to be executed on the same environment. Once ADPACK completes calculations, the other calculations are performed by Python. If you copy the data from ADPACK, you can continue calculations on different environments.

Figure 2.6 shows an example using C6.0.pao and C_PBE19.vps. Calculations are specified by `Analysis type`; now, it calculates pseudo-atomic orbitals before and after the optimization. The center table specifies orbitals to be plotted in the left bottom figure; s0 ($2s$ orbital) is now selected. The right bottom table can show linear combination coefficients or norms of orbitals. Now it shows the contraction coefficients for s orbitals ($l = 0$); the upper ones are from the `Contraction.coefficients` data block, and the lower ones are calculated from inner products of orbitals before and after the optimization.

Some errors occurred when files in OpenMX were directly used. `Docs/DFT_DATA19_mod.md` lists necessary modifiecations to perform calculations.

2.2.4 `OpenMX_band`

The tool can show band dispersion and LCAO coefficients. It is generated during the development of `Main_GUI/SPADExp_GUI.py`, so users are recommended to use the latter.

2.3 OpenMX_tools directory

The tools included in the OpenMX_tools directory are described. They are necessary as the interface with OpenMX.

2.3.1 Compilation

The programs are complied with the make command and a C++ compiler. Users need to install HDF5 [15] before the compilation. When they install HDF5, they need to set --enable-cxx option in the configre command.

Users create Makefile referring to Makefile_example and specify the path where HDF5 is installed. Then they can compile programs.

2.3.2 preproc.o

preproc.o create the input file to calculate LCAO coefficients in OpenMX. It needs two arguments, the paths of the input and output files.

```
> preproc.o (input file) (output file)
```

The input file includes input parameters for OpenMX and keywords in Table 2.3. All keywords are mandatory; the values of minN maxN are not loaded in preproc.o but are necessary for postproc.o. We recommend to set 0 to num.HOMOs and num.LUMOs. Three numbers to specify the point in the reciprocal space are fractional coordinates of the reciprocal lattice. The basis set is the reciprocal lattice vectors of Band.KPath.UnitCell or Atom.UnitVectors. If both unit cells are in the input file, the former is used as the band dispersion calculations.

Table 2.3: Keywords for preproc.o.

Keyword	Value	Description
SPADExp.dimension	Number 1 or 2	Dimension of the reciprocal space
SPADExp.curved	Boolean	Whether the target is curved or flat
SPADExp.origin	Three real numbers	Origin of the target space
<SPADExp.range SPADExp.range>	Five real numbers, one integer Same numbers of lines as the dimension	Reciprocal space Three in the beginning are for the vector Following two are for the range The last integer is for the number of points
SPADExp.minN	Integer	The lowest band index to be considered
SPADExp.maxN	Integer	The highest band index to be considered

The output file includes the same content as the input and MO.fileout, MO.Nkpoint, and MO.kpoint keywords according to values in Table 2.3. Although keywords in Table 2.3 remain in the output, they cause no error because OpenMX neglects unnecessary keywords.

The reciprocal space is specified by origin and range as follows. In this explanation, dimension is fixed to 1 and $\mathbf{a}_i$ $(i = 1,\ 2,\ 3)$ represent the bases for the reciprocal lattice.

1. Values of origin $(o_1,\ o_2,\ o_3)$ determines the origin $\mathbf{o} = \sum_i o_i \mathbf{a}_i$.
2. Values of range $(x_1,\ x_2,\ x_3$, three in the beginning) determines the direction vector $\mathbf{x} = \sum_i x_i \mathbf{a}_i$.
3. It checks that $\mathbf{o}$ and $\mathbf{x}$ are orthogonal.
4. Values of range $(p_1,\ p_2,\ n$, three in the end) determines the distance $d = (p_2 - p_1)/(n-1)$.
5. The ith reciprocal point is

$$\mathbf{v}_i = \mathbf{o} + (p_1 + i \times d)\mathbf{x} \tag{2.1}$$

if curved is false (flat plane/straight line) and

$$\mathbf{v}_i = r \cdot \mathbf{o} + (p_1 + i \times d)\mathbf{x} \tag{2.2}$$

if curved is true (curved plane/curve). The coefficient r is determined so that $|\mathbf{v}_i| = |\mathbf{o}|$ holds.

2.3.3 `postproc.o`

`postproc.o` loads the output of OpenMX and generate a HDF5 file. It requires one argument, the path of the input for OpenMX (output of `preproc.o`).

```
> postproc.o (input file)
```

It reads the unit cell, band dispersion, LCAO coefficients, and so on from the input file and the output of OpenMX *System.Name*`.out`. In the output of OpenMX, LCAO coefficients are written in the form of a list like Ref. [16]; the loops to determine the order are atom label, angular quantum number, principal quantum number, and magnetic quantum number, from the outside. Basis sets used in OpenMX are not eigenstates of the magnetic quantum number m but real functions obtained by combining eigenstates of the magnetic quantum number $\pm m$. For the order of the magnetic quantum number, see `source/Band_DFT_MO.c` in the OpenMX source.

2.4 SPADExp_GUI tools

Tools included in the SPADExp_GUI directory are described. One is the Python-based photoemission angular distribution (PAD) calculator SPADExp_GUI.py, and the other is the viewer SPADExp_Viewer.py.

We recommend performing calculations on the C++ version if the reciprocal space is two-dimensional or the system is large. The Python version does not include the matrix element calculations using the modified plane wave and the weighting, which are included in the C++ version.

2.4.1 SPADExp_GUI

The tool calculates the photoemission angular distribution from the HDF5 file output from postproc.o. Users need to set the path of PAO_and_AO_after_opt.hdf5 to the variable PAO_and_AO in Config.py. Also, they need to set the path of elements.ini in VESTA [17] to the variable elements_file.

Figure 2.4.1 shows the execution example. The left bottom panel shows the unit cell and the Boundaries determines the number of repetitions. The straight line in pen_pol represents the angle for the polarization (Θ, Φ). The straight lines in pen_kx and pen_ky represent the directions to specify the calculation region.

The center panel is the band dispersion or the PAD. Each band is stretched according to the Gaussian with the width dE to obtain the color map. In the case of 2D (dimension is one), green vertical and horizontal lines appear. The right table shows the LCAO coefficients or orbital shape at the crossing point of the cursors. The left and right keys change the k point, and the top and bottom keys change the band index. In case of 3D (dimension is two), the left and the right are for kx, the top and the bottom are for ky, Page Up/Page Dn are for the constant-energy map, home/end are for the band index.

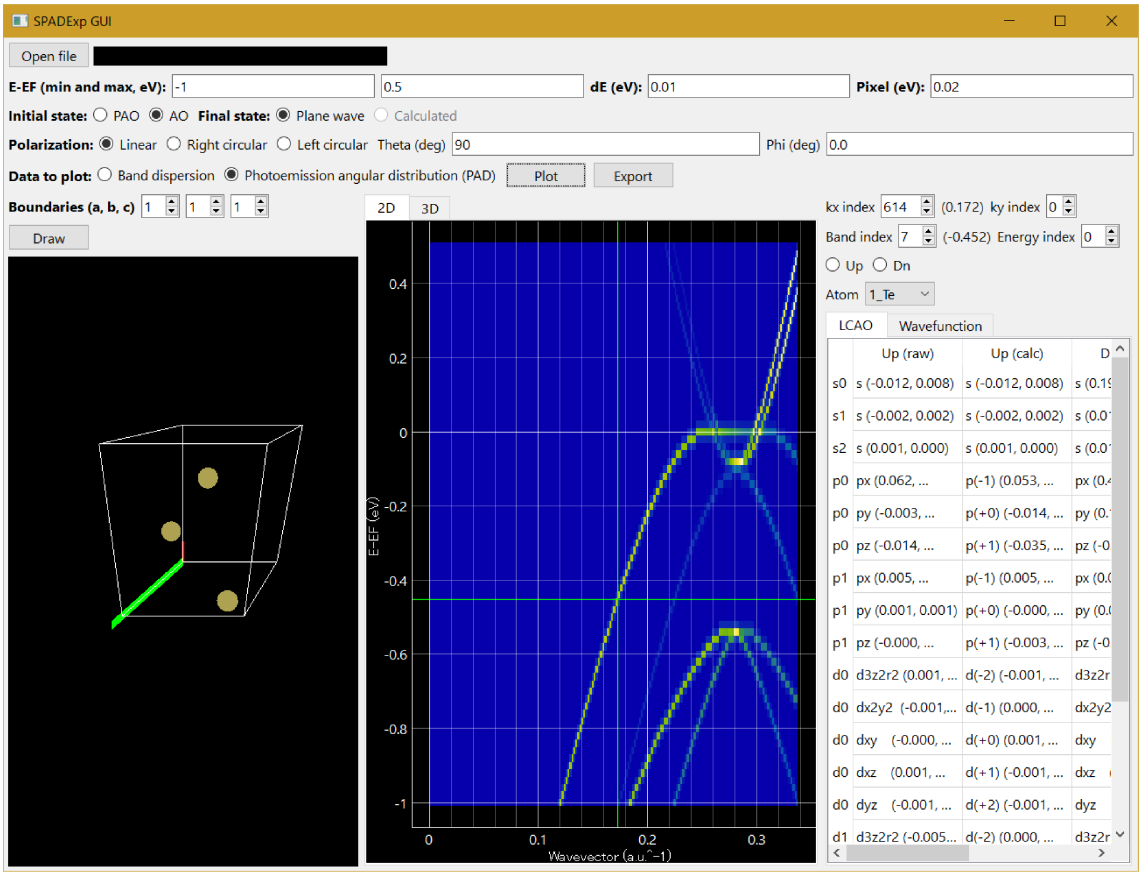

Figure 2.7: Example of SPADExp_GUI.py.

2.4.2 SPADExp_Viewer

It displays the PAD in the HDF5 exported by SPADExp.o or SPADExp_GUI.py. Figure 2.4.2 shows the example Users can control the cursors in the 3D case in the same way as SPADExp_GUI.py. In the case

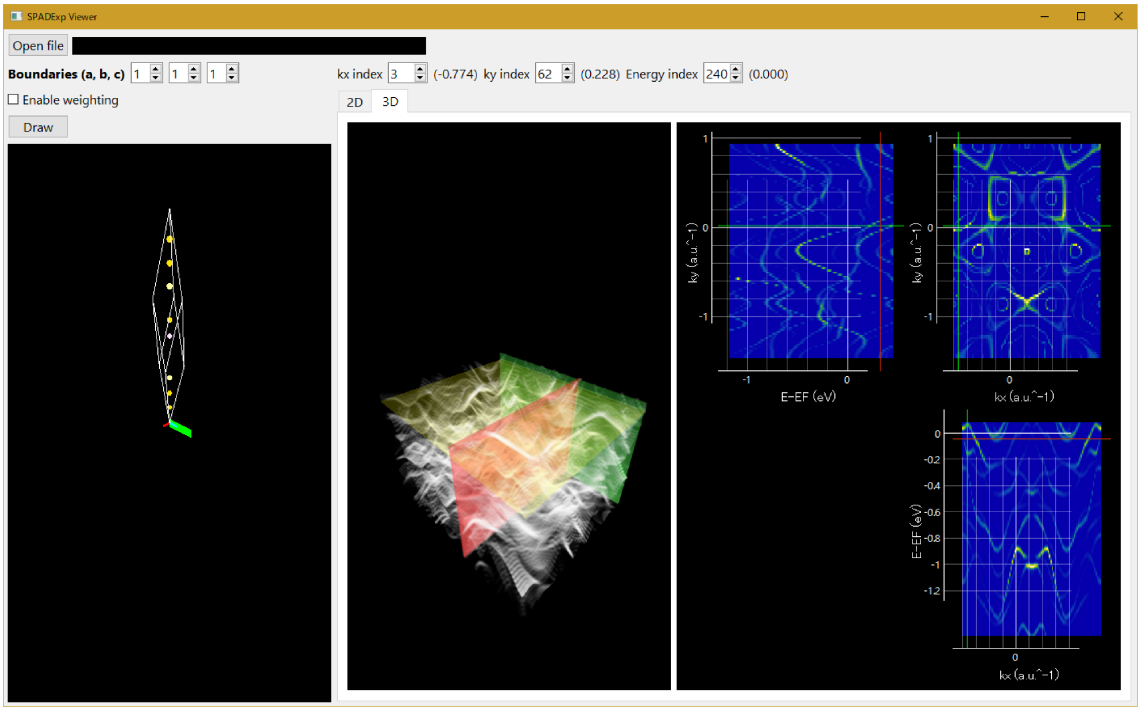

Figure 2.8: Example of `SPADExp_Viewer.py`.

of the PAD calculations with the weighting function, `Enable weighting` changes the transparency of atoms according to their weight of them.

2.5 Main_program directory

Tools in Main_program directory are described. The executable SPADExp.o can calculate atomic potentials and PADs.

2.5.1 Compilation

Similarly to the OpenMX_tools directory, users need to make Makefile based on Makefile_example and compile the program by the make command. In addition to HDF5, libraries for the OpenMP parallelization and BLAS, such as Intel MKL, are necessary.

2.5.2 Overview

The successful compilation generates the executable SPADExp.o. Users can perform calculations by loading the input file to the standard input.

```
> SPADExp.o < input.dat
```

The input file is a text file with a similar format to Quantum ESPRESSO. It containt several blocks, which start with &*block_name* and end with /. In a block, each line contains the keyword and the value with spaces between them. Lines starting with ! or # and blank lines are neglected. There is no rule for the order of blocks, while multiple blocks with the same name are forbidden.

The keywords and values are case-sensitive. The values have the following types.

Integer 1

Real number 1.5 or 1.0e-2

Boolean TRUE True true or FALSE False false

String /path/to/file

2.5.3 &Control block

The &Control block specifies the calculation type and input and output files. Table 2.4 describes the keyword. Keywords without default values are generally mandatory; the calculations cannot be executed if the values are given.

Table 2.4: Keywords and values for the &Control block.

Keyword	Type	Description	Default
Calculation	String	Calculation type	None
Log_file	String	Path to the log file Calculations are performed without the log when not specified.	None
Console_log	Boolean	Whether the log is output to the console or not	True
Output_file	String	Path to the output file	None

2.5.4 Calculation of the Thomas-Fermi potential

When Calculation is set to Thomas-Fermi, the software calculates the Thomas-Fermi potential $g(x)$. The differential equation to be solved is

$$\frac{\mathrm{d}}{\mathrm{d}x^2} g(x) = \frac{g(x)^{3/2}}{\sqrt{x}}. \tag{2.3}$$

See Section 1.2 for the details of the calculation process.

The keywords are specified in the &Thomas-Fermi blocks. Table 2.5 shows the keywords. In the test calculation, the software calculates $g(x)$ for given $g'(0)$ values. In the actual calculation, the software finds the solution satisfying $g(x) \to 0$ ($x \to \infty$) by the bisection method using the given minimum and maximum of $g'(0)$. The default values for Initial_diff_min and Initial_diff_max are chosen so that it successfully finds the solution with the 4th-order Runge-Kutta method.

Table 2.5: Keywords and values for the `&Thomas-Fermi` block.

Keyword	Type	Description	Default
`Calculation_test`	Boolean	Test calculation or actual calculation	`False` (actual)
`Initial_diff_offset`	Real number	[Test] the initial value of $g'(0)$	None
`Initial_diff_delta`	Real number	[Test] increment for $g'(0)$	None
`Initial_diff_size`	Real number	[Test] number of points for $g'(0)$	None
`Initial_diff_min`	Real number	[Actual] the initial bottom for $g'(0)$	`-1.49`
`Initial_diff_max`	Real number	[Actual] the initial top for $g'(0)$	`-1.51`
`Threshold`	Real number	Convergence threshold	`1e-5`
`Solution`	String	Method to solve the differential equation `RK1`(Euler method) `RK4`(4th-order Runge-Kutta method)	`RK4`

In the calculations of the Thomas-Fermi potential, the `&Radial-grid` block can specify the sequence of points x_i for the calculations of $g(x_i)$. The number of lines in the block is described in the `&Radial-grid` line. Each line in the block specifies the increment (real number) and the number of points (integer). The default is the same as Ref. [2].

```
&Radial_grid 11
0.0025 40
0.005  40
0.01   40
0.02   40
0.04   40
0.08   40
0.16   40
0.32   40
0.64   40
1.28   40
2.56   40
/
```

2.5.5 Calculations of atomic wave functions

When `Calculation` is set to `Atomic-wfn`, the software calculates the radial wave function in the spherically isotropic atomic potential. See Section 1.2 for the details of the calculations.

The keywords are specified in the `&Atomic-wfn` block, as well as the `&Radial-grid` block for x_i. Table 2.6 shows the keywords. For the principal quantum number, users can specify multiple values by `n_min` and `n_max` or one value by `n`; both ways cannot be used simultaneously. A similar limitation is applied for the angular quantum and atomic numbers.

The potential is set to $V(x) = -Z/\mu x$ for `H-like` (hydrogen-like atom), $V(x) = -Z/\mu x \cdot g(x)$ for `Thomas-Fermi` (g(x) is given by the file), and the values in the file for `file`. In the above equation, μ is the Thomas-Fermi scaling coefficient.

The output includes eigenvalues for each atom.

Table 2.6: Keywords and values for the `&Atomic-wfn` block.

Keyword	Type	Description	Default
`n_min`	Integer	Minimum of the principal quantum number n	None
`n_max`	Integer	Maximum of the principal quantum number n	None
`n`	Integer	Value of the principal quantum number n	None
`l_min`	Integer	Minimum of the angular quantum number l	None
`l_max`	Integer	Maximum of the angular quantum number l	None
`l`	Integer	Value of the angular quantum number l	None
`Z_min`	Integer	Minimum of the atomic number Z	None
`Z_max`	Integer	Maximum of the atomic number Z	None
`Z`	Integer	Value of the atomic number Z	None
`Potential`	String	Type of the potential `H-like` (hydrogen-like atom) `Thomas-Fermi`(Thomas-Fermi potential) `file` (from file)	None
`Potential_file`	String	File containing the potential	None
`Solution`	String	Method to solve the differential equation `RK1` (Euler method) `Numerov` (Numerov method)	`Numerov`
`Bisubsection_step`	Real number	Initial step size in the bisection method	`1e-3`
`E_threshold`	Real number	Threshold for the energy convergence	`1e-5`
`Radius_factor`	Real number	Coefficient to determine the calculation range of x	`8.0`

2.5.6 Calculations of the self-consistent atomic potential

When `Calculation` is set to `SCF-atom`, the software calculates the self-consistent atomic potential. See Section 1.2 for the details of the calculations.

The keywords are specified in the `&SCF-atom`, `&Atomic-wfn`, `&Occupation`, and `&Radial-grid` blocks. Table 2.7 shows the valuable keywords in the `&Atomic-wfn` block. The input potential is used as the initial value for the self-consistent calculations.

Table 2.7: The keywords in the `&Atomic-wfn` block used in the self-consistent calculations.

Keyword	Note
`Z`	`Z_min` and `Z_max` are forbidden
`Potential`	Set to `Thomas-Fermi` regardless of the input
`Potential_file`	
`Solution`	
`Bisubsection_step`	
`Radius_factor`	

Table 2.8 shows the keywords for the `&SCF-atom` block.

Table 2.8: Keywords and values for the `&SCF-atom` block.

Keyword	Type	Value	Default
`Mix_weight`	Real number	Mixing ratio in the self-consistent calculations	`0.5`
`Criterion_a`	Real number	Convergence threshold for α	`0.001`
`Criterion_b`	Real number	Convergence threshold for β	`0.001`

The `&Occupation` block specifies the occupation number in the shape of stairs. In case of a carbon atom with two electrons in $1s$, $2s$, and $2p$ orbitals, the input becomes like

```
&Occupation 2
2
2 2
/
```

The output is an HDF5 file containing the self-consistent potential and the atomic number.

2.5.7 Calculations of excited states and phase shifts

When `Calculation` is set to `Phase-shift`, the software calculates excited states and phase shifts with the atomic potential.

The keywords are specified in the `&Phase-shift`, `&Atomic-wfn`, `&Radial-grid`, `&Excitation-energy`, and `&Orbital` blocks. Table 2.9 shows the valuable keywords in the `&Atomic-wfn` block. Users set the path of an HDF5 file, obtained by the self-consistent calculations or given by us as a database, to `Potential_file` If the file is not specified, the potential becomes the hydrogen potential $V(x) = -1/\mu x$, so the calculations give the Coulomb wave function and the phase difference $\arg \Gamma(l + 1 - \mathrm{i}/k)$.

Table 2.9: The keywords in the `&Atomic-wfn` block used in the phase shift calculations.

Keyword	Note
`Z`	`Z_min` and `Z_max` are forbidden
`Potential_file`	
`Solution`	

Table 2.10 shows the keywords for the `&Phase-shift` block.

Table 2.10: Keywords and values for the `&Phase-shift` block.

Keyword	Type	Description	Default
`Skip_points`	Integer	Number of skipped local minimum/maximum points	2
`Calc_points`	Integer	Number of points used for the phase calculation	5

The `&Orbital` block specifies the angular quantum number and the binding energy of the ground states. For example,

```
&Orbital 1
2p 6.0
/
```

means the $2p$ orbital has a binding energy of 6 eV. The `&Excitation-energy` block specifies the excitation energies;

```
&Excitation-energy 1
21.2
/
```

means the excitation by the helium lamp (21.2 eV).

The default values of the `&Radial-grid` block is inappropriate because they do not have enough points for large x. The calculation examples use the following grid.

```
&Radial-grid
0.0025 40
0.005  40
0.01   40000
/
```

The output includes the wave functions for the excited states with $l \pm 1$. The beginning of the output file has comments for the phase shift calculated from local minima and maxima.

2.5.8 Photoemission intensity calculations

When `Calculation` is set to `PAD`, the software calculates the PAD. See Section 1.5 for the details of the calculations.

The `&PAD` block is used. Tables 2.11 and 2.12 show the keywords. The Gauss distribution with the width `dE` is introduced to realize smooth distribution from discretized dispersions, maybe due to slab calculations. `Final_state_step` is used to reduce the number of k points where the software calculates the atomic potential effect. When `Final_state` is set to `Calc`, the `&Radial-grid` block, `Potential_file` and `Solution` in the `&Atomic-wfn` bock, and the `&Phase-shift` block are used.

The `FP_PAO` and `FP_AO` values in the `Final_state` mean unoccupied states of the Kohn-Sham system, discussed in the Sec. 1.4. When `Ignore_nonlocal` is `false` and `Final_state` is `FP_AO`, the radial wave function with the non-local term is transformed using the expansion coefficients by pseudo-atomic orbital and atomic orbital wave functions. However, the transformation may be inappropriate because the expansion by pseudo-atomic orbitals does not completely reproduce the original radial wave function.

When users use `Extend`, they need to check that the first and last points are different by the reciprocal vector, and the repetition of the region gives the periodic reciprocal space. Therefore, they cannot use `Extend` if `curved` is set to `true` in `preproc.o`. The software does not check the periodicity. In the one-dimensional case, the second (right) and fourth (left) values are used.

The weighting is applied by the following process. For an atom at $\mathbf{r}_i$, the software determines the distance z_i by the inner product with the unit vector $\mathbf{v}$ specified by `Weighting_axis`. The following equation gives the weight; if $\lambda > 0$,

$$W_{\mathrm{Rect}}(z_i) = \begin{cases} 1 & z_0 < z_i < z_0 + \lambda \\ 0 & \text{otherwise} \end{cases} \tag{2.4}$$

$$W_{\mathrm{Exp}}(z_i) = \begin{cases} 0 & z_i < z_0 \\ \exp\left(-\dfrac{z_i - z_0}{\lambda}\right) & z_i > z_0 \end{cases} \tag{2.5}$$

$$W_{\mathrm{Tri}}(z_i) = \begin{cases} 1 - \dfrac{z_i - z_0}{\lambda} & z_0 < z_i < z_0 + \lambda \\ 0 & \text{otherwise} \end{cases} \tag{2.6}$$

$$W_{\mathrm{Sqrt}}(z_i) = \begin{cases} \sqrt{1 - \dfrac{z_i - z_0}{\lambda}} & z_0 < z_i < z_0 + \lambda \\ 0 & \text{otherwise} \end{cases} \tag{2.7}$$

and if $\lambda < 0$,

$$W_{\mathrm{Rect}}(z_i) = \begin{cases} 1 & z_0 - |\lambda| < z_i < z_0 \\ 0 & \text{otherwise} \end{cases} \tag{2.8}$$

$$W_{\mathrm{Exp}}(z_i) = \begin{cases} 0 & z_i > z_0 \\ \exp\left(\dfrac{z - z_0}{|\lambda|}\right) & z_i < z_0 \end{cases} \tag{2.9}$$

$$W_{\mathrm{Tri}}(z_i) = \begin{cases} 1 + \dfrac{z_i - z_0}{|\lambda|} & z_0 - |\lambda| < z_i < z_0 \\ 0 & \text{otherwise} \end{cases} \tag{2.10}$$

$$W_{\mathrm{Sqrt}}(z_i) = \begin{cases} \sqrt{1 + \dfrac{z_i - z_0}{|\lambda|}} & z_0 - |\lambda| < z_i < z_0 \\ 0 & \text{otherwise} \end{cases} \tag{2.11}$$

where z_0 represents `Weighting_origin` and λ represents `Weighting_width` [Fig. 2.9].

Figure 2.10 shows the polarizations and angles Θ, Φ. Table 2.13 represents the $\mathbf{r} \cdot \mathbf{e}$ term for each polarization.

If the $\mathbf{g}_{/\!/}$ is unlimited, all $\mathbf{g}_{/\!/}$'s satisfying $|\mathbf{g}_{/\!/}| < \sqrt{2h\nu} \times$ `FPFS_kRange` are used.

The solving strategy of the Kohn-Sham unoccupied states is determined by the following rules.

- If `FPFS_Numerov` is `True`, the Numerov method is used ($\mathbf{g}_{/\!/}$ is limited).
- If `FPFS_Numerov` is `False` and `FPFS_bulk` is not set, the simultaneous equations are used.

- If `FPFS_Numerov` is `False` and `FPFS_bulk` is set, bulk wave functions are used.

When `Interpolate_wfn` is `True`, the grid step of the initial state radial wave functions is changed to the z step multiplied by `Interpolate_wfn_coef`. The original (pseudo-)atomic orbital wave function uses the logarithmic grid and the grid is too precise for matrix element calculations. Therefore, this interpolation can reduce the calculation cost.

The output file is an HDF5 file containing the PAD, unit cell, and so on.

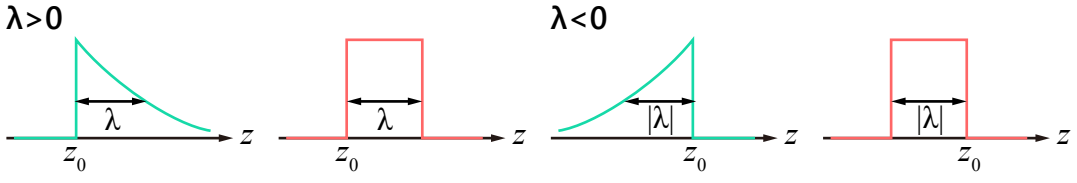

Figure 2.9: Schematic of the weighting functions.

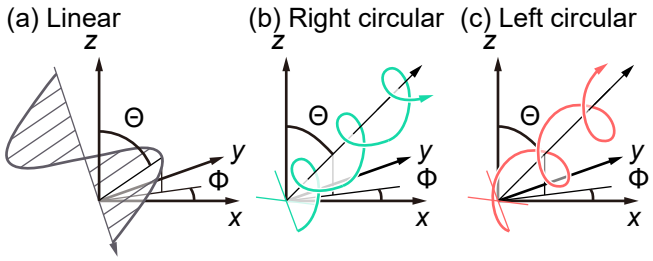

Figure 2.10: Schematic of linear and circular polarizations and angle Θ, Φ.

Table 2.11: Keywords and values for the `&PAD` block.

Keyword	Type	Description	Default
`Input_file`	String	File path to the output of `postproc.o`	None
`E_min`	Real number	Minimum of the energy range	None
`E_max`	Real number	Maximum of the energy range	None
`E_pixel`	Real number	Step along the energy direction	None
`dE`	Real number	Width of the gaussian	None
`Initial_state`	String	Initial states `AO` or `PAO`	None
`Final_state`	String	Final states `PW` (plane wave) `Calc` (modified plane wave) `FP_PAO` (Kohn-Sham unoccupied, PAO) `FP_AO` (Kohn-Sham unoccupied, AO)	None
`Final_state_step`	Real number	Discretization width for the atomic potential effect calculations	0.01
`Polarization`	String	Polarization `Linear` (linear) `LCircular` (left circular) `RCircular` (right circular)	None
`Theta`	Real number	Angle Θ [degree] for the polarization direction	None
`Phi`	Real number	Angle Φ [degree] for the polarization direction	None
`Atomic_orbitals_file`	String	Database file for AO and PAOs	None
`Extend`	4 integers	Extension width for top, right, bottom, and left	Zero
`Weighting`	Boolean	Whether weighting is applied	`False`
`Weighting_axis`	3 real numbers	Axis for the weighting	None
`Weighting_shape`	String	Shape of the weighting function `Rect` (rectangular) `Exp` (exponential) `Tri` (triangular) `Sqrt` (square root)	None
`Weighting_origin`	Real number	Origin for the weighting	None
`Weighting_width`	Real number	Width of the weighting function	None
`Use_angstrom`	Boolean	Å is used for the unit of `Weighing_origin` and `Weighting_width`, or Bohr is used	`True`
`Ignore_core`	Boolean	Whether the region with non-local is discarded	`False`
`Output_data`	String	Output data `PAD` (normal PAD) `Band` (the matrix element is fixed to 1)	`PAD`

Table 2.12: Keywords and values for `&PAD` block (FP calculation related ones)

Keyword	Type	Description	Default
`Excitation_energy`	Real number	Excitation energy [eV]	None
`FPFS_energy_step`	Real number	Energy step for eigenstate calculations [eV]	0.01
`FPFS_kRange`	Real number	Coefficients for $\mathbf{g}_{/\!/}$	2.0
`FPFS_Numerov`	Boolean	Use the Numero method ($\mathbf{g}_{/\!/}$ limited)	`False`
`FPFS_bulk`	2 real, 1 integer	Lower end, upper end, number of layers	None
`VPS_file`	String	Pseudopotential database file	None
`Ignore_nonlocal`	Boolean	Whether non-nonlocal term is discarded	`False`
`Interpolate_wfn`	Boolean	Whether interpolation is applied to radial wave functions	`True`
`Interpolate_wfn_coef`	Real number	Coefficients for interpolation	0.5
`FPFS_nonloc_offset`	Real number	Offset to move the cutoff of the non-local term	0.0
`Calc_all_nonloc`	Boolean	Whether non-local wave functions are calculated for all atoms	`True`
`FPFS_file`	String	Export file path of FP wave functions	None

Table 2.13: $\mathbf{r}\cdot\mathbf{e}$ terms for linear and circular polarization.

Polarization	$\mathbf{e}$	$\mathbf{r}\cdot\mathbf{e}$
Linear	$\begin{pmatrix}\sin\theta\cos\varphi\\ \sin\theta\sin\varphi\\ \cos\theta\end{pmatrix}$	$-\sqrt{\frac{2\pi}{3}}\sin\theta e^{-\mathrm{i}\varphi}\cdot rY_{1,1}$ $+\sqrt{\frac{4\pi}{3}}\cos\theta\cdot rY_{1,0}$ $+\sqrt{\frac{2\pi}{3}}\sin\theta e^{\mathrm{i}\varphi}\cdot rY_{1,-1}$
Right circular	$\begin{pmatrix}-\cos\theta\cos\varphi\\ -\cos\theta\sin\varphi\\ \sin\theta\end{pmatrix}+\mathrm{i}\begin{pmatrix}\sin\varphi\\ -\cos\varphi\\ 0\end{pmatrix}$	$\sqrt{\frac{2\pi}{3}}(1+\cos\theta)e^{-\mathrm{i}\varphi}\cdot rY_{1,1}$ $+\sqrt{\frac{4\pi}{3}}\sin\theta\cdot rY_{1,0}$ $+\sqrt{\frac{2\pi}{3}}(1-\cos\theta)e^{\mathrm{i}\varphi}\cdot Y_{1,-1}$
Left circular	$\begin{pmatrix}-\cos\theta\cos\varphi\\ -\cos\theta\sin\varphi\\ \sin\theta\end{pmatrix}-\mathrm{i}\begin{pmatrix}\sin\varphi\\ -\cos\varphi\\ 0\end{pmatrix}$	$\sqrt{\frac{2\pi}{3}}(-1+\cos\theta)e^{-\mathrm{i}\varphi}\cdot rY_{1,1}$ $+\sqrt{\frac{4\pi}{3}}\sin\theta\cdot rY_{1,0}$ $-\sqrt{\frac{2\pi}{3}}(1+\cos\theta)e^{\mathrm{i}\varphi}\cdot Y_{1,-1}$

Bibliography

[1] https://physics.nist.gov/cuu/Constants/index.html

[2] Herman and Skillman "Atomic Structure Calculations ", 1963.

[3] R. Latter, Phys. Rev. **99**, 510 (1955).

[4] E. Heirer, S.P. Nørsett, and G. Wanner, "Solving Ordinary Differential Equations I", Springer, 1993.

[5] 西森 秀稔、「物理数学 II」、丸善出版、2015。

[6] NIST Digital Library of Mathematical Functions, https://dlmf.nist.gov .

[7] E. U. Condon and G. H. Shortley, "The Theory of Atomic Spectra", Cambridge Univ. Press, 1999.

[8] 猪木 慶治、川合 光、「量子力学 II」、講談社、2007。

[9] http://www.openmx-square.org/

[10] http://www.openmx-square.org/adpack_man2.2/

[11] R. M. Martin "Electronic Structure: Basic Theory and Practical Methods", 2nd edition, Cambridge University Press, 2020.

[12] T. Ozaki, Phys. Rev. B **67**, 155108 (2003).

[13] http://www.openmx-square.org/video_lec/OrderN-Part2.pdf, pp.4-20.

[14] http://www.openmx-square.org/adpack_man2.2_jp/node22.html

[15] https://www.hdfgroup.org/downloads/hdf5/

[16] http://www.openmx-square.org/openmx_man3.8jp/node93.html

[17] https://jp-minerals.org/vesta/en/

[18] J. A. Sobota, Y. He, and Z. X. Shen, Rev. Mod. Phys. **93**, 025006 (2022).

[19] T. Matsushita *et al.*, Phys. Rev. B **56**, 7687 (1997).

[20] S. Moser, J. Electron Spectrosc. **214**, 29 (2017).

[21] J. Stöhr, and H. C. Siegmann, "Magnetism: From Fundamentals to Nanoscale Dynamics", Springer, 2007.

[22] N. H. March, Advances in Physics **6**, 1 (1957).

[23] G. Breit and H. A. Bethe, Phys. Rev. **93**, 888 (1954).

[24] H. Tanaka, e-J. Surf. Sci. Nanotechnol. **21**, 139 (2023).

[25] https://people.sc.fsu.edu/~jburkardt/cpp_src/sphere_lebedev_rule/sphere_lebedev_rule.html